GIGYF recruits mRNA decay factors to repress target mRNA expression

Dissertation

der Mathematisch-Naturwissenschaftlichen Fakultät
der Eberhard Karls Universität Tübingen
zur Erlangung des Grades eines
Doktors der Naturwissenschaften
(Dr. rer. nat.)

vorgelegt von
Vincenzo Ruscica
aus Treviglio, Italy

Tübingen
2019

Gedruckt mit Genehmigung der Mathematisch-Naturwissenschaftlichen Fakultät der Eberhard Karls Universität Tübingen.

Tag der mündlichen Qualifikation:	02.05.2019
Dekan:	Prof. Dr. Wolfgang Rosenstiel
1. Berichterstatter:	Prof. Dr. Ralf-Peter Jansen
2. Berichterstatter:	Prof. Dr. Doron Rapaport

Declaration

This thesis describes my work conducted in the laboratory of Prof. Dr. Elisa Izaurralde in the Department of Biochemistry at the Max Planck Institute for Developmental Biology, Tübingen, Germany, from November 2014 to May 2019. The work was co-supervised by Prof. Dr. Ralf-Peter Jansen at the Eberhard Karls University of Tübingen, Germany, and was supported by a fellowship from the International PhD Program in the Biological Sciences, Tübingen. I declare that this thesis is the product of my own work. The parts that have been published or where other sources have been used were cited accordingly.

Table of contents

1 Abbreviations ... 1
2 Summary ... 5
2.1 Zusammenfassung ... 6
3 Introduction ... 9
3.1 Eukaryotic gene expression ... 9
3.2 Translation ... 12
3.2.1 Translation initiation ... 13
3.2.2 Translation elongation, termination, and ribosome recycling ... 15
3.3 Control of translation ... 16
3.3.1 Regulation of translation initiation via the 5’ cap structure ... 17
3.3.2 Competition for binding to eIF4E ... 17
3.3.3 Competition for binding the 5’ cap structure ... 19
3.4 mRNA quality control and decay ... 22
3.4.1 Cytoplasmic mRNA turnover ... 24
3.5 Interplay between translation repression and mRNA decay ... 27
3.5.1 3’ UTR mRNA binding protein ... 27
3.5.2 microRNAs ... 28
3.6 GIGYF proteins: enigmatic multifunctional players ... 30
4 Aims and significance ... 33
5 Materials and methods ... 35
5.1 Materials ... 35
5.1.1 Plasmids ... 35
5.1.2 Oligonucleotides ... 38
5.1.3 Antibodies ... 41
5.1.4 Solutions and reagents ... 42
5.1.5 Media for cell culture ... 45
5.1.6 Enzymes ... 45
5.2 Methods ... 46

5.2.1 PCR, restriction digestion, and ligation 46
5.2.2 Site-directed mutagenesis 47
5.2.3 Transformation, plasmid extraction, and sequencing 47
5.2.4 S2 cells transfection 47
5.2.5 Knock downs 48
5.2.6 mRNA half-life assay 49
5.2.7 Tethering assay 50
5.2.8 RNA extraction 51
5.2.9 Northern blot 52
5.2.10 Immunoprecipitation assay 52
5.2.11 Western blot 53
5.2.12 Protein expression from *E. coli* and purification 53
5.2.13 Protein crystallization 54
5.2.14 Crystal data collection and structure determination 54
5.2.15 *in vitro* pull-down assay 55

6 Results 57

6.1 4EHP requires GIGYF to promote mRNA degradation 57

6.1.1 4EHP interacts with GIGYF, via a conserved tripartite binding mode 57
6.1.2 GIGYF is the main 4EHP-binding protein in S2 cells 60
6.1.3 4EHP requires GIGYF to repress mRNA expression 61

6.2 GIGYF recruits mRNA decay factors to induce mRNA decay 64

6.2.1 The N-term of GIGYF represses translation and induces mRNA decay 64
6.2.2 GIGYF regulates mRNA stability 65
6.2.3 GIGYF promotes deadenylation-dependent decapping 67
6.2.4 GIGYF interacts with mRNA decay factors 68
6.2.5 TTP, ZNF598, and GW182 do not recruit GIGYF on RNA in S2 cells 71
6.2.6 Me31B and HPat interact with the effector domain of GIGYF 72
6.2.7 GIGYF contains a conserved Me31B-binding motif 73

6.2.8 GIGYF and Me31B interact through a unique structural arrangement 76
6.2.9 HPat is a GYF domain-interacting protein 78
6.2.10 GIGYF requires Me31B and HPat to induce translational repression and mRNA decay 80
6.2.11 Me31B and HPat are required for GIGYF-mediated translational repression 82
6.3 4EHP-mediated mRNA repression requires the recruitment of Me31B and HPat via GIGYF 86
6.3.1 GIGYF is necessary to recruit Me31B and HPat to 4EHP repressor complexes 86
6.3.2 GIGYF bridges 4EHP to Me31B and HPat 87
6.3.3 4EHP requires HPat and Me31B to repress target mRNA expression 88
6.3.4 NOT1 might be involved in 4EHP/GIGYF-mediated translational repression 89
7 Discussion 93
7.1 *D. melanogaster* 4EHP and GIGYF are different from their cognate human proteins 93
7.2 4EHP/GIGYF-mediated mRNA-repression 95
7.3 GIGYF allows the formation of a network of interactions 96
7.3.1 GIGYF-HPat interaction 96
7.3.2 GIGYF-NOT1 interaction 97
7.3.3 GIGYF-Me31B interaction 98
7.3.4 4EHP/GIGYF and HPAT/Me31B/NOT1 interaction 99
7.4 4EHP/GIGYF require HPat and Me31B for mRNA regulation 101
7.5 GIGYF biological role 103
8 References 105
9 Acknowledgments 123
10 Curriculum vitae 125

1 Abbreviations

4E-T	eIF4E-transporter
4EBP	eIF4E-binding protein
4EHP	eIF4E-homologous protein
A	auxiliary sequence
AA	amino acid
aa-tRNA	aminoacyl-tRNA
ABCE1	ABC-family ATPase 1
AGO	argonaute
AKT	protein kinase B
AREs	AU (Adenylate-Uridylate) -rich elements
BCD	Bicoid
BRAT	brain tumour
C	canonical eIF4E binding motif
CAF1	CCR4-associated factor 1
CBC	cap binding complex
CCR4	carbon catabolite repressor 4
CDS	coding sequence
D	dorsal surface
DCP2	decapping enzyme subunit 2
DDX6	DEAD-box helicase 6
DEAD	Aspartic Acid-Glutamic Acid-Alanine-Aspartic Acid box
DMSO	dimethyl sulfoxide
dNTPs	deoxyribonucleotide triphosphates
EDCs	enhancer of mRNA decapping proteins
eEFs	eukaryotic elongation factors
EGFP	enhanced green fluorescent protein
EGFR	epidermal growth factor receptor
eIF	eukaryotic initiation factor
EJC	exon-exon junction complex
eRF1	eukaryotic release factor 1
ERK	extracellular signal-regulated kinase
F-Luc	firefly luciferase

GIGYF1/2	Grb10-interacting GYF proteins 1 and 2
Grb10	growth factor-receptor bound protein 10
GYF	glycine-tyrosine-phenylalanine
HEPES	4-(2-hydroxyethyl)-1-piperazineethanesulfonic acid
HhR	hammerhead ribozyme
HOXB4	homeobox B4
HPat	PAT1 homolog protein 1
HRP	horse-radish peroxidase
IGF	insulin-like growth factor
IPTG	isopropyl ß-D-1-thiogalactopyranoside
IRES	internal ribosomal entry site
L	lateral surface
LSM14	sm-like protein 14
LSM15	sm-like protein 15
MAPK	mitogen activated protein kinase
Met-tRNA$_i^{met}$	initiator methionyl-tRNA
MIF4G	middle domain of eukaryotic IF4G
miRISC	microRNA-induced silencing complex
miRNA	microRNA
MOPS	3-(*N*-morpholino) propanesulfonic acid
mRNP	messenger-ribonucleoprotein particle
mTOR	mechanistic target of rapamycin
mTORC1	mTOR complex 1
NC	non-canonical eIF4E binding motif
NET	NaCl-EDTA-tris
NGD	no-go decay
NMD	non-sense-mediated mRNA decay
NOS	Nanos
NOT1	negative on TATA less protein
NPC	nuclear pore complex
NSD	non-stop decay
ORF	open reading frame
PABP	poly(A)-binding protein

PAGE	polyacrylamide gel electrophoresis
PAN	poly(A)-nucleases
PAP	polyadenylate polymerase
PB	P-body
PBS	phosphate-buffered saline
PCR	polymerase chain reaction
PDB	protein data bank
PI3K	phosphoinositide 3-kinase
PIC	pre-initiation complex
polyA	polyadenylation
PPGF	Proline rich sequence – pro-pro-gly-phe
pre-mRNA	precursor-messenger RNA
pri-miRNA	primary-miRNA
PSB	protein sample buffer
PUM	Pumilio
R-Luc	*Renilla* luciferase
RAN	Ras-related nuclear protein
RBPs	RNA-binding proteins
RE	responsive elements
RecA-like	recombinase A-like
RNA pol II	RNA polymerase II
RNP	ribonucleoprotein
rRNAs	ribosomal RNAs
S	4EHP-specific surface
S6K1	S6 kinase beta 1
SDS	sodium dodecylsulfate
SKI7	Superkiller protein 7
SLiMs	short linear motifs
TBE	tris-boric acid-EDTA
TCA	trichloroacetic acid
TEMED	*N, N, N', N'*-tetramethylenediamine
Tis11	TPA-**i**nducible sequence-11
TNRC6	trinucleotide repeat-containing 6A proteins

TRAMP	trf4/air2/mtr4p polyadenylation
tRNAs	transfer RNAs
TTP	tristetraprolin
UTR	untranslated region
XRN1	exoribonuclease 1
ZNF598	zinc finger protein 598

2 Summary

Gene expression is fundamental for all living organisms and involves different pathways that act to regulate the amount and quality of gene products. Translation initiation is one of the most heavily regulated steps. It is negatively modulated by a protein called 4E-homologous protein (4EHP), which is recruited to different mRNAs through the binding to specific RNA binding proteins (RBPs), forming transcript-specific repressor complexes. One such complex, contains the Grb10-interacting GYF (GIGYF) protein that in turn associates with the zinc finger RBPs ZNF598 and tristetraprolin (TTP). These RBPs are involved in mouse embryonic development and AU-rich element-containing mRNAs regulation, respectively. Moreover, the 4EHP/GIGYF complex interacts with the CCR4-NOT deadenylase complex altering mRNA abundance. This preliminary information suggests an important role of the 4EHP/GIGYF complex in translational repression and possibly in mRNA degradation, although the interacting partners, the mechanism and the significance remain substantially elusive. In my doctoral studies, I demonstrated that the 4EHP-GIGYF interaction is conserved between human and fly and is characterised by a tripartite binding mode. 4EHP repressor function is strongly dependent on the interaction with GIGYF, which post-transcriptionally regulates mRNA abundance by inducing deadenylation-dependent mRNA decay. Subsequently, I identified novel *Drosophila melanogaster* (*Dm*) GIGYF-interacting mRNA decay factors such as NOT1, Me31B, and HPat and I mapped their interaction to previously uncharacterized motifs/domains. By generating several GIGYF mutants that disrupt single or multiple protein interactions, I analysed the relevance of these interactions in GIGYF-mediated mRNA repression. I observed that both Me31B and HPat contribute to the repressor function of GIGYF. Moreover, since 4EHP requires GIGYF to repress translation of target mRNA, I tested the relevance of the interactions of GIGYF with Me31B/HPat in the control of mRNA expression by 4EHP. I observed that 4EHP can only reduce mRNA expression if GIGYF is able to interact with the mRNA decay partners. Taken together, these results indicate that 4EHP and GIGYF do not only elicit translational repression but also induce mRNA degradation via the recruitment of several mRNA decay factors.

2.1 Zusammenfassung

Die Genexpression ist eine grundlegende Voraussetzung für die Entwicklung lebender Organismen. Bestandteil dieses Prozesses sind verschiedene Mechanismen, welche die Menge und Qualität der Genprodukte regulieren. Die Initiation der Translation ist einer der am stärksten regulierten Schritte. Sie wird durch das sogenannte 4E-homologe Protein (4EHP) negativ beeinflusst, welches durch Interaktion mit spezifischen RNA-bindenden Proteinen (RBPs) zu unterschiedlichen mRNAs rekrutiert wird um Transkript-spezifische Inhibitionskomplexe zu bilden. Ein solcher Komplex enthält das Grb10-interagierende GYF (GIGYF) Protein, welches wiederum an die Zinkfinger-RBPs YNF598 und Tristetraprolin (TTP) bindet. Diese RBPs spielen eine Rolle in der Embryonalentwicklung von Mäusen und bei der Regulation von mRNAs mit AU-reichen Elementen. Des Weiteren interagiert der 4EHP/GIGYF Komplex mit dem CCR4-NOT Deadenylase Komplex und beeinflusst dadurch die mRNA-Menge. Diese Informationen lassen darauf schließen, dass der 4EHP/GIGYF Komplex eine wichtige Rolle bei der Regulation der Translation und möglicherweise auch beim Abbau der mRNA einnimmt, allerdings sind die Interaktionspartner, der Mechanismus und die Relevanz bislang weitgehend unbekannt. In meiner Doktorarbeit zeige ich, dass die Interaktion zwischen 4EHP und GIGYF bei Menschen und Fliegen konserviert ist und durch ein dreigeteiltes Bindemotiv gekennzeichnet ist. Die inhibitorische Wirkung von 4EHP beruht vornehmlich auf seiner Interaktion mit GIGYF. GIGYF reguliert den mRNA-Spiegel posttranskriptional, indem es deadenylierungsabhängigen mRNA-Abbau einleitet. Außerdem habe ich neue *Drosophila melanogaster* (*Dm*) GIGYF Interaktionspartner identifiziert, wie zum Beispiel die mRNA-Degradation induzierenden Faktoren NOT1, Me31B, und HPat, und habe deren Bindung zu bisher nicht charakterisierten Motiven oder Domänen zurückführen können. Mit Hilfe von GIGYF-Mutanten, bei welchen einzelne oder mehrere dieser Bindungen blockiert sind, untersuchte ich den Einfluss dieser Interaktionen auf die GIGYF-abhängige mRNA-Regulation. Ich beobachtete, dass sowohl die Interaktion mit Me31B als auch HPat zur inhibitorischen Wirkung von GIGYF beitragen. 4EHP benötigt GIGYF um die Translation bestimmter mRNAs zu hemmen, daher habe ich auch die Bedeutung der Interaktionen von GIGYF mit Me31B und HPat für die regulatorische Funktion

von 4EHP getestet. Ich stellte fest, dass 4EHP die mRNA-Expression nur dann beeinflussen kann, wenn die Interaktion von GIGYF mit den mRNA-Abbaufaktoren gewährleistet ist. Zusammengefasst deuten diese Ergebnisse darauf hin, dass 4EHP und GIGYF nicht nur die Translation hemmen, sondern auch durch das Rekrutieren von mRNA-Abbaufaktoren die Degradation der mRNA initiieren.

3 Introduction

3.1 Eukaryotic gene expression

Gene expression is a fundamental process composed by a myriad of steps, countless reactions and an enormous number of precise spatial-temporal regulated activities (Fig. 1). It is responsible for the existence of the biological life as we know, starting from simple protein production to the complexity of cell differentiation and development. The central dogma of molecular biology is the simplified representation of the whole gene expression events, describing the flow of information from DNA to RNA and in many cases to proteins. In fact, not all the products of gene expression are represented by proteins, but a very fascinating group is composed by diverse non-coding RNAs which regulate and are essential for many aspects of gene expression.

In eukaryotic cells, the protein-encoding genomic information flow initiates in the nucleus where RNA polymerase II (RNA pol II) transcribes the nucleotide information present in the DNA into a primary transcript called precursor-messenger mRNA (pre-mRNA). The pre-mRNA is co-transcriptionally processed to mature mRNA as a consequence of modification steps such as 5' RNA capping, pre-mRNA splicing, and 3' RNA polyadenylation (Heck and Wilusz, 2018; Moore, 2005).

RNA capping consists in the insertion of a specifically-modified guanine nucleotide to the nascent mRNA molecule. It requires the involvement of three enzymatic reactions: removal of the γ-phosphate of the 5'-terminal nucleotide, followed by the covalent link of a guanosine to the 5'-terminal nucleotide in an unusual 5'-5'-triphosphate linkage and a final N7-methylation of the guanosine (Ramanathan et al., 2016). The cap structure is crucial for the initiation of cap-dependent translation, it protects the 5'-end of the mRNA from exonuclease degradation and promotes the recruitment of pre-mRNA splicing, 3'-polyA, and nuclear export protein factors (Galloway and Cowling, 2018).

During splicing, the interspersed non-coding RNA sequences, introns, of the pre-mRNA, are removed from the primary RNA transcript to form contiguous stretch of coding sequences, known as exons. This is a sophisticated and complex mechanism that requires the recognition of consensus sequences on the introns, that specifically define the intron-exon border and are recognized by a

ribonucleoprotein (RNP) complex called spliceosome (Baralle and Baralle, 2018; Shi, 2017).

3' end RNA processing involves the recognition of the cleavage/polyadenylation sequence on the nascent mRNA by the cleavage factor complex which cleaves and adenylates the 3' end of the mRNA to length of about 200 nucleotides (Heck and Wilusz, 2018; Wu and Bartel, 2017).

Every step of the mRNA maturation is under surveillance by the nuclear RNA quality control mechanisms that ensure the fidelity of each step (Frye et al., 2018; Hollerer et al., 2014; Nasif et al., 2018; Simms and Zaher, 2016; Singh et al., 2018). The resulting mature mRNA is composed of the 5'-end cap structure, 5' untranslated region (UTR), coding sequence (CDS), 3' UTR, and the polyA tail.

Every RNA molecule is coated with several, and different, RNA-binding proteins (RBPs) from the beginning of its existence (transcription) to the moment of its end (degradation), aiding the RNA in every task of its cellular life (Mitchell and Parker, 2014). In the nucleus, some of these RBPs include the cap binding complex (CBC), the exon-exon junction complex (EJC) and the nuclear poly-A-binding protein (PABP). These proteins are crucial for translocation of the messenger-ribonucleoprotein particle (mRNP) from the nucleus into the cytoplasm of the cell in a process called nuclear export (Björk and Wieslander, 2014; Eliscovich and Singer, 2017). In fact, the nuclear export of the mRNA requires the interaction of the newly formed mRNPs and different nuclear export factor proteins with the giant multi-protein nuclear pore complex (NPC), which undergoes several conformational changes, essential for RNA export (Beck and Hurt, 2016; Björk and Wieslander, 2014; Carmody and Wente, 2009).

Upon mRNA export to the cytosol, the mRNP undergoes remodelling, a requisite for the next step of the gene expression (Carmody and Wente, 2009; Eliscovich and Singer, 2017). The cap binding protein eukaryotic initiation factor (eIF) 4E, together with several other eIFs, replaces the CBC and promotes ribosome recruitment and mRNA translation, the process of protein production (Jackson et al., 2010; Shirokikh and Preiss, 2018).

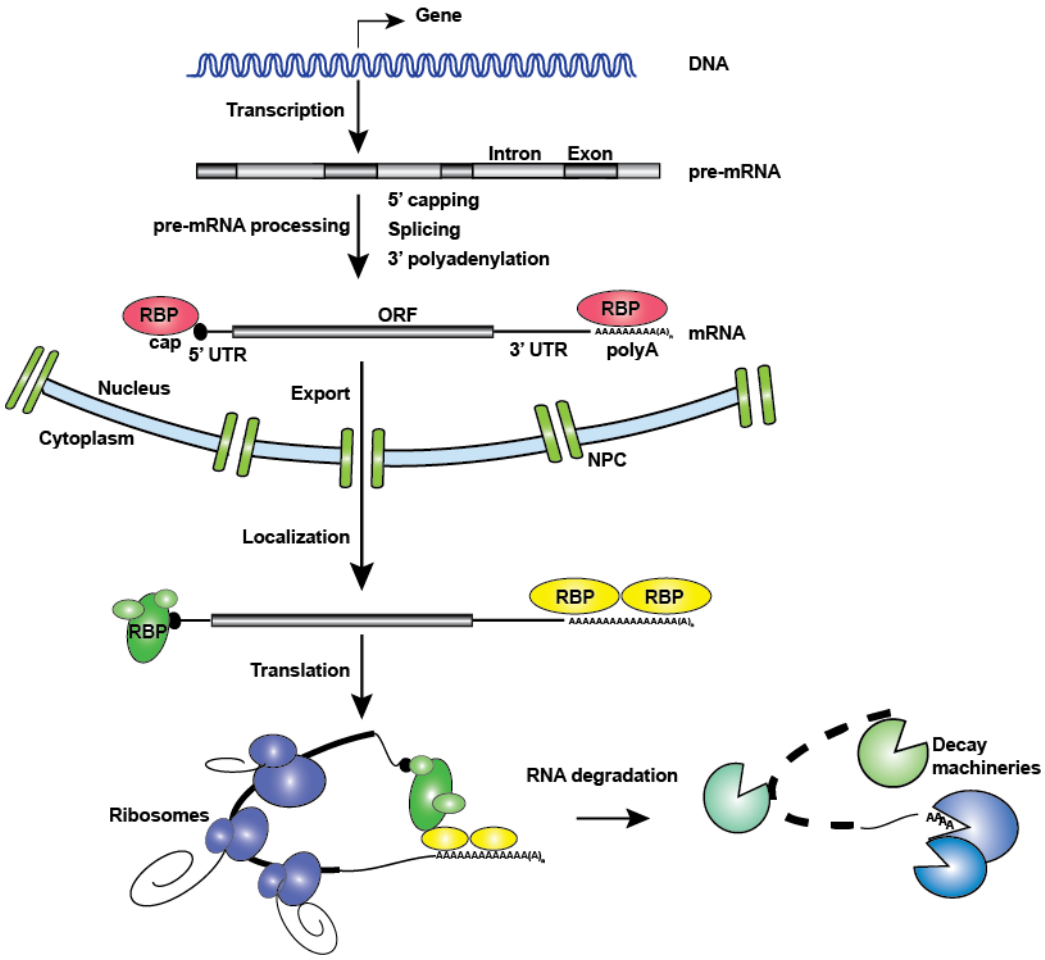

Figure 1. Eukaryotic gene expression
Schematic overview of eukaryotic gene expression. It begins in the nucleus with the transcription process, which generates a pre-mRNA molecule constituted by intron and exons. Pre-mRNA undergoes several processing events which protect the mRNA at the 5' end with the addition of a cap and at the 3' with the addition of the polyA-tail and that excise the non-coding sequences forming the mature mRNA. The mature mRNA is covered with RBPs which assist in the nuclear export of the mRNA to the cytoplasm trough the nuclear pore (NPC). Once in the cytoplasm, a new set of RBPs associate with the mRNA which can localize to several different cellular structures. Thereafter, the information carried by the nucleotide sequence of the mRNA is translated into the amino acid sequence of proteins. The final step of gene expression removes the message when it is no longer necessary and is operated by many effector complexes. Every single step of the gene expression is controlled to ensure the correct flow of information.

Alternatively, the mRNP in the cytoplasm can be actively transported to specific subcellular localisations by a process that involves the recognition of a definite sequence localisation element on the mRNA and subsequent transport to the final destination (Eliscovich and Singer, 2017; Mitchell and Parker, 2014). The final step of gene expression which removes the mRNA from the cell, mRNA decay, requires

the activity of numerous molecular complexes (Ghosh and Jacobson, 2010; Roy and Jacobson, 2013). Eventually the mRNA can also be temporarily stored in specialized non-membranous cytosolic bodies, such as stress granules and P-bodies (PBs) (Standart and Weil, 2018; Zlotorynski, 2014).

3.2 Translation

Once exported to the cytoplasm, the mature mRNA, coated with the appropriate set of proteins, is engaged into a process called translation (Eliscovich and Singer, 2017; Shirokikh and Preiss, 2018), during which, each consequent nucleotide triplet of the mRNA, called codon, is decoded into a specific amino acid (AA) (Jackson et al., 2010; Shirokikh and Preiss, 2018). mRNA translation is characterised by the coordinated action of two specialized non-coding RNAs, transfer RNAs (tRNAs) and ribosomal RNAs (rRNAs), in combination with a myriad of associated proteins (Graifer and Karpova, 2015; Lafontaine, 2015; Schimmel, 2017; Yusupova and Yusupov, 2017).

tRNAs are adaptor RNA molecules equipped with an anti-codon stem loop, which base pairs with the codon of the mRNA, and an acceptor stem at the 3' end of its structure, that harbours the AA specific for the corresponding mRNA codon, forming an aminoacyl-tRNA (aa-tRNA) (Graifer and Karpova, 2015).

rRNAs are a class of distinct RNA molecules that constitute the scaffold for a complex RNP machinery, the 80S ribosome composed of the 60S large subunit and the 40S small subunit (Graifer and Karpova, 2015; Shirokikh and Preiss, 2018). The ribosome contains three sites that accommodate the tRNAs during translation; A (acceptor) site, where the aa-tRNA decodes the nucleotide triplets of the mRNA, P (peptidyl) site, where the tRNA associated with the growing peptide is located, and E (exit) site, where the uncharged tRNA is released (Peña et al., 2017; Steitz and Moore, 2017; Yusupova and Yusupov, 2017).

The concerted actions of ribosome, tRNA, mRNA and associated proteins delineate the molecular mechanism of protein synthesis, which can be identified by four stages called initiation, elongation, termination, and ribosome recycling (Shirokikh and Preiss, 2018).

3.2.1 Translation initiation

Translation initiation is one of the most studied and characterized steps of gene expression. Eukaryotic cells rely on different mechanisms to initiate translation (Sriram et al., 2018).

The canonical cap-dependent translation initiation requires the formation of numerous protein-protein and protein-RNA complexes that interact with each other to assemble the macromolecular machinery that executes translation (Aylett and Ban, 2017; Hinnebusch and Lorsch, 2012; Jackson et al., 2010; Shirokikh and Preiss, 2018). It begins with the recognition of the 5' cap structure of a mRNA by a heterotrimeric protein complex called eIF4F, composed of the 5' cap-binding protein eIF4E, the DEAD (Asp-Glu-Ala-Asp)-box RNA helicase eIF4A, and the scaffold protein eIF4G (Aylett and Ban, 2017; Jia et al., 2012; Marcotrigiano et al., 1999; Sonenberg and Hinnebusch, 2009). eIF4G simultaneously interacts with eIF4E, at the 5' end of the mRNA, and with PABP, at the 3' end polyA tail, causing the circularization of the mRNA in a closed loop structure. mRNA circularization facilitates translation initiation and protects the mRNA from degradation (Shirokikh and Preiss, 2018; Wu and Bartel, 2017).

In parallel to the association of the eIF4F complex to the 5' cap structure, distinct sequential events ensure the correct execution of the first reactions of translation that ultimately require the formation of a competent ribosome and its positioning at the AUG start codon.

The initiator methionyl-tRNA (Met-$tRNA_i^{met}$) binds the eIF2 (constituted by α, β, and γ subunits) and a GTP molecule, thus constituting the ternary complex. The interaction of the ternary complex with the 40S small ribosomal subunit bound to the associated eIFs (eIF1, eIF1A, eIF3, and eIF5) leads to the assembly of the 43S pre-initiation complex (PIC) (Cate, 2017; des Georges et al., 2015; Majumdar et al., 2003). The combination of this sequence of events allows the accommodation of the Met-$tRNA_i^{met}$ into the P site of the 40S small ribosomal subunit (Aylett and Ban, 2017; Graifer and Karpova, 2015). Recruitment of the 43S PIC to the 5' end of the mRNA occurs upon binding of eIF4G (in the eIF4F complex) to eIF3 (in the PIC), and results in the formation of a larger complex known as the 48S PIC (Shirokikh and Preiss, 2018; Villa et al., 2013).

The loading of the 43S PIC onto the mRNA is aided by the ATP-dependent mRNA secondary structure unwinding activity of eIF4A, in collaboration with eIF4B (Andreou and Klostermeier, 2014; Garcia-Garcia et al., 2015).

Once the 48S PIC is assembled onto the mRNA, the 5' UTR is meticulously examined to identify the AUG initiation codon in a process called 5' UTR scanning. This requires the unwinding activity of eIF4A, assisted by other members of the DEAD-box RNA helicases, such as DDX3 and DHX29, eIF4G, and eIF4B (Hinnebusch, 2014; Leppek et al., 2017; Shirokikh and Preiss, 2018). 5' UTR scanning continues until the 43S PIC recognizes the starting AUG triplet located in a favourable nucleotide environment known as the Kozak sequence. In mammals, this sequence is defined by the GCCPuCC**AUG**G motif. Within the motif, the purine (Pu=A or G) localized three nucleotides upstream the AUG starting codon and the guanine (G) localized four nucleotides downstream of it are the most important (Jackson et al., 2010; Kozak, 1991). The fidelity of AUG recognition is granted by the activity of eIF1 that is able to discriminate between AUG and non-AUG codons (Hinnebusch, 2014; Pestova et al., 1998). The interaction between the 43S PIC and the starting codon occurs by codon-anticodon association and causes conformational changes that tight the interaction between mRNA and 43S PIC, and provoke the dissociation of eIF1 (Hinnebusch, 2014; Passmore et al., 2007; Shirokikh and Preiss, 2018). The last event of the initiation step requires the activity of eIF5B that favours the joining of the 60S large ribosomal subunit with the 43S PIC, forming the fully competent 80S ribosome (Hinnebusch, 2014; Shirokikh and Preiss, 2018).

Alternatively, translation can be initiated in a cap-independent fashion mediated by *cis*-acting RNA elements present in the 5' UTR of some mRNAs. These RNA elements are called internal ribosomal entry sites (IRES) and do not require the aforementioned eIF4E or the cap to initiate translation. Cap-independent protein synthesis occurs in many biological conditions in which cap-dependent translation is blocked by regulatory cellular pathways, for example during hypoxia and viral infection (Terenin et al., 2017; Yamamoto et al., 2017).

3.2.2 Translation elongation, termination, and ribosome recycling

The accurate identification of the AUG start codon by the Met-tRNA$_i^{met}$ in the P site of the ribosome and the joining of the 60S large ribosomal subunit is the prerequisite for the assembly of a fully functional 80S ribosome and the start of the elongation phase of translation. Translation elongation is characterized by the progressive addition of aminoacids (AA) according to the information provided by the mRNA codons and involves three main reactions: tRNA selection, peptide-bond formation, and tRNA translocation (Dever et al., 2018).

The translation elongation cycle begins with tRNA selection. Specifically, the aa-tRNA harbouring the corresponding anticodon is loaded onto the A site of the ribosome, aided by the activity of different eukaryotic elongation factors (eEFs). The accommodation of the aa-tRNA in the site A triggers peptide bond formation between the AAs associated to the tRNAs present in the P and A sites of the ribosome. Upon peptide bond formation, translocation of the ribosome along the mRNA shifts the tRNAs from the P to the E site and form the A to P site of the ribosome allowing the release of the discharged tRNA and the selection of a new aa-tRNA to the free A site, respectively (Dever et al., 2018; Schuller and Green, 2018).

Several circumstances may hamper the activity of the ribosome during elongation. For example, a sequence of specific AA, codon usage, and mRNA secondary structures can result in ribosome stalling that must be resolved to permit the continuation of protein synthesis (Bicknell and Ricci, 2017; Chen and Shyu, 2017; Hanson and Coller, 2018).

The tri-step process of translation elongation is repeated until the ribosome encounters one of the three stop codons in the A site. This event initiates the termination phase of translation (Dever et al., 2018; Hellen, 2018). The pivotal player involved in translation termination is the eukaryotic release factor 1 (eRF1), which shares unique similarities in size and shape with a tRNA, functioning as a molecular mimic. Together with associated factors such as eRF3, eIF5, and the ABC-family ATPase 1 (ABCE1), eRF1 promotes the release of the newly synthetized polypeptide chain and the termination of translation (Hellen, 2018; Schuller and Green, 2018). Subsequently, the 80S ribosome containing the deacylated tRNA is split into the 40S and 60S subunits, by the activity of ABCE1, and the 40S is re-

associated with eIFs, recycling the small ribosomal subunit for a new round of translation (Hellen, 2018; Schuller and Green, 2018).

3.3 Control of translation

Every step of gene expression, from transcription till degradation of the mRNA, is subjected to regulation to ensure a spatial-temporal regulation of the expression of a gene. Among these, translational control extensively contributes to the complexity of gene expression modulation (Kong and Lasko, 2012; Tahmasebi et al., 2018). Because protein synthesis requires the consumption of approximately 20% of the cellular energy, its dynamic regulation is important in various cellular situations (Cao, 2018; Lindqvist et al., 2018; Topisirovic and Sonenberg, 2011). Moreover, translational control allows the cell to quickly adapt to environmental and cellular stresses, via the activation of distinct cellular mechanisms that evolved to monitor the different steps of translation (Cao, 2018; Hernandez et al., 2010; Pakos-Zebrucka et al., 2016). Interestingly, mRNA can also be locally confined in specific subcellular areas to restrict protein production. An example of the coupling of mRNA localisation with translational inhibition is observed in the control of synaptic plasticity (Shirokikh and Preiss, 2018; Sriram et al., 2018). Furthermore, translational regulation has a pivotal role in several physiological processes, including, but not limited to, cell growth, development, and stress response (Galloway and Cowling, 2018; Kong and Lasko, 2012; Meng et al., 2018; Pakos-Zebrucka et al., 2016). Protein synthesis is controlled at a global- or message-specific level. Regulation of the different phases of translation, through the modulation of the function of general initiation and elongation factors has a global impact on protein synthesis. Alternatively, translational control can specifically repress the expression of only a subset of mRNAs (Aylett and Ban, 2017; de la Parra et al., 2018; Kong and Lasko, 2012). This intricate regulatory network is extremely important to maintain cellular homeostasis and its dysregulation is the cause of a vast number of human diseases (Biffo et al., 2018; Lindqvist et al., 2018; Robichaud et al., 2018; Tahmasebi et al., 2018).

3.3.1 Regulation of translation initiation via the 5' cap structure

Translational regulation occurs at the different steps of protein synthesis. However, the majority of the translational control mechanisms regulate the assembly of the eIF4F complex onto the cap structure. In particular, two alternative mechanisms control the binding of eIF4E to the cap structure. These mechanisms rely on the function of two groups of proteins: the eIF4E-binding proteins (4EBPs) and a member of the eIF4E protein family, eIF4E2 (or eIF4E-homologous protein, 4EHP) (Joshi et al., 2004; Joshi et al., 2005; Kong and Lasko, 2012).

3.3.2 Competition for binding to eIF4E

Eukaryotic cells express a group of proteins, generally defined as 4EBPs, that compete with eIF4G for eIF4E binding (Kong and Lasko, 2012; Marcotrigiano et al., 1999). Thus, the interaction between 4EBPs and eIF4E inhibits the assembly of the eIF4F complex, impairing the recruitment of the 43S PIC to the 5' cap structure (Fig. 2) and repressing translation (Cate, 2017; Kong and Lasko, 2012; Marcotrigiano et al., 1999; Shirokikh and Preiss, 2018). Both 4EBPs and eIF4G interact with the dorsal surface of eIF4E via a highly conserved binding motif, termed the canonical motif (C) of sequence TyrX_4LeuΦ (YX_4LΦ, where X is any AA and Φ is any hydrophobic AA) (Hernandez et al., 2010; Mader et al., 1995; Marcotrigiano et al., 1999). Furthermore, 4EBPs and eIF4G also bind to a second and lateral surface of eIF4E. Lateral binding is mediated by poorly conserved and hydrophobic non-canonical eIF4E binding motifs (NC) (Gruner et al., 2016; Gruner et al., 2018; Igreja et al., 2014). Interestingly, beside C and NC motifs, some 4EBPs also possess a third auxiliary motif (A), adopting a tripartite eIF4E-binding mode, which confers stronger binding affinity (Peter et al., 2015b).

The interaction between some 4EBPs and eIF4E is reversible and regulated by phosphorylation. In detail, hyper-phosphorylated 4EBPs have reduced binding affinity to eIF4E, while hypo-phosphorylated 4EBPs bind strongly to eIF4E and repress translation (Gingras et al., 1999; Gingras et al., 1998; Kong and Lasko, 2012; Topisirovic and Sonenberg, 2011). 4EBP phosphorylation cascade is mediated by one of the most important signalling pathways in the cell, that involves the phosphoinositide 3-kinase (PI3K), the protein kinase B (AKT), and the downstream serine/threonine kinase called mechanistic target of rapamycin

(mTOR), part of a multi subunit complex called mTOR complex 1 (mTORC1) (Cao, 2018; Lindqvist et al., 2018; Robichaud et al., 2018; Saxton and Sabatini, 2017; Tahmasebi et al., 2018). The PIK3-AKT-mTORC1 pathway is activated by several stimuli, either internal or external of the cell, such as growth factors, energy status, and nutrients, recognized by different sensor membrane proteins (Cao, 2018; Lindqvist et al., 2018). The importance of PIK3-AKT-mTORC1 is highlighted by the evidence that its dysregulation is linked to a plethora of disorders including but not limited to cancer (Tahmasebi et al., 2018). mTORC1 phosphorylation targets include, besides 4EBPs, the serine/threonine ribosomal protein S6 kinase beta 1 (S6K1) which regulates S6 ribosomal protein and eIF4B, a co-activator of eIF4A, and eEF2 (Cao, 2018). Thus, mTORC1 has a general and central role of in regulating translation, by modulating many of its players and maintaining the cell under physiological conditions (Chu et al., 2018; de la Parra et al., 2018; Sriram et al., 2018; Tahmasebi et al., 2018).

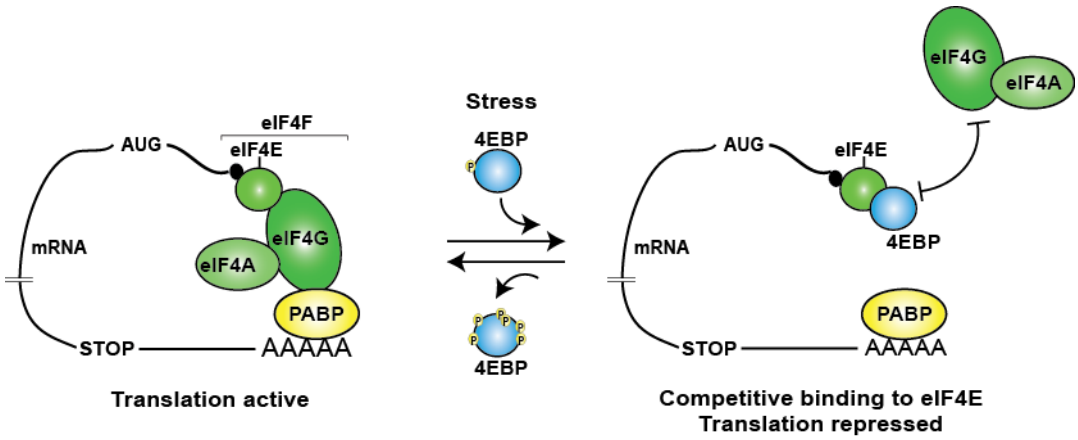

Figure 2. Competition mechanism for binding to eIF4E
Representation of translational repression mediated by 4EBP. To promote translation, the eIF4F complex binds to the cap of the mRNA, via the eIF4E subunit, while the RBP PABP connects it to the 3' polyA-tail circularizing the mRNA. Moreover, eIF4F recruits the small ribosomal subunit to the mRNA. In stress conditions, cap-dependent mRNA translation is blocked by hypophosphorylated 4EBPs, which compete with eIF4G for the binding to eIF4E. This is a reversible process controlled by phosphorylation of 4EBP.

4EBPs not only regulate general translation repression but also act on specific mRNA targets. Transcript-specific translational regulation is mediated by specific RBPs that recognize RNA elements in the 3' UTR of the mRNA and bind to the 4EBP, thus tethering the repressor and increasing the local competition with

eIF4G. Examples of this repression mechanism are represented, among many others, by the insect-specific CUP protein, and the eIF4E-transporter (4E-T) protein (Kamenska et al., 2014a; Kamenska et al., 2014b; Kong and Lasko, 2012; Lewis et al., 2017; Nakamura et al., 2004; Nelson et al., 2004; Peter et al., 2015a).

3.3.3 Competition for binding the 5' cap structure

Translational control can also be exerted by another member of the eIF4E-proteins family, called 4EHP (Hernandez et al., 2010; Joshi et al., 2004; Joshi et al., 2005), which shares high sequence and structural similarities with its cognate protein (Joshi et al., 2004; Peter et al., 2017; Rosettani et al., 2007). 4EHP interacts with the 5' cap structure of the mRNA, although with lower binding affinity than eIF4E. However, it fails to bind eIF4G and therefore represses translation initiation by hampering the assembly of eIF4F complex at the cap structure (Cho et al., 2005; Rom et al., 1998). Therefore, 4EHP represses translation by competing with eIF4E for cap-binding (Fig. 3).

This alternative control mechanism is usually employed in the regulation of translation in a messenger-specific manner (Cho et al., 2005). In fact, in *Drosophila melanogaster,* 4EHP is recruited to *caudal* and *hunchback* mRNAs by the RBPs Bicoid (BCD), and brain tumour (BRAT) in complex with the RBPs Nanos (NOS), and Pumilio (PUM) (Cho et al., 2006; Cho et al., 2005). This selective translational repression mechanism is crucial for embryonic pattern formation and in particular to define the anterior-posterior axis of the fly embryo (Cho et al., 2006; Cho et al., 2005). In addition, binding of 4EHP to the Prep1 protein translationally represses the expression of *homeobox B4* (*HOXB4*) mRNA, a regulator of stem cell renewal during mouse oogenesis (Antonchuk et al., 2002; Villaescusa et al., 2009). In mammalian cells, human 4EHP contributes to microRNA (miRNA)-mediated gene silencing by binding to 4E-T and other factors of the miRISC (miRNA-Induced Silencing Complex) (Chapat et al., 2017). In this context, 4EHP translationally controls the expression of *Dusp6* mRNA, a target of miR-145. DUSP6 is an extracellular signal regulated kinase (ERK)1/2- phosphatase which modulates the mitogen activated protein kinase (MAPK) pathway and affects cell proliferation and apoptosis (Jafarnejad et al., 2018).

Furthermore, 4EHP is part of two translational repressor complexes that are recruited to mRNA by the RBPs zinc finger protein 598 (ZNF598) or tristetraprolin (TTP, or Tis11 in *D. melanogaster*), repressing the translation of mRNAs essential for mouse development or possessing AU-rich elements (AREs) in the 3' UTR, respectively (Fu et al., 2016; Morita et al., 2012; Tao and Gao, 2015). Interestingly, in both complexes the Grb10-interacting GYF (glycine-tyrosine-phenylalanine) protein 2 (GIGYF2) (Fig. 4 A) acts as a scaffold and bridges the interaction between the cap binding protein 4EHP and ZNF598 or TTP (Fu et al., 2016; Morita et al., 2012; Tao and Gao, 2015). Both these zinc finger proteins are characterized by the presence of proline rich sequences (PPGΦ, where Φ is a F or L hydrophobic AA) that mediate the interaction with GIGYF2. Indeed, the GYF domain of the latter protein (Fig. 4 A) adopts a cradle structural arrangement that accommodates the hydrophobic AA of the PPGΦ sequences of both ZNF598 and TTP (Ash et al., 2010; Fu et al., 2016; Kofler and Freund, 2006; Morita et al., 2012). In addition to these two RBPs, the GYF domain can potentially interact with several other proteins of the miRISC complex as highlighted by mass spectrometry data analysis (Ash et al., 2010; Schopp et al., 2017).

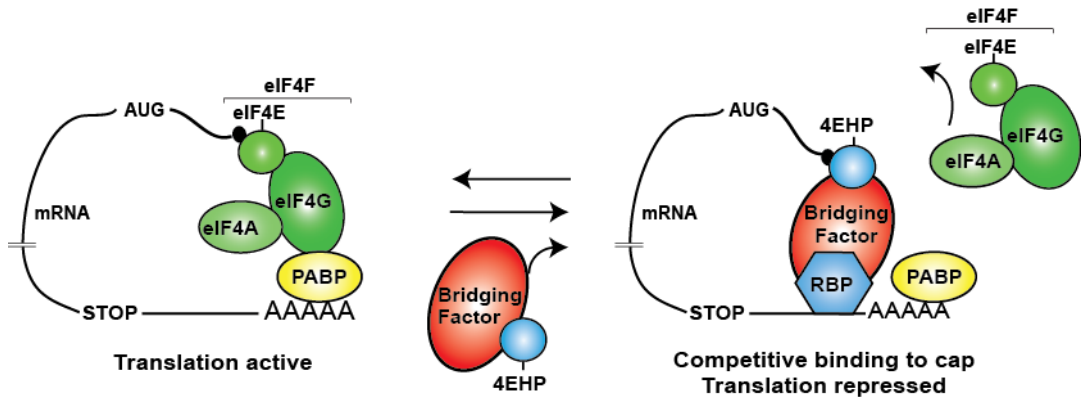

Figure 3. Competition mechanism for binding the cap
Model representing the translational repressor function of 4EHP. The eIF4F complex binds the cap, it is connected to the polyA tail through PABP and promotes translation by recruiting the ribosome. 4EHP, in complex with an RBP and in some cases a bridging factor, can hamper translation by competing with eIF4E to bind the cap structure.

4EHP-interacting proteins contain a highly conserved motif called canonical (C) 4EHP-binding motif, with the consensus sequence $YXYX_4L\Phi$, that is highly similar to the C eIF4E-binding motif. The interaction with 4EHP-binding proteins, in

combination with several post-translational modifications such as ISGylation and ubiquitination, enhances the binding of 4EHP to the cap (Chapat et al., 2017; Kubacka et al., 2013; Okumura et al., 2007; von Stechow et al., 2015). Interestingly, despite the high sequence similarity between the C motif of 4EBPs and 4EHP-binding proteins, GIGYFs proteins specifically interact with 4EHP and fail to interact with eIF4E (Morita et al., 2012). In detail, the binding between 4EHP and GIGYF is mediated by three different contact points (Fig. 4 B and C). First, the GIGYF C motif adopts a helical conformation and addresses the dorsal surface of 4EHP. A flexible linker region connects the C to the non-canonical (NC) motif, located twelve residues downstream, which harbours conserved hydrophobic AAs that mediate the interaction with the lateral surface of 4EHP, in the second contact point. This structural arrangement is very similar to the one adopted by 4EBPs to bind eIF4E, but the binding specificity between 4EHP and GIGYF is achieved by a complex molecular architecture mediated by a tripartite binding. In fact, C-terminally to the NC binding region, GIGYF proteins contain an auxiliary (A) sequence, adopting mainly a helical secondary structure, which interacts with a region of 4EHP that is not conserved in its cognate eIF4E, termed 4EHP-specific surface (S). This unique structural arrangement does not only provide a strong binding affinity of GIGYF to 4EHP, but also confers specificity towards 4EHP instead of eIF4E (Peter et al., 2017).

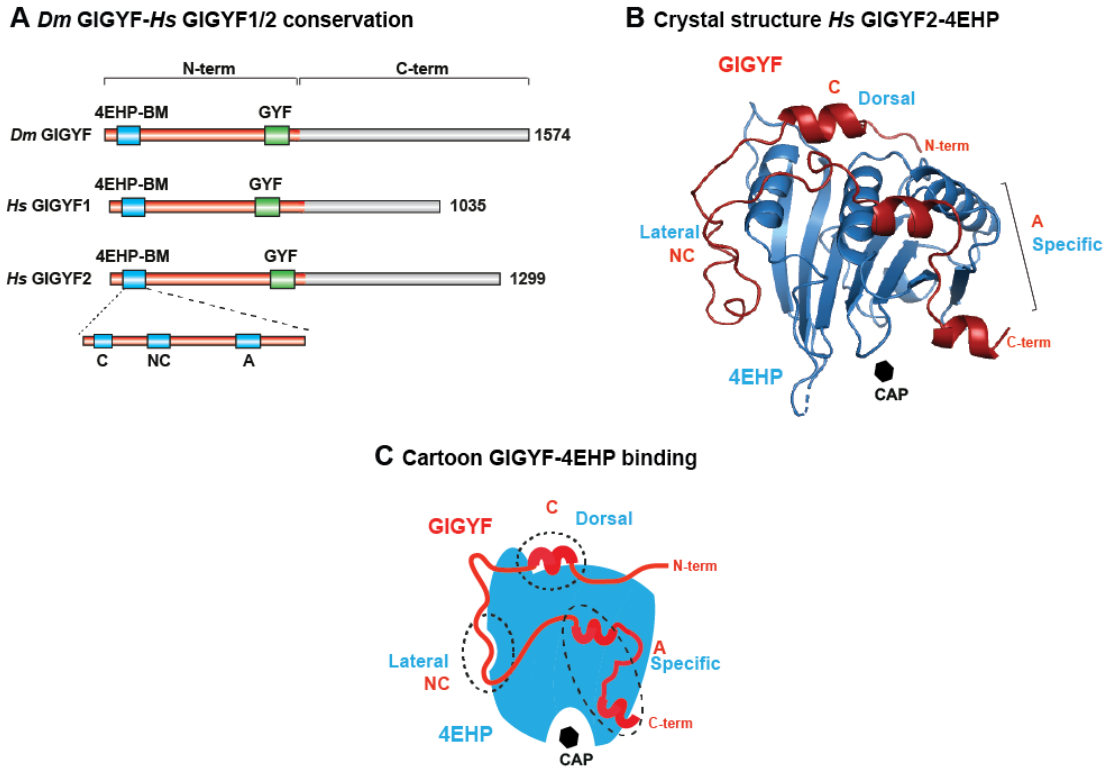

Figure 4. 4EHP binding to GIGYF

(A) Overview of the domain organization of *D. melanogaster* GIGYF (CG11148) and the two human paralogs GIGYF1/2. The N-terminal (N-term) region (red) is the most conserved part of the protein, while the C-terminal (C-term) region (grey) is the less conserved. All the GIGYF proteins contain a 4EHP binding motif (4EHP-BM, blue box) and a GYF domain (green box). The number at the end of the protein indicate the last amino acid of the protein. At the bottom of the figure it is depicted an enlargement of the 4EHP-BM, highlighting the Canonical (C) and non-canonical (NC) motifs, and the auxiliary sequence (A). **(B)** Human GIGYF2-4EHP crystal structure. GIGYF-4EHP-BM is shown in red and are highlighted the C, NC and the A sequences. 4EHP is shown in blue; dorsal, lateral and specific surfaces are highlighted. The structure image as been modified from the Protein Data Bank (PDB: 5NVL) (Peter et al., 2017). **(C)** Schematic representation of the interaction between GIGYF (red) and 4EHP (blue). The three interacting regions of GIGYF, Canonical (C), Non-Canonical (NC), and Auxiliary sequence (A) interact with three surfaces on 4EHP, Dorsal, Lateral and Specific, respectively. The dashed black circles indicate the three different contact points. In B and C, the black octagon represents the cap of an mRNA and highlights the position of the cap-binding pocket on 4EHP.

3.4 mRNA quality control and decay

The control of gene expression guarantees the quality, the abundance and spatial-temporal localization of all gene products (Heck and Wilusz, 2018). The formation of the mature mRNA molecule is an extremely complex and elaborated process, that produces a large quantity of different RNA molecules (Ghosh and

Jacobson, 2010; Kong and Lasko, 2012). Upon completion of specific cellular functions, all RNA molecules are eliminated from the cell (Bicknell and Ricci, 2017; Collart, 2016; Singh et al., 2018). RNA decay is accomplished by several mechanisms and plays a major role in the modulation of the quality and quantity of a gene product in response to different requirements (Heck and Wilusz, 2018; Pérez-Ortín et al., 2013).

RNA decay is required for the elimination of RNA molecules that accumulated errors during its life cycle (Chen and Shyu, 2017; Frye et al., 2018; Simms and Zaher, 2016; Singh et al., 2018). These errors consist of sequence abnormalities and structural RNA defects and are recognized by RNA-surveillance mechanisms. These mechanisms operate both in the nucleus and in the cytoplasm through the activity of different effector complexes (Kilchert et al., 2016; Pérez-Ortín et al., 2013). In the nucleus, the surveillance pathways aim to recognize errors occurring during the three major RNA processing events (5' cap formation, splicing, and 3'-end processing) and the constitution of the nuclear export mRNPs. These quality control steps are mediated by different multiprotein complexes, the nuclear exosome and the trf4/air2/mtr4p polyadenylation (TRAMP) complex (Jamar et al., 2018; Nasif et al., 2018; Singh et al., 2018). In the cytoplasm, the mRNP undergoes a second round of scrutiny to avoid the translation of aberrant mRNA which could lead to accumulation of faulty and harmful proteins (Jamar et al., 2018; Singh et al., 2018). Three main mRNA quality control pathways have been identified in the cytoplasm: the non-sense-mediated mRNA decay (NMD), non-stop decay (NSD), and no-go decay (NGD). NMD is the best characterized RNA surveillance mechanism and its function is important during embryonic development and cell differentiation (Ghosh and Jacobson, 2010; Nasif et al., 2018). NMD mediates the degradation of mRNAs which harbour premature termination codons (Jamar et al., 2018; Lykke-Andersen and Jensen, 2015; Nasif et al., 2018). Inversely, the NSD induces degradation of mRNA transcripts with stalled ribosomes at the end of the transcript due to the lack of a stop codon (Bicknell and Ricci, 2017; Ghosh and Jacobson, 2010). Finally, the NGD promotes the degradation of RNA species in which the ribosome is stalled during translation, for example, due to damaged nucleotides or the presence of secondary structures (Bicknell and Ricci, 2017; Jamar et al., 2017; Jamar et al., 2018; van Hoof and Wagner, 2011).

Beside the mRNA quality control pathways, RNA degradation also influences the concentration of different mRNA transcripts in the cell and thus constitutes an important mean to regulate gene expression. Cytoplasmic mRNA decay is mediated by two different kind of nucleases: endo- and exonucleases (Heck and Wilusz, 2018). The exonuclease-dependent mRNA turnover occurs via two alternative mechanisms called 5'-3' decay and 3'-5' decay pathways (Radhakrishnan and Green, 2016). Instead, the turnover of mRNA mediated by endonucleases leads to the recognition and cleavage of the mRNA generating either 5'-monophosphate termini or 3'-hydroxil termini that are substrate for exonucleases in the cell (Bartel, 2018; Heck and Wilusz, 2018).

3.4.1 Cytoplasmic mRNA turnover

According to the direction of ribonucleotide removal, cytoplasmic mRNA decay is divided into two alternative pathways, 5'-3' decay and 3'-5' decay (Heck and Wilusz, 2018; Pérez-Ortín et al., 2013). Both of the degradation pathways begin with the removal of the adenosines from the 3'-end of the mature mRNA (Fig. 5). This is the rate-limiting step of the degradation process and it is mainly executed by two deadenylase complexes, the poly(A)-nucleases (PAN) 2-PAN3 and the CCR4-NOT. The first acts in a distributive fashion and catalyses the removal of a short stretch of adenosines from the mRNA. Subsequently, the CCR4-NOT complex degrades the remaining polyA tail in a processive fashion (Heck and Wilusz, 2018; Tucker et al., 2001; Wahle and Winkler, 2013).

The CCR4-NOT is a conserved multisubunit complex that, not only deadenylates mRNA, but also modulates several steps in gene expression, having a role in assisting transcription, nuclear export and in translation (Collart, 2016; Collart and Panasenko, 2017). NOT1 is the scaffolding subunit of the CCR4-NOT that mediates interaction with the other subunits of the complex. CCR4-associated factor 1 (CAF1) and CCR4, dock onto the MIF4G domain (MIF4G: middle domain of eukaryotic initiation factor 4G) of NOT1, are active deadenylases and form the catalytic module of the complex. Other non-catalytic subunits of the CCR4-NOT complex are NOT2, NOT3, CAF40, NOT10, and NOT11 (Collart and Panasenko, 2017). The shortening of the polyA tail causes the dissociation of PABP and the destabilization of the mRNA (Collart and Panasenko, 2017; Heck and Wilusz, 2018;

Shirokikh and Preiss, 2018). Following deadenylation, the two canonical mRNA degradation pathways undertake different actions that lead to the complete degradation of the mRNA (Heck and Wilusz, 2018).

In the 5'-3' decay pathway (Fig. 5), the protective 5' cap structure is removed from the mRNA (Bicknell and Ricci, 2017; Chen and Shyu, 2017; Houseley and Tollervey, 2009). Decapping is mainly executed by the decapping enzyme subunit 2 (DCP2) in complex with DCP1. DCP2 belongs to the Nudix hydrolase superfamily of proteins and catalyses the hydrolysis of the 5' cap structure, releasing m^7GDP and a mRNA with a 5' monophosphate end (Arribas-Layton et al., 2013; Grudzien-Nogalska and Kiledjian, 2017; Valkov et al., 2017; Valkov et al., 2016). Several associated decapping factors assist the DCP1/DCP2 complex in this fundamental step. These factors recruit the DCP1/DCP2 complex to an mRNA, form a docking platform for the assembly and activation of the complex, identify the target mRNA and probably assist in the remodelling of the mRNP for efficient assembly (Heck and Wilusz, 2018). The decapping factors include enhancers of mRNA decapping (EDCs), which vary among different species, such as the sm-like protein 14 (LSM14), LSM15 (Trailer hitch - Tral in *D. melanogaster*), the LSM1-7 complex, the PAT1 homolog protein 1 (PATL1, HPat in *D. melanogaster*) and the RNA helicase DEAD-box 6 (DDX6, or maternal expression at 31B - Me31B in *D. melanogaster*) (Arribas-Layton et al., 2013; Jonas and Izaurralde, 2013). The decapping associated factors selectively interact with each other and form a highly orchestrated molecular complex, with different functions according to the specific binding partner (Arribas-Layton et al., 2013; Jonas and Izaurralde, 2013; Tritschler et al., 2009). This is represented by PATL1/HPat and DDX6/Me31B that mediate multiple protein-protein interactions between the decapping associated factors and, in addition, link deadenylation to decapping by binding to NOT1 (Chen et al., 2014; Grudzien-Nogalska and Kiledjian, 2017; Haas et al., 2010; Jonas and Izaurralde, 2013; Marnef and Standart, 2010; Tritschler et al., 2008; Valkov et al., 2017).

DDX6/Me31B is a DEAD-box (Asp-Glu-Ala-Asp) RNA helicase able to bind RNA in an ATP-independent fashion. It is characterized by the presence of a tandem RecA-like domains (RecA1 and RecA2) and is involved in a multitude of functions in RNA metabolism (Brandmann et al., 2018; Cordin et al., 2006; Wang et al., 2017; Yu et al., 2011). DDX6/Me31B interacts with PATL1/HPat, EDC3, and LSM15/Tral,

among others, via a hydrophobic patch located in the C-terminal RecA like domain (RecA-C) that binds a conserved phenylalanine-aspartate-phenylalanine (FDF) motif of the mentioned proteins (Brandmann et al., 2018; Jonas and Izaurralde, 2013; Tritschler et al., 2008; Tritschler et al., 2007). In addition, other DDX6-interacting proteins, such as 4E-T, address DDX6/Me31B trough different binding mode, that include the interaction with the CUP-homology domain (CHD) and a second motif called IEL (Kamenska et al., 2014a; Kamenska et al., 2016; Nishimura et al., 2015; Ozgur et al., 2015). DDX6/Me31B also has a distinct binding spot for the NOT1 subunit of the CCR4-NOT complex. In the case of 4E-T, the presence of a polar residue upstream of the IEL motif of 4E-T allow the binding with a negative reside of NOT1, forming the trimeric complex with DDX6/4E-T/NOT1 (Ozgur et al., 2015). Moreover, beside assisting in decapping, DDX6/Me31B is important for translational repression and for miRNA- mediated gene silencing (Kuzuoglu-Ozturk et al., 2016; Ostareck et al., 2014).

As a consequence of decapping, the mRNA harbours a 5’-monophosphate terminus, which is the substrate for the highly processive 5’-3’ exoribonuclease 1 (XRN1), responsible for the complete degradation of the mRNA body (Heck and Wilusz, 2018; Jones et al., 2012; Nagarajan et al., 2013).

Alternatively, the mRNA can be degraded in a 3’ to 5’ direction by the RNA exosome, a conserved multisubunit protein responsible for the degradation of RNA species that possess 3’-hydroxyl termini (Heck and Wilusz, 2018; Zinder and Lima, 2017). This degradation machinery has a complex structural organization, constituted by a core complex of nine catalytically-inactive proteins called exo9 and one catalytic subunit called RRP44, forming the active exo10 complex (Kilchert et al., 2016; Labno et al., 2016). Upon completion of the RNA decay the final step of degradation is executed by the decapping scavenger complex DCPS which hydrolyse the cap structure. Furthermore, the exosome is necessary for cell proliferation and differentiation, defence against viruses, and quality control of the telomerase RNA (Heck and Wilusz, 2018; Hoshino, 2012; Labno et al., 2016; Singh et al., 2018; Zinder and Lima, 2017)

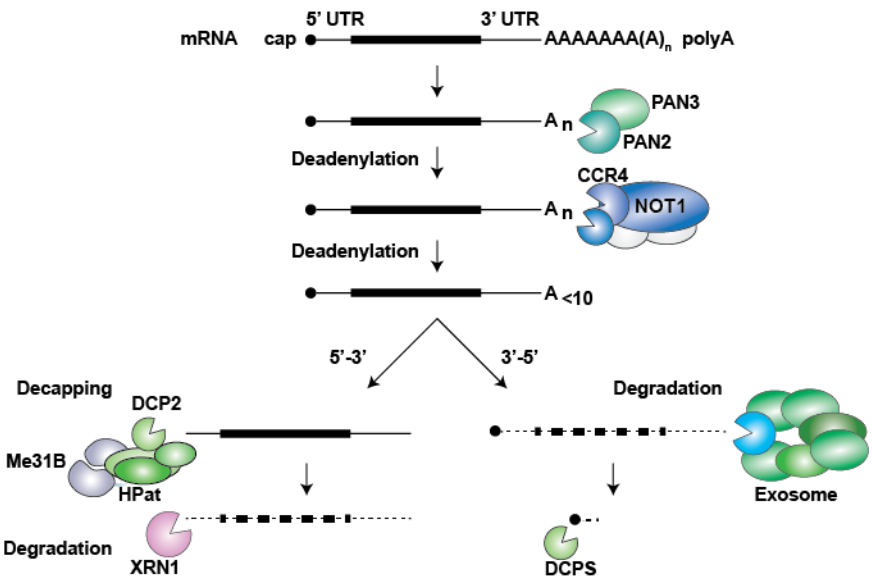

Figure 5. Cytoplasmic mRNA turnover

Schematic representation of the two major mRNA decay mechanisms in the cell, both beginning with the deadenylation of the mRNA at the 3'-end. A short stretch of adenosines is removed from the 3'-end by the PAN2-PAN3 complex and afterwards the CCR4-NOT complex is responsible for complete deadenylation of the mRNA. After the removal of the polyA-tail, the mRNA can be degraded by two different mechanisms acting in opposite directions: 5' to 3' or 3' to 5'. The first one requires the decapping of the mRNA, executed by DCP2 assisted by several proteins, for example Me31B and HPat, followed by degradation from the 5' end operated by the XRN1 exonuclease. The second mechanism requires the activity of the exosome complex that degrades the mRNA from its 3' end and the final hydrolysis of the cap structure by the DCPS enzyme.

3.5 Interplay between translation repression and mRNA decay

3.5.1 3' UTR mRNA binding protein

A precise response to different cellular conditions requires the fast adaptability of the cell. Mature eukaryotic mRNA contains 5' and 3' UTRs that are fundamental in post-transcriptional gene regulation. Indeed, these regions contain RNA elements that modulate in *cis* the expression of the mRNA, either favouring the stabilization and translation of the mRNA or accelerating its degradation (Heck and Wilusz, 2018; Schimmel, 2017). Control of mRNA stability is crucial in several cellular processes like development, differentiation, and immune response. The majority of these regulatory *cis*-elements are located in the 3' UTR of the mRNA, that are usually much longer and more complex than the regulatory elements on the 5' UTR (Chen and Shyu, 2017; Leppek et al., 2017; Rissland, 2017). RBPs

selectively bind to specific RNA elements and in turn influence the stability, localization, transport, and degradation of the mRNA molecule.
Among the RNA *cis*-elements that regulate mRNA stability are AREs, GU-rich and U-rich regions, and several protein specific responsive elements (RE), for example the Nanos responsive element (Cho et al., 2006; Collart, 2016; Fu et al., 2016; Raisch et al., 2016; Schoenberg and Maquat, 2012; Sgromo et al., 2018; Tao and Gao, 2015; Yamaji et al., 2017; Yamashita and Takeuchi, 2017). Interestingly, these sequence elements do not only induce mRNA decay but also promote translational repression by various mechanisms. For example, AREs are recognized by TTP, which in turn recruits the CCR4-NOT complex by binding to NOT1 (Fabian et al., 2013). Indeed, beside deadenylating bulk mRNA in the cytoplasm, the CCR4-NOT complex is recruited to and deadenylates specific transcripts via the interaction with TTP and several others RBPs. The importance of the AREs is corroborated by their localization on the 3' UTR of many short-lived mRNAs encoding for inflammatory factors, cytokines, and oncoproteins (Bartel, 2018).
TTP also recruits the GIGYF/4EHP translational repressor complex, and consequently blocks translation (Fu et al., 2016; Tao and Gao, 2015). An additional level of complexity has been highlighted by the intriguing possibility that GIGYF may also act as an RBP, targeting specific mRNA transcripts and recruiting the CCR4-NOT complex. The recruitment of the CCR4-NOT complex occurs through different binding regions of GIGYF and promotes degradation of mRNAs in a 4EHP-independent fashion (Amaya Ramirez et al., 2018).

3.5.2 microRNAs

Gene expression is also regulated by a class of small regulatory non-coding RNAs, microRNAs (miRNA), in complex with different effector proteins. miRNA-mediated gene silencing is a widespread mechanism of regulation that acts post-transcriptionally on complementary mRNA targets. It influences the vast majority of mRNA expression and is fundamental for many developmental and pathological processes in humans (Bartel, 2018; Jonas and Izaurralde, 2015; Treiber et al., 2018). miRNA-encoding genes are transcribed by the RNA pol II as primary-miRNA (pri-miRNA) intermediate, capped at the 5' end and modified at the 3'-end, although they do not necessarily harbour a polyA tail, and possess hairpins required for the

maturation of the miRNA (Bartel, 2018; Wu and Bartel, 2017). This is performed by the microprocessor heterotrimeric complex containing the endonuclease Drosha, that cleaves the RNA hairpin, forming the pre-miRNA. This is exported to the cytoplasm by the exportin5-Ras related nuclear protein (RAN)-GTP complex. In the cytoplasm, Dicer, a second RNA endonuclease, cleaves the terminal loop of the pre-miRNA forming a dsRNA duplex, that is recognised by the Argonaute (AGO) protein and its associated proteins. AGO in turn unwinds the two strands of the dsRNA duplex leaving only the so-called guide strand loaded into the miRISC (Bartel, 2018; Ha and Kim, 2014). The recognition of the target mRNA occurs by Watson-Crick base pairing between the miRNA and the 3' UTR of the target mRNA. The miRISC regulates gene expression by a direct or an indirect mechanism. In the direct mechanism, the AGO protein of the miRISC directly cleaves the complementary mRNA sequence where it is bound and required the full complementarity between miRNA and mRNA. This is not very frequent in mammals but common in plants (Bartel, 2018; Iwakawa and Tomari, 2015; Treiber et al., 2018).

In mammals, miRISC-dependent gene regulation involves the recruitment of the CCR4-NOT deadenylase complex, does not require full base pair complementarity between miRNA and mRNA, and requires the binding of the scaffold protein TNRC6/GW182 to AGO. TNRC6/GW182 in turn interacts and destabilizes PABP, while simultaneously interacting with NOT1, which initiates the 5'-3' mRNA degradation pathway (Behm-Ansmant et al., 2006; Braun et al., 2011; Chen et al., 2014; Iwakawa and Tomari, 2015; Jonas and Izaurralde, 2015). In addition, the consequent recruitment of DDX6 by NOT1 causes translational repression, mediated by 4E-T and 4EHP (Bartel, 2018; Chapat et al., 2017; Jafarnejad et al., 2018; Jonas and Izaurralde, 2015; Wang et al., 2017). GIGYF2 is also involved in miRNA-mediated gene regulation since it interacts with TNRC6/GW182 and AGO in human cell lines. This interaction occurs through the GYF domain of GIGYF2 and the PPGΦ motif of TNRC6/GW182. However, the involvement of GIGYF proteins in miRNA-mediated gene silencing remains poorly understood (Kryszke et al., 2016; Schopp et al., 2017).

All the aforementioned pathways are only a portion of the whole gene expression control and highlight the amazing complexity and intricacy of this regulation.

3.6 GIGYF proteins: enigmatic multifunctional players

GIGYF is a protein conserved in all metazoan either as one single copy or as two paralogous. Human cells express two GIGYF proteins, GIGYF1 and GIGYF2, which possess very similar domain composition characterised by the presence of a 4EHP binding region and the GYF domain at the N-terminal of the protein (Fig. 4 A). They are ubiquitously expressed in cellular tissue, and they mainly localize in the cytoplasm.

GIGYF1/2 have been originally identified as interactors of an adaptor protein called growth factor-receptor bound protein 10 (Grb10), which bind to activated tyrosine kinase receptor, such as insulin and insulin-like growth factor (IGF) receptor (Giovannone et al., 2003; Giovannone et al., 2009; Xie et al., 2014). Grb10 negatively regulates the insulin signalling not only by destabilizing the IGF receptor, favouring its degradation through ubiquitination signal, but also by preventing the association of the substrate to the receptor. However, Grb10 may act as a dual regulator, since it can also promote tyrosine receptor signalling (Desbuquois et al., 2013; Kabir and Kazi, 2014). The interaction between GIGYF1/2 and Grb10 may be important in the control of different hormones-induced signalling. In fact, it has been reported that in breast cancer cells, the GIGYF1/2-Grb10 complex interacts with the downstream regulators of the epidermal growth factor receptor (EGFR), AKT and CNOT9, and is involved in the activation of the AKT by phosphorylation (Ajiro et al., 2009; Ajiro et al., 2010). In addition, GIGYF2 expression increase the IGF-1-induced phosphorylation of ERK1/2 (Higashi et al., 2010).

Despite the number of publications reporting the involvement of GIGYF1/2 in the modulation of this signalling pathway, the exact molecular mechanism of this regulation remains elusive. Nevertheless, *gigyf2* null mice have been associated with an adult onset neurodegeneration phenotype, such as motor dysfunction and cognitive impairments, and these phenotypes were linked to the altered insulin signalling (Giovannone et al., 2009). Moreover, the involvement of GIGYF2 in age related neurodegenerative diseases, such as Parkinson's disease, has been inferred from several genetic studies that identified the location of the GIGYF2 gene within the PARK11, a Parkinson's disease-linkage region. In addition, the orthologue GIGYF in *D. melanogaster* is associated with neurodegeneration phenotypes in null mutants, and it is required for starvation-induced, developmental, and physiological

autophagy, affecting life span and mobility of the fly (Kim et al., 2015). However, the involvement of GIGYF in Parkinson's disease remains very controversial (Giovannone et al., 2009; Higashi et al., 2010; Tan and Schapira, 2010; Zhang et al., 2015).

4 Aims and significance

The regulation of gene expression is crucial to control the spatiotemporal localization of gene products. From transcription to mRNA degradation, all steps of mRNA metabolism are regulated. One regulatory mechanism operating at the interplay between mRNA decay and translational repression involves the activity of an eIF4E family member, 4EHP. This protein directly competes for binding to the 5'-cap structure of the mRNA, preventing its association with eIF4E and the recruitment of 43S ribosomal subunit. To exert transcript-specific translational repression, 4EHP is recruited to mRNAs by RNA-associated proteins, such as GIGYF, which bridges 4EHP to specific RBPs. GIGYF proteins also interact with the scaffold subunit of the CCR4-NOT complex to regulate mRNA expression. However, their function in the control of mRNA expression is poorly understood.

In this work, I extensively studied the 4EHP/GIGYF complex to elucidate the molecular mechanisms employed by these proteins in the control of translation and mRNA stability. In detail, I aimed to:

- identify the specific role of 4EHP and GIGYF on mRNA regulation;
- identify their downstream effector partners;
- unravel the downstream effectors intricate reciprocal interconnection;
- highlight the molecular mechanism mediated by 4EHP/GIGYF complex in mRNA degradation and translation repression.

The detailed information obtained by this study will bring us a step closer to understand the entire mRNA decay process and its interplay with translation repression, paving the way to design new studies.

5 Materials and methods

5.1 Materials

5.1.1 Plasmids

Table 1. Plasmids
All the plasmid listed below correspond to *D. melanogaster* proteins (with the exception of: Luciferase enzymes: F-Luc, firefly luciferase, from *Photinus pyralis* and R-Luc, *Renilla* luciferase from *Renilla reniformis*).

Name of the construct	Binding site/motif mutants (AA)
pAC5.1B-EGFP-V5	(Behm-Ansmant et al., 2006)
pAC5.1B-λN-HA	(Rehwinkel et al., 2005)
pAC5.1B-EGFP-MBP	(Behm-Ansmant et al., 2006)
pAC5.1B-EGFP-F-Luc	(Behm-Ansmant et al., 2006)
pAC5.1C-F-Luc-5BoxB	(Rehwinkel et al., 2005)
pAC5.1C-F-Luc-5BoxB-$A_{95}C_7$-HhR	(Igreja and Izaurralde, 2011)
pAC5.1C-F-Luc-V5	(Rehwinkel et al., 2005)
pAC5.1C-R-Luc-A_{90}-HhR	(Behm-Ansmant et al., 2006)
pAC5.1B-EGFP-4EHP (isoform 1 CG33100)	Full-length (1–223)
pAC5.1B-λN-HA-4EHP	Full-length (1–223)
pAC5.1B-EGFP-4EHP D*	W85A, Dorsal surface
pAC5.1B-λN-HA-4EHP D*	W85A, Dorsal surface
pAC5.1B-EGFP-4EHP L*	V75A, L91A, Lateral surface
pAC5.1B-EGFP-4EHP S*	R93P, E139L, specific surface
pAC5.1B-EGFP-4EHP CAP*	W114A, Cap-binding pocket
pAC5.1B-λN-HA-4EHP CAP*	W114A, Cap-binding pocket

pAC5.1B-EGFP-GIGYF (isoform G CG11148)	Full-length (1–1574)
pAC5.1B-λN-HA-GIGYF	Full-length (1–1574)
pAC5.1B-EGFP-GIGYF N-term region	1–640
pAC5.1B-λN-HA-GIGYF N-term region	1–640
pAC5.1B-EGFP-GIGYF C-term region	641–1574
pAC5.1B-λN-HA-GIGYF C-term region	641–1574
pAC5.1B-EGFP-GIGYF C*	Y58A, Y60A, M65A, Canonical
pAC5.1B-λN-HA-GIGYF C*	Y58A, Y60A, M65A, Canonical
pAC5.1B-λN-HA-GIGYF NC*	L79A, F82A, L85A, Non-canonical
pAC5.1B-λN-HA-GIGYF A*	P93D, L94A, Auxiliary
pAC5.1B-EGFP-GIGYF ΔMBM	Δ331-374, Me31B binding motif
pAC5.1B-λN-HA-GIGYF ΔMBM	Δ331-374, Me31B binding motif
pAC5.1B-λN-HA-GIGYF W*	W348A, Me31B binding motif (PEW-sequence)
pAC5.1B-λN-HA-GIGYF FF*	F360A, F366A, Me31B binding motif (FDF)
pAC5.1B-λN-HA-GIGYF WFF*	W348A, F360A, F366A, Me31B binding motif (PEW-sequence + FDF)
pAC5.1B-EGFP-GIGYF GYF*	Y571A, F582A, W590A, F596A, GYF domain
pAC5.1B-λN-HA-GIGYF GYF*	Y571A, F582A, W590A, F596A, GYF domain
pAC5.1B-λN-HA-GIGYF C*+GYF*	Y58A, Y60A, M65A, Y571A, F582A, W590A, F596A, Canonical + GYF domain
pAC5.1B-EGFP-GIGYF ΔMBM+GYF*	Δ331-374, Y571A, F582A, W590A, F596A, Me31B binding motif + GYF domain
pAC5.1B-λN-HA-GIGYF ΔMBM+GYF*	Δ331-374, Y571A, F582A, W590A, F596A, Me31B binding motif + GYF domain
pAC5.1B-HA-GIGYF C* (dsRNA-resistant)	Y58A, Y60A, M65A, Canonical
pAC5.1B-HA-GIGYF ΔMBM+GYF* (dsRNA-resistant)	Δ331-374, Y571A, F582A, W590A, F596A, Me31B binding motif + GYF domain

pAC5.1B-EGFP-HPat (CG5208)	Full-length (1–968), (Haas et al., 2010)
pAC5.1B-EGFP-HPat PPGF*	P286A, P287A, F289A, P328A, P329A, F331A, GYF-domain binding mutant
pAC5.1B-EGFP-Me31B	Full-length (1–459), (Tritschler et al., 2007)
pAC5.1B-EGFP-Me31B RecA2	268-459, (Tritschler et al., 2007)
pAC5.1B-EGFP-DCP1 GSSG (CG11183)	T70G, N71S, N72S, T73G, NR-loop mutant, (Kuzuoglu-Ozturk et al., 2016)
pAC5.1B-EGFP-Bicoid	Department plasmid databank
pAC5.1B-λN-HA-Brat	Department plasmid databank
pAC5.1B-EGFP-ZNF598	Department plasmid databank
pAC5.1B-EGFP-Tis11	Department plasmid databank
pAC5.1B-EGFP-NOT1	(Zekri et al., 2009)
pAC5.1B-EGFP-NOT2	(Zekri et al., 2009)
pAC5.1B-EGFP-NOT3	(Zekri et al., 2009)
pAC5.1B-EGFP-PAN2	(Braun et al., 2011)
pAC5.1B-EGFP-PAN3	(Braun et al., 2011)
pAC5.1B-EGFP-CCR4	(Zekri et al., 2009)
pAC5.1B-EGFP-POP2	(Zekri et al., 2009)
pAC5.1B-EGFP-CAF40	(Haas et al., 2010)
pAC5.1B-EGFP-EDC3	(Tritschler et al., 2007)
pAC5.1B-EGFP-EDC4	(Eulalio et al., 2007)
pAC5.1B-EGFP-Tral	(Tritschler et al., 2007)
pAC5.1B-EGFP-DCP1	(Tritschler et al., 2007)
pAC5.1B-DCP2-V5	(Tritschler et al., 2007)
pAC5.1B-XRN1-V5	(Haas et al., 2010)

pAC5.1B-EGFP-GW182	(Behm-Ansmant et al., 2006)
pAC5.1B-λN-HA-GW182	(Behm-Ansmant et al., 2006)
pAC5.1B-EGFP-4E-T	Department plasmid databank
pAC5.1B-λN-HA-eIF4E	Department plasmid databank

5.1.2 Oligonucleotides

Table 2. Oligonucleotides used for site-directed mutagenesis and plasmid cloning
Numbers represent amino acid residues of the specified protein. F and R stand for forward and reverse, respectively.

Oligonucleotide name	Sequence (5' to 3')
4EHP_W85A_F	ggtgcgccagcgtgcagcagtgggcgtcgctctactcgcacctcatccg
4EHP_W85A_R	cggatgaggtgcgagtagagcgacgcccactgctgcacgctggcgcac c
4EHP_V75AL91A_F	cagcaagtcgctgcacatggccggccggtgcgccagcgtgcagcagtg gtggtcgctctactcgcacgccatccggcccaccgccctgaag
4EHP_ V75AL91A _R	cttcagggcggtgggccggatggcgtgcgagtagagcgaccaccactgc tgcacgctggcgcaccggccggccatgtgcagcgacttgctg
4EHP_R93P_F	gtcgctctactcgcacctcatcccgcccaccgccctgaagccctacc
4EHP_R93P_R	ggtagggcttcagggcggtgggcgggatgaggtgcgagtagagcgac
4EHP_E139L_F	agaacaaggtcgaccgggcctggctgaacgtttgtatggcgatgctcg

4EHP_E139L_R	cgagcatcgccatacaaacgttcagccaggcccggtcgaccttgttct
4EHP_W114A_F	tcaagcagggcatcataccgatggcggaggacccggcgaacagcaag g
4EHP_W114A_R	ccttgctgttcgccgggtcctccgccatcggtatgatgccctgcttga
GIGYF_L79AF82AL85A_F	ggaactgcctactgccgcagatcgctccatcggctaaaaaggccttcgtg gaaaaggttcagtg
GIGYF_ L79AF82AL85A _R	cactgaacctttccacgaaggccttttagccgatggagcgatctgcggca gtaggcagttcc
GIGYF_P93DL94A_F	cttcgtggaaaaggttcagtgcgatgctgcactgacaccgagctccgagg
GIGYF_P93DL94A_R	cctcggagctcggtgtcagtgcagcatcgcactgaacctttccacgaag
GIGYF_640_F	tccgaattctattcctgttggtcaaatacc
GIGYF_640_R	ggacgagcggccgctcagttctctagttctatcggag
GIGYF_Y58AY60AM65A_F	gcttcccgtaatctatttccagaagcccgggccggacgcgaggaagcgct gtccttgttcgatcggaactg
GIGYF_ Y58AY60AM65A_R	cagttccgatcgaacaaggacagcgcttcctcgcgtccggcccgggcttct ggaaatagattacgggaagc
GIGYF_Y571AF582AW590AF596A_F	aatctaaacgaattgtggtttgcccgggatccgcaggcaaatgttcagggg ccagctagtgccgttgagatgacggaagcgtatcgcgctggctacgctaa tgagaacctgtttgtacg

GIGYF_Y571AF582AW590AF596A_R	cgtacaaacaggttctcattagcgtagccagcgcgatacgcttccgtcatctcaacggcactagctggcccctgaacatttgcctgcggatcccgggcaaaccacaattcgtttagatt
GIGYF_delta331-370_F	gtcgagttctaaaatatctcaaactgatctaaaacctatcaaaa
GIGYF_delta331-370_R	ttttgataggttttagatcagtttgagatattttagaactcgac
GIGYF_F361AF367A_F	atccatcgaaattgggtggcagtgctgatgctagtggagccgctcatggagatactgatctaaaacc
GIGYF_F361AF367A_R	ggttttagatcagtatctccatgagcggctccactagcatcagcactgccacccaatttcgatggat
GIGYF_W348A_F	gatgccgacgaaaatctacccgaagcggcaattgaaaatccatcgaaatt
GIGYF_W348A R	aatttcgatggattttcaattgccgcttcgggtagattttcgtcggcatc
GIGYF_W348AF361AF367A_F	gatgccgacgaaaatctacccgaagcggcaattgaaaatccatcgaaattgggtggcagtgctgatgctagtggagccgctcatggagatactgatctaaaacct
GIGYF_W348AF361AF367A_R	aggttttagatcagtatctccatgagcggctccactagcatcagcactgcccacccaatttcgatggattttcaattgccgcttcgggtagattttcgtcggcatc
HPat_P286AP287AF289A_site1_F	cacaacaagcgcagcacaaggtagccgctggcgccttgggcacgccgcacacctctcc
HPat_P286AP287AF289A_site1_R	ggagaggtgtgcggcgtgcccaaggcgccagcggctaccttgtgctgcgcttgttgtg
HPat_P328AP329AF331A_site2_F	ggtattggtggcaaccgagtggcggccggagctatttacccgcaaggtctgccc

HPat_P328AP329AF331A_site2_R	gggcagaccttgcgggtaaatagctccggccgccactcggttgccacca atacc

Table 3. Oligonucleotides used in KDs and in the generation of F-Luc and R-Luc northern blotting probes

Oligonucleotide name	Sequence (5' to 3')
T7_Neo_F	ttaatacgactcactatagggaggatgattgaacaagatggattgcacgc
T7_Neo_R	ttaatacgactcactatagggaggcgccaagctcttcagcaatatcacg
Me31B-T7F	taatacgactcactatagggaggatgatgactgaaaagtaa
Me31B-T7R	taatacgactcactatagggaggcttgactgttagtggaaat
T7_NOT1_F	taatacgactcactatagggagagctcactcagcatcgccatcg
T7_NOT1_R	taatacgactcactatagggagagtaggcgaaggccgacacaat
T7_F_GIGYF	ttaatacgactcactatagggagatgacagattcaatgaaatt
T7_R_GIGYF	ttaatacgactcactatagggagcgggtccgctcatggaaccg
T7_F_HPat	taatacgactcactatagggaggcgtgctgctgaagccgccaatccg
T7_R_HPat	taatacgactcactatagggaggctaatcaatttgatgcctggcttc
F-Luc probe_R	ccggaattcttacaatttggactttccgcc
R-Luc probe_R	ccctcgagttgttcatttttgagaactc

5.1.3 Antibodies

Table 4. Antibodies

Antibody	Source	Cat. number	Dilution
Anti-HA-HRP (Western blot)	Roche	12 013 819 001	1:5000
Anti-HA (Immunoprecipitation)	Covance	MMS-101P	1:150

Anti-GFP (Immunoprecipitation)	In house		1:150
Anti-GFP	Roche	11814460001	1:2000
Anti-rabbit-HRP	GE Healthcare	NA934V	1:10000
Anti-mouse-HRP	GE Healthcare	RPN4201	1:10000
Anti-V5	QED Bioscience Inc.	18870	1:5000
Anti-V5	LSBio LifeSpan BioSciences, Inc.	LS-C57305	1:5000
Anti-*Dm* Me31B	In house		1:3000
Anti-*Dm* HPat	In house		1:3000
Anti-*Dm* PABP	In house		1:5000
Anti-*Dm* NOT3	In house		1:3000
Anti-*Dm* DCP1	In house		1:2000

5.1.4 Solutions and reagents

Table 5. Solutions and reagents for DNA analysis

Name	Composition
TBE	89 mM Trizma base (Sigma), 88.9 mM boric acid (Merck), 2.5 mM ethylenediaminetetraacetic acid (EDTA; Merck)
Agarose gel	1% agarose dissolved in TBE, 0.003% Ethidium bromide (Roth)
5x DNA dye	20% Ficoll PM 400 (Sigma), 1 mM EDTA (Merck), 0.1% Sodium dodecylsulfate (SDS; Serva), 0.05% Bromophenol Blue (Sigma)
10x in-house Taq buffer	200 mM Trizma base-HCl pH 8.55 (Sigma), 160 mM ammonium sulfate (Merck), 0.1% Tween (Sigma), 20 mM magnesium chloride (Merck)
DNA ladder	20% 100 bp or 1 kbp DNA ladder (New England Biolabs, NEB), 20% 5x DNA dye, 60% 10 mM Trizma-HCl (Sigma), 1 mM EDTA (Merck)

Table 6. Solutions and reagents for RNA analysis

Name	Composition
5x DNase treatment buffer	400 mM HEPES-KOH pH 7.5 (Roth), 120 mM magnesium chloride (Merck), 10 mM Spermidine (Sigma), 20 mM Dithiothreitol (DTT; Biomol)
Agarose gel	1.2% agarose ultra-pure (Invitrogen) n 270 mL of MilliQ water (Merck) and MOPS
Glyoxal	60% Dimethylsulfoxide (DMSO; VWR), 50% deionised Glyoxal, 12% 10x MOPS, 6% Glycerol (Sigma)
RNA dye	95% deionized formamide, 0.05% SDS (Serva), 0.05% xylene cyanol FF (Sigma), 0.05% bromophenol blue (Sigma)
10x MOPS	200 mM 3-(*N*-morpholino) propanesulfonic acid (MOPS; Roth), 80 mM sodium acetate (Merck), 10 mM EDTA (Merck), pH 7 light-sensitive
20x SSC	3 M sodium chloride (Roth), 300 mM trisodiumcitrate dehydrate (Roth)
Northern blot Washing buffer	40 mM sodium phosphate pH 7, 1% SDS (Serva), 1 mM EDTA (Merck)
Sodium phosphate pH 7	Titrate 1 M di-sodium hydrogen phosphate (Roth) with 1 M sodium dihydrogen phosphate monohydrate (Merck) up to pH 7
Deionized Glyoxal	20 g AG 501-X8 mixed-bed resin (Bio-Rad) in 20 mL Glyoxal solution
Deionized formamide	5 g of AG 501-X8 mixed-bed resin (Bio-Rad) in 50 mL Formamide (Merck)

Table 7. Solutions and reagents for protein analysis

Name	Composition
NET buffer	50 mM Trizma base-HCl pH 7.5 (Sigma), 150 mM NaCl (Roth), 0.1 % Triton-X 100 (Merck), 1 mM EDTA pH 8 (Merck)
2x Protein sample buffer (2xPSB)	100 mM Trizma base-HCl pH 6.8 (Sigma), 4% (w/v) SDS (Serva), 20% Glycerol (Sigma), 200 mM DTT (Biomol), 0.05% Bromophenol Blue (Sigma)

1x PSB	50% 2x PSB, 200 mM Trizma base (Sigma)
8% Resolving gel	375 mM Trizma base pH 8.7 (Sigma), 26% Rotiphorese Gel 30 (Roth), 0.1% SDS (Serva), 0.5% Ammonium persulfate (10% w/v) (APS 10%; Sigma), 0.15% *N, N, N', N'*-Tetramethylenediamine (TEMED; Sigma).
Stacking gel	100 mM Trizma base pH 6.8 (Sigma), 16% Rotiphorese Gel 30 (Roth), 0.08% SDS (Serva), 0.5% APS 10% (w/v) (Sigma), 0.12% TEMED (Sigma)
Laemmli buffer	3.5 mM SDS (Serva), 0.19 mM Glycin (Roth), 24.8 mM Trizma base (Sigma) in deionized water
Wet transfer buffer	20 mM Trizma base (Sigma), 149 mM Glycin (Roth), 0.1% SDS (Serva), 20% Methanol (Roth) in deionized water
PBS	10 mM Na_2HPO_4 (Roth), 1.8 mM Potassium dihydrogen phosphate (Merck), 0.137 M NaCl (Roth), 2.7 mM KCl (Merck)
Western blot Blocking buffer	PBS, 0.3% Tween20 (Sigma), 5% w/v Skimmed milk powder (Reform)
Western blot Washing buffer	PBS, 0.3% Tween20 (Sigma)
Detection solution A	2 mM Luminol (light-sensitive; Roth), 100 mM Trizma base-HCl pH 8.6 (Sigma)
Detection solution B	7 mM *p*-Coumaric acid (Sigma) dissolved in DMSO (VWR)
Detection solution mix	90% detection solution A, 10% detection solution B, 0.01% Hydrogen peroxide 35% (Sigma)
Coomassie stain	45% Methanol (Roth), 10% Acetic acid (Merck), 0.1% w/v Brilliant Blue R-250 (Thermo Fischer)
Coomassie destaining	25% Isopropanol (Roth), 10% Acetic acid (Merck)
Lysis buffer Pulldown for *E. coli*	50 mM sodium phosphate buffer (pH 7.0), 200 mM NaCl (Roth), 2 mM DTT (Biomol), 5 µg/ml DNAse I, 1 mg/ml Lysozyme, cOmplete™ Protease Inhibitor (Roche)
Pulldown buffer for *E. coli*	20 mM sodium phosphate buffer (pH 7.0), 200 mM NaCl (Roth), 2 mM DTT (Biomol).

crystallization solution (initial crystal)	0.1 M sodium acetate (pH 5.0) (Sigma), 0.2 M ammonium chloride (Sigma) and 20% PEG 6000 (Sigma).
crystallization solution (optimization crystal)	0.1 M sodium acetate (pH 5.0) (Sigma), 0.15 M ammonium chloride (Sigma) and 16% PEG 6000 (Sigma).

5.1.5 Media for cell culture

Table 8. Cell culture media

Cells	Media
Schneider S2	Schneider's *Drosophila* powder (Serva Electrophoresis) supplemented with 10% Foetal Calf Serum (FCS - Thermo Fischer) and with 1:200 Penicillin/Streptomycin (Gibco)
TOP10 and DH5α	LB media: 0.5% w/v Yeast extract (Roth), 1% w/v Peptone ex casein (Roth), 85 mM NaCl (Roth)
BL21 Star™ (DE3)	TB media: 2.4% w/v Yeast extract (Roth), 1.2% w/v tryptone (Roth), Glycerol 86-89% (Sigma), 0.17M KH_2PO_4 (Merck), 0.72M K_2HPO_4,

5.1.6 Enzymes

Table 9. Enzymes

Type	Enzymes
Polymerases	Taq polymerase (lab-made), *Pfu* DNA Polymerase (Thermo Fischer and Promega), Phusion® High-Fidelity DNA polymerase (Thermo Scientific)
Restriction enzymes	SacII, FastDigest SalI, FastDigest XbaI, FastDigest BspTI, FastDigest DpnI (Thermo Fischer)
Other DNA modifying enzymes	RevertAid H Minus Reverse Transcriptase (Thermo Fischer), T4 DNA Ligase (Thermo Fischer), FastAP Thermosensitive Alkaline Phosphatase (Thermo Fischer), TOPO TA cloning (Invitrogen)
Enzymes for RNA studies	DNaseI RNase-free (Thermo Fischer), RNase H (NEB), RiboLock RNase Inhibitor (Thermo Fischer)

Enzymes for protein studies	Lysozyme (Sigma), DNaseI (Roche), RNase A (Qiagen)

5.2 Methods

5.2.1 PCR, restriction digestion, and ligation

DNA template was amplified by Phusion® HF DNA polymerase (Thermo Fischer) according to manufacturer instructions. A standard PCR reaction contains 50 ng of DNA template, 10 mM dNTPs, 5X buffer PCR, 20 μM of specifically designed oligonucleotides (forward and reverse) and 0.5 μM Phusion® HF DNA polymerase in a final reaction volume of 50 μl.

Table 10. Standard PCR cycles

Step	Temperature (°C)	Time	Cycles
Initial denaturation	98	30s	1
Denaturation	98	10	30
Annealing	Primers melting temperature	30	
Elongation	72	30s/kbp	
Final elongation	72	10m	1
storage	4		

The PCR product was separated on an agarose gel, visualized with UV light on a Quantum Gel Documentation Imager (Vilber), and purified with GeneJET Gel Extraction kit (Thermo Fischer Scientific). The purified PCR product and vector were digested using the appropriate FastDigest restriction enzymes (1μl) per 30 minutes at 37°C. The vector was treated with FastAP and subsequently inactivated at 75°C for 5 minutes. The digested vector, five times in excess, was mixed with the digested PCR product, the T4 DNA Ligase buffer, and 1 μL of T4 DNA ligase (5 U/μl) in a total volume of 20 μL and incubated over night at 22°C. Successful DNA cloning was verified with a control test digestion and UV light-based visualization of ethidium bromide stained PCR insert after agarose gel electrophoresis.

5.2.2 Site-directed mutagenesis

Mutations, insertions, and deletions were obtained by PCR amplification using the *Pfu* polymerase and a specific set of oligonucleotides containing the desired mutation according to the manufacturer's protocol (Stratagene). The PCR product was treated with DpnI enzyme at 37°C for 3 hours to digest template DNA.

5.2.3 Transformation, plasmid extraction, and sequencing

Transformation of chemically competent DH5α or TOP10 *E. coli* cells was performed by adding the plasmid of interest to the cells, incubating on ice for 20 minutes, followed by heat shock at 42°C for 45 s and again on ice for 2 minutes. Cells were then incubated in 700 μL of media at 37°C with 700 rpm shaking for 30 minutes and finally plated in agar media supplemented with the appropriate antibiotic. After an overnight incubation at 37°C, single colonies were picked and inoculated into 3 ml of selective liquid media and grown overnight at 37°C. Plasmid DNA was extracted using QIAGEN® Plasmid Mini kit according to the manufacturer's protocol. Colonies were analysed by test digestion and sequencing reaction, which was performed with the BigDye™ Terminator v3.1 Cycle Sequencing Kit (Thermo Fischer) and ran at the Genome centre of the Max Planck Institute for Developmental Biology, Tübingen. Positive colonies were incubated in 100 ml media containing the appropriate antibiotic and the plasmid DNA extracted with *Plus* Midi kit or the QIAfilter Plasmid Midi kit. DNA concentration was finally measured with the NanoDrop ND-1000 (PeqLab).

5.2.4 S2 cells transfection

Drosophila S2 cells were transfected using the Effectene Transfection Reagent QIAGEN® according to manufacturer's instructions, seeded at a concentration of 2.5×10^6 cells/ml in a 6-wells plate and transfected with the desired plasmids. Cells were incubated at 25°C and collected the third day after transfection and processed according to the planned experiment.

Tethering assays (section 5.2.7) transfections were performed in a 6-wells plate. The amount of DNA transfected was as follow:

- 0.1 µg of F-Luc reporters (F-Luc-5BoxB, F-Luc-V5, F-Luc-5BoxB-$A_{95}C_7$-HhR);
- 0.4 µg of R-Luc-A_{90}-HhR reporter;

- 0.05 µg of WT λN-HA-4EHP;
- 0.08 µg D* λN-HA-4EHP;
- 0.05 µg S* and CAP* λN-HA-4EHP;
- 0.01 µg of WT, C-term, C*, GYF*, C*+GYF*, ΔMBM, and ΔMBM+GYF* λN-HA-GIGYF for F-Luc-5BoxB and F-Luc-V5 experiments, while half of the amount were used for the F-Luc-5BoxB-$A_{95}C_7$-HhR reporter;
- 0.005 µg of N-term λN-HA-GIGYF for F-Luc-5BoxB and F-Luc-V5 experiments, while half of the amount were used for the F-Luc-5BoxB-$A_{95}C_7$-HhR reporter;
- 0.01 µg λN-HA-GW182;
- 0.025 µg GFP-V5;
- 1.0 µg V5-tagged HA-DCP1 GSSG-mutant;
- 0.03 µg dsR GIGYF WT, C*, and ΔMBM+GYF*.

5.2.5 Knock downs

Knock down (KD) of specific proteins in S2 cells was performed by mixing $7.5x10^6$ cells with 50 µl of appropriate double strand RNA (dsRNA) (3 µg/µl) and incubated for two hours at 25°C in 3 ml of serum-free media. 3 ml of 2X serum-supplemented media was added and cells were incubated at 25°C for four days. In the fourth day, new dsRNA was added as described before. At the seventh day, cells were seeded for transfection as described previously (section 5.2.4). Cells were collected and used to determine KD efficiency or subjected to transfection.

700 bp long dsRNAs were obtained by standard PCR amplification using cDNA of the target gene (Neomycin, GIGYF, NOT1, HPat, and Me31B) cloned in a vector and specific primers carrying the T7 promoter sequence followed by 20 nucleotides of the target gene (5'-TTAATACGACTCACTATAGGGAGA-3'). PCR amplicon DNA was purified with the GeneJET Gel Extraction kit (Thermo Fischer Scientific) according to the manufacturer's protocol. The purified DNA was transcribed using homemade T7 RNA polymerase, as shown in Table 11, and incubated overnight at 37°C.

Table 11. *in vitro* transcription

5x buffer	20 µl
25 mM rNTPs	30 µl
cDNA	5 µg
T7 RNA polymerase	10 µl
H_2O	up to 100 µl

The newly transcribed RNA was treated with 2 U of DNAseI in the appropriate buffer (Thermo Fischer Scientific) and incubated 1 hour at 37°C. Subsequently, 100 µL of RNase-free MilliQ water and 200 µL of Phenol:Chloroform:Isoamylalcohol (25:24:1) (ITW Reagents) were added and the RNA solution was vortexed for 30 seconds. After centrifugation at 13000 rpm for 30 minutes at 4°C, the upper phase of the RNA sample was transferred to a solution containing 20 µL of 3 M sodium acetate pH 5.2 and 600 µL of pure ethanol (Merck) and precipitated for 1 hour at -20°C. The RNA was pelleted for 30 minutes 13000 rpm at 4°C and washed with 75% ethanol (Merck). The RNA was dissolved in 200 µL of RNAse-free MilliQ water by shaking at 80°C for 5 minutes. Subsequently, it was placed in a warm bath water at 80°C that cooled down to 30°C at room temperature. RNA concentration was measured with NanoDrop ND-1000-coefficient factor 45 (PeqLab) and the concentration was adjusted to 3µg/µl with RNAse-free MilliQ water.

The dsRNA resistant version of HA-GIGYF (WT, C*, and ΔMBM+GYF*) was obtained by inserting a nucleotide modified sequence, resistant to the action of the corresponding dsRNA, in the CDS of GIGYF via site-directed mutagenesis. The modified nucleotide sequence has of silent point mutations of every third base of GIGYF sequence.

5.2.6 mRNA half-life assay

To determine the mRNA half-lives, cells were collected three days after transfection and treated with actinomycin D (5 µg/ml final concentration) and collected at the indicated time points for tethering assay and Northern blot. The stable ribosomal *rp49* mRNA was used as control. The mean value of three experiments was plotted in a time-dependent graph and the fitting curves were determined with the Levenberg-Marquardt algorithm for single exponential decay

functions. The R^2 values associated with the fitting curves were calculate with SciDAVis program.

5.2.7 Tethering assay

Dual-Luciferase® Reporter Assay system (Promega) is based on the measuring of light production from two luciferase enzymes, F-Luc (firefly luciferase, from *Photinus pyralis*) and R-Luc (*Renilla* luciferase from *Renilla reniformis*), detected in a Centro LB 960 Mikroplatten Luminometer (Berthold Technologies) (Gehring et al., 2005). The ORFs for the two luciferases were cloned in different expression vectors and were always transfected together. The λN-HA/BoxB system from phage λ was employed: the F-Luc vector contained five repeats of the BoxB RNA element in the 3' UTR of the reporter. The λN peptide, which was fused to the N-terminal region of a protein of interest, recognizes with high affinity the BoxB elements (Fig. 6). The R-Luc vector was employed as normalization control because it did not contain BoxB elements and is not affected by the expression of the fusion protein. λN-HA was expressed as a control and the ratio of the F-Luc/R-Luc values were set to 100%. The same samples used for measuring the luciferase activity were analysed by Northern blot and the mRNA steady state levels were quantified as described in section 5.2.9. In addition, the expression levels of all tethered proteins were analysed by Western blot.

Different F-Luc reporters were used in this work. The F-Luc-5BoxB reporter (Fig. 6 A) has a cleavage/polyadenylation site that allows the expression of a polyadenylated mRNA used to determine effects at the protein and mRNA levels. The F-Luc-5BoxB-A_{96}-HhR (Fig. 6 B) contains at the 3'-end a stretch of 96 adenosines followed by the hammerhead ribozyme (HhR) sequence, to analyse effects on the reporter expression only at the protein/translation level. To exclude possible trans effects of the protein of interest on the reporter mRNA expression, an F-Luc vector lacking of the BoxB elements was used (F-Luc-V5; Fig. 6 C).

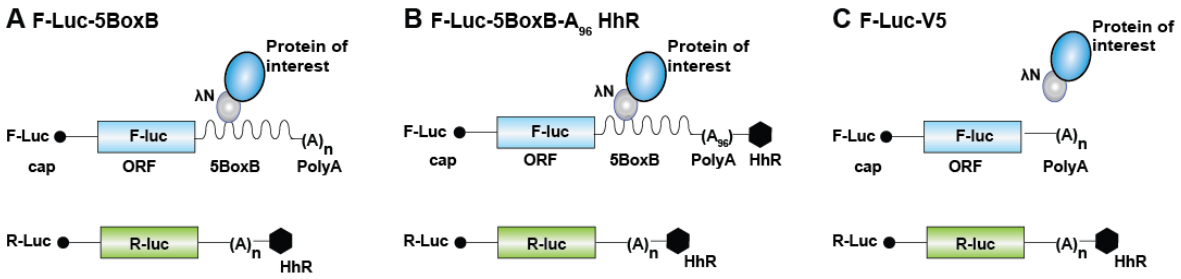

Figure 6. Schematic representation of the tethering assay
(A-C) The tethering assay is a luciferase-based reporter assay where the production of light of two different enzymes, the F-Luc and transfection control R-Luc, are measured in a luminometer instrument, in the presence or absence of the protein of interest. The R-Luc vector includes the ORF for the *Renilla* luciferase enzyme (green rectangle) followed by the hammerhead ribozyme (HhR) sequence (black hexagon). The protein of interest (blue circle) fused to the λN peptide (grey circle) binds to the reporter mRNAs containing 5BoxB elements in the 3' UTR. **(A)** The F-Luc-5BoxB reporter includes the ORF of the firefly luciferase (blue rectangle) and the BoxB RNA element (repeated five times) followed by a polyA tail (A_n). **(B)** The F-Luc-5BoxB-A_{96}-HhR includes the ORF of the firefly luciferase, the BoxB RNA element (repeated five times), an internal polyA stretch and the HhR sequence. **(C)** The F-Luc-V5 reporter contains the ORF of the firefly luciferase and lacks the BoxB RNA element.

5.2.8 RNA extraction

Cells collected for RNA extraction were resuspended in TRIzol™ Reagent (Thermo Fischer). RNA extraction was performed according to the manufacturer's recommendations. To degrade possible plasmid DNA present upon cell transfection, the RNA was then treated with 2 U of DNAseI in the appropriate DNAseI buffer (Thermo Fischer) containing 20 U of RiboLock RNAse Inhibitor (Thermo Fischer) and incubated one hour at 37°C. Subsequently, 150 μL of RNase-free MilliQ water and 200 μL of Phenol:Chloroform:Isoamylalcohol (25:24:1) (ITW Reagents) were added and the samples were vortexed for 30 seconds. After centrifugation at 13000 rpm for 30 minutes at 4°C, the upper-phase of the solution was transferred to into a tube containing 20 μL of sodium acetate 3 M pH 5.2 and 600 μL of pure ethanol (Merck), and precipitated for one hour at -20°C. The RNA was pelleted via centrifugation for 30 minutes at 13000 rpm and 4°C, washed with 75% ethanol (Merck) and dissolved in 11 μL of RNAse-free MilliQ water. RNA concentration was measured with NanoDrop ND-1000 (PeqLab).

5.2.9 Northern blot

RNA samples mixed with glyoxal solution and RNA dye were loaded on a 1.2% agarose gel soaked in 1X MOPS buffer. The RNA was transferred to a nylon membrane (GeneScreen Plus, NEN Life Sciences) soaked in 10X MOPS buffer. The transfer chamber consists of a big container filled with 10X MOPS buffer and a glass plate that serves as a support of the gel. Rotilabo® blotting paper 0.35 mm thick (Roth) soaked in 10X MOPS was used as a bottom part of a sandwich, consisting of the agarose gel with RNA samples and the nylon membrane that directly contacts the gel. On top of the membrane two Rotilabo® blotting paper 0.35 mm thick (Roth) soaked in 2X MOPS were placed and ten non-soaked blotting papers. RNA transfer was performed overnight and subsequently the RNA was crosslinked to the membrane by UV (120 mJ/cm^2, Stratalinker UV crosslinker, Stratagene) and saturated in the presence of sonicated salmon sperm DNA 0.1 /L in Church buffer for one hour at 65°C. ^{32}P-radiolabelled single stranded DNA specific probes (complementary to F-Luc and R-Luc ORFs) were added to the solution in which the membrane is soaked and hybridized overnight. The membrane was washed five times for 1 hour with washing buffer and the radioactive signal was exposed onto a GE Storage Phosphor Screen (Fujifilm). After 2 days of exposure, the signal was detected in a STORM 860 Imager (Molecular Dynamics) or the Amersham Typhoon RGB Biomolecular Imager and quantified with the ImageQuant TL program (GE Healthcare).

^{32}P-labelled specific DNA probes were generated by standard PCR in the presence of α-^{32}P-labelled dATP and α-^{32}P-labelled dCTP and a reverse primer, specific for the amplification of F-Luc or R-Luc in order to generate a single strand DNA probe. The radioactively labelled PCR product was purified by centrifugation using Sephadex G50 beads (Sigma) and Silanized Glass Wool (Sigma). The purified probe was immediately used for RNA membrane hybridization.

5.2.10 Immunoprecipitation assay

Co-immunoprecipitation assays were performed three days after transfection of the plasmid encoding for the protein of interest in 2.5x10^6 S2 cells /ml in a 6-wells plate (two wells for each sample). Cells were collected, washed in cold PBS and resuspended in 500 μl of NET buffer supplemented with 10% glycerol (Sigma) and

cOmplete™ Protease Inhibitor (Roche). Subsequently, cells were sonicated in a water bath (Bandolin Sonorex) three times for 30 seconds and treated with 2 μl of RNAseA 7000 U/ml (Qiagen) for 30 minutes at 4°C. After centrifuging for 15 minutes at 13000 rpm, 50 μL of the supernatant were collected as input samples and mixed with 50 μL of protein sample buffer (PSB). The remaining supernatant was mixed with 3 μl of polyclonal anti-GFP or polyclonal anti-HA antibodies (Covance) and incubated at 4°C for one hour on a wheel. The anti-GFP antibody was immunoprecipitated by adding 50 μl of Gammabind G Sepharose® (GE Healthcare) and incubated for one hour at 4°C. The beads were washed three times with NET buffer supplemented with 10% glycerol (Sigma) and cOmplete™ Protease Inhibitor (Roche) and one last time with NET buffer and finally resuspended in 100 μl of 2x PSB.

5.2.11 Western blot

Proteins resuspended in PSB were heat denatured at 95°C and separated on an SDS-polyacrylamide gel electrophoresis (PAGE) together with a protein ladder (Thermo Fischer). The proteins were then transferred onto a nitrocellulose membrane (Santa Cruz Biotechnology) by applying for three hours a 55 V current to the gel-membrane sandwich formed between sponges and blotting paper soaked with blotting buffer and immerged in a transfer chamber filled with transfer buffer. The membrane was then incubated for one hour in a 5% milk blocking solution. The primary antibody was then added to the membrane overnight at 4°C. Next, the membrane was washed three times in PBS buffer and incubated for one hour with the secondary antibody. Detection ECL solution was applied to the membrane and chemiluminescence was detected by the Fusion FX from Vilber Lourmat.

5.2.12 Protein expression from *E. coli* and purification

The GST-tagged RecA2 domain of *D. melanogaster* Me31B used for crystallization or for *in vitro* pull-down assays was expressed in *E. coli* BL21 (DE3) Star cells (Invitrogen) grown in suspension at 37°C in TB medium at 180 rpm in a Multitron Standard incubator (Infors-HT) till an OD_{600} of 0.6. The temperature was dropped to 20°C and cells were induced with 0.5 mM IPTG (Roth). Cells were harvested approximately 18 hours after induction, lysed by sonication in lysis buffer

supplemented with DNaseI (5 µg/ml), lysozyme (1 mg/ml) and cOmplete EDTA-free Protease inhibitor cocktail (Roche). Cells were purified using Protino® Glutathione Agarose 4B (Macherey-Nagel). For crystallization purposes, the GST-tag was cleaved with HRV3C protease overnight at 4°C. Subsequently the protein was purified using a heparin column (HiTrap Heparin HP 5ml, GE Healthcare) and eluted from the column using an increasing salt gradient. The buffer was finally exchanged to 10 mM HEPES (pH7.2), 200 mM NaCl, 2 mM DTT using a VivaSpin 20 centrifugal concentrator (Sartorius; 10000 MWCO) and the protein was stored at -80°C.

5.2.13 Protein crystallization

For crystallization, 500 µM of purified Me31B-RecA2 domain (E266-N435) was mixed with 750 µM synthetic GIGYF peptide (synthesized by EMC microcollections GmbH), in order to have a molar excess of the peptide. The sitting-drop vapor diffusion method was used to obtain the initial crystals that appeared at 20°C three days after mixing the protein complex solution and the crystallization solution consisting of 0.1 M sodium acetate (pH 5.0), 0.2 M ammonium chloride and 20% PEG 6000. Consecutive rounds of microseeding were performed to optimise the crystals in a final buffer with 0.1 M sodium acetate (pH 5.0), 0.15 M ammonium chloride and 16% PEG 6000. The crystals were grown at 18°C using hanging-drop vapor diffusion and soaked in mother liquor supplemented with 15% glycerol for cryoprotection before flash-freezing.

5.2.14 Crystal data collection and structure determination

Data of the Me31B-GIGYF crystals were collected at a wavelength of 0.99961 Å at 100K on a PILATUS 6M detector at the PXII beamline of the Swiss Light Source. XDS and XSCALE were used to process and scale the diffraction data respectively (Kabsch, 2010). PHASER was used to solve the structure by molecular replacement (McCoy et al., 2007). *Hs* DDX6 RecA2 domain structure (PDB 5ANR) was used as a search model (Ozgur et al., 2015). Because the data showed a strong anisotropy, the data were further submitted to STARANISO server (http://staraniso.globalphasing.org/cgi-bin/staraniso.cgi). In addition, the anisotropic scaling and B-factor sharpening were also used to correct for the diffraction anisotropy. COOT (Emsley et al., 2010) was used for the cycles of model building

and PHENIX (Afonine et al., 2012) was used for refinement of the structure. GIGYF chain was built manually into the difference density in COOT and further refined with PHENIX.

5.2.15 *in vitro* pull-down assay

50 μg of purified GST-Me31B-RecA2 domain was mixed with glutathione agarose beads (Macherey-Nagel) for 30 minutes at 4°C on a rotating wheel and then washed five times with washing buffer. MBP-tagged GIGYF fragment (348-360 AA) was expressed in bacteria and the lysate was added to the GST-Me31B-RecA2-coupled beads. The samples were then incubated 30 minutes at 4°C on a rotating wheel and subsequently washed five times with washing buffer. The elution step was performed by adding glutathione 25mM to the mix for 15 minutes at 4°C and centrifuged at 10000 rpm. The supernatant was mixed with 5X PSB. Samples were analysed by SDS-PAGE and stained with Coomassie blue stain solution and washed with Coomassie destaining solution.

6 Results

6.1 4EHP requires GIGYF to promote mRNA degradation

6.1.1 4EHP interacts with GIGYF, via a conserved tripartite binding mode

4EHP is a cap-binding protein that interacts with GIGYF and represses translation of an mRNA target. Human GIGYF1/2 proteins bind to three distinct surfaces of 4EHP as shown in Fig. 4 (Chapat et al., 2017; Fu et al., 2016; Morita et al., 2012; Peter et al., 2017). To obtain detailed molecular knowledge on the control of mRNA expression by the 4EHP/GIGYF repressor complex, I studied the uncharacterised *Dm* 4EHP/GIGYF complex.

To confirm that *Dm* GIGYF and *Dm* 4EHP (from now on GIGYF and 4EHP, respectively) interact in Schneider S2 *Drosophila* cells (S2), I performed an anti-HA co-immunoprecipitation assay (see 5.2.10 for full protocol), with overexpressed HA-tagged GIGYF and GFP-tagged 4EHP (Fig. 7 A). To exclude any unspecific binding to GFP-4EHP, I used as a negative control the HA-tagged maltose binding protein (MBP). The input fractions of the experiment show the similar expression levels of the tested proteins (Fig. 7 A, lane 1-5). Indeed, GIGYF immunoprecipitated 4EHP in *Dm* cells (Fig. 7 A, lane 7 versus 6) and the binding between the two proteins occurred in the 4EHP-binding region, since mutations on the canonical motif (GIGYF C*, Y58A Y60A M65A), and not in the GYF domain (GYF*, F582A W590A F596A), abolished the interaction (Fig. 7 A, lane 8 and 10 versus 9).

Based on the structure of the human 4EHP/GIGYF1/2 complexes (Peter et al., 2017) and sequence alignment of the 4EHP-binding region of GIGYF orthologues, I generated GIGYF proteins carrying amino acid substitutions in the three 4EHP-binding motifs (Fig. 4): C* (Y58A Y60A M65A), non-canonical (NC*, L79A F82A L85A), and auxiliary sequence (A*, P93D L94A). The mutations were inserted in an N-terminal (N-term; 1-640 AA) fragment of HA-GIGYF which was then used in co-immunoprecipitation assays to assess the interaction with 4EHP (Fig. 7 B). This experiment showed that the N-term of GIGYF is sufficient for the interaction and that each of these binding motifs is necessary for the interaction with 4EHP (Fig. 7 B, lane 8, 9, and 10 versus 7). HA-MBP was used as negative control. Alternatively, I also generated 4EHP proteins with amino acid substitutions in

conserved residues of the dorsal (D*, W85A), lateral (L*, V75A L91A) and 4EHP-specific (S*, R93P E148L) surfaces. In co-immunoprecipitation assays, overexpressed GFP-tagged 4EHP efficiently immunoprecipitated HA-tagged GIGYF N-term (Fig. 7 C, lane 7), while the 4EHP mutants failed to interact with GIGYF (Fig. 7 C, lane 8-10). These results indicate that GIGYF addresses all the three surfaces of 4EHP to establish a tripartite binding mode. In this experiment, GFP-MBP has been used as a negative control for the interaction with 4EHP (Fig. 7 C, lane 6).

Since, 4EHP is a cap-binding protein that interacts with different partners and mediates translational repression (Chapat et al., 2017; Cho et al., 2005; Peter et al., 2017; Rosettani et al., 2007), I also investigated whether a HA-4EHP mutant that does not bind the cap structure (CAP*), still associated with GFP-GIGYF (Fig. 7 D). As expected, the mutation in the cap-binding pocket did not affect the interaction with GIGYF (Fig. 7 D lane 8 and 6). GFP-F-Luc was used as a negative control and did not bind to HA-4EHP (Fig. 7 D lane 7 and 5). Taken together the co-immunoprecipitation experiments confirmed that GIGYF efficiently interacts with 4EHP in S2 cells using a conserved tripartite binding mode.

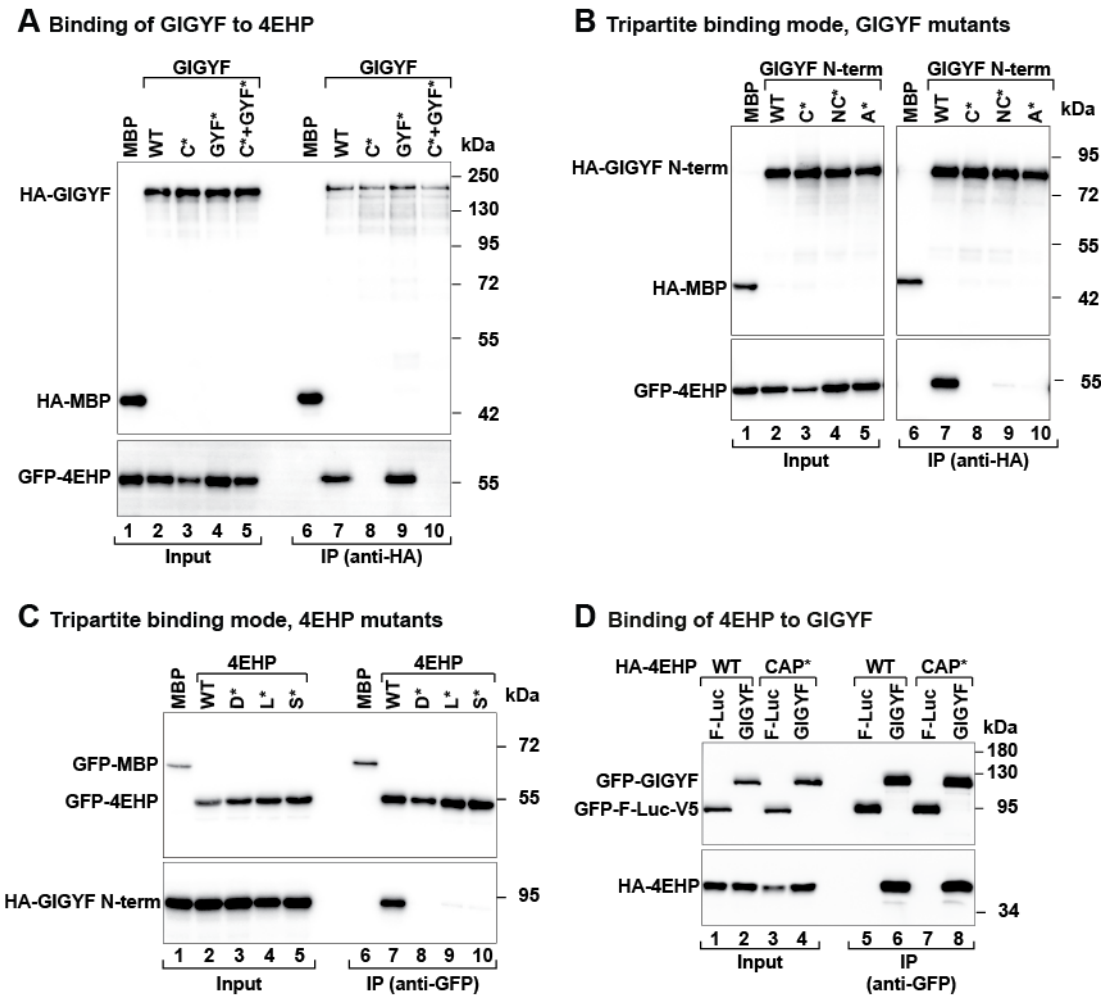

Figure 7. 4EHP interacts with GIGYF using a tripartite binding mode

(A) Immunoprecipitation assay displaying the interaction of HA-GIGYF, WT or the indicated mutants (canonical: C*, GYF domain: GYF*, and double mutant: C*+GYF*), with GFP-4EHP. The proteins were immunoprecipitated using an anti-HA antibody. HA-MBP served as a negative control. The input (0.5%) and bound fractions (35%) were analysed by WB using anti-HA and anti-GFP antibodies. **(B)** Immunoprecipitation assay displaying the interaction between HA-GIGYF N-term or the indicated HA-GIGYF N-term mutants (canonical: C*, non-canonical: NC*, and Auxiliary sequence: A*) and GFP-4EHP. The proteins were immunoprecipitated using an anti-HA antibody. HA-MBP served as a negative control. The input (2%) and bound fractions (30%) were analysed by WB using anti-HA and anti-GFP antibodies. **(C)** Immunoprecipitation assay displaying the interaction between GFP-4EHP, WT or the indicated mutants (dorsal: D*; lateral: L* and 4EHP-specific: S*), and HA-GIGYF N-term (residues 1-640). The proteins were immunoprecipitated using an anti-GFP antibody. GFP-MBP served as a negative control. The input (2.8%) and bound fractions (10%) were analysed by WB using anti-GFP and anti-HA antibodies. **(D)** Immunoprecipitation assay showing the interaction between GFP-GIGYF and HA-4EHP (WT or CAP* mutant). GFP-F-Luc-V5 served as a negative control. The input (3% for GFP-tagged proteins and 1% for HA-tagged proteins) and bound fractions (15% for GFP-tagged proteins and 20% for HA-tagged proteins) were analysed by WB using anti-HA and anti-GFP antibodies.

6.1.2 GIGYF is the main 4EHP-binding protein in S2 cells

4EHP-interacting partners have been characterised in different species, including fly, mouse, and human, and are relevant in different biological processes, especially during *Dm* embryogenesis (Cho et al., 2006; Cho et al., 2005; Kubacka et al., 2013). To determine if these interactions are maintained in S2 cells, I performed co-immunoprecipitation assays in cells overexpressing 4EHP and the different known partners, namely 4E-T, Brat, and Bicoid (Fig. 8 A, B, and C) and (Cho et al., 2006; Cho et al., 2005; Kubacka et al., 2013). Interestingly, none of the reported 4EHP-interacting proteins were efficiently detected as binding partners. In each of these assays GIGYF or eIF4E were employed as positive control. Moreover, a negative control, GFP-F-Luc-V5 or HA-MBP, allowed to exclude the possibility of unspecific interactions. These unexpected results indicate that in *Dm* S2 cells GIGYF appears to be the main 4EHP-binding protein.

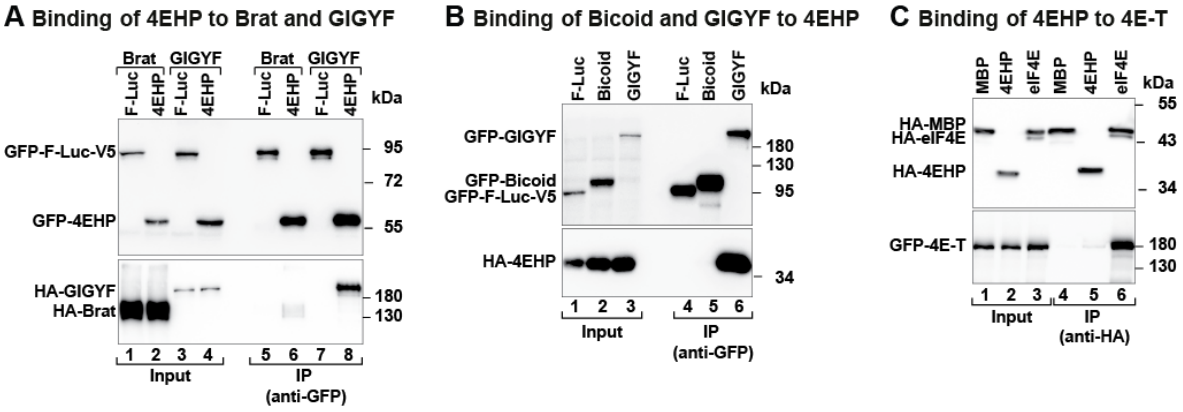

Figure 8. 4EHP efficiently interacts with GIGYF
(A) Anti-GFP immunoprecipitation assay showing the interaction between GFP-4EHP and HA-Brat or the positive control HA-GIGYF. GFP-F-Luc-V5 served as a negative control. The input (3% for GFP-tagged proteins and 1% for HA-tagged proteins) and bound fractions (15% for GFP-tagged proteins and 30% for HA-tagged proteins) were analysed by WB using anti-HA and anti-GFP antibodies. **(B)** Anti-GFP immunoprecipitation assay showing the interaction between GFP-Bicoid with HA-4EHP. GFP-GIGYF served as a positive control and GFP-F-Luc-V5 as a negative control. The input (3% for GFP-tagged proteins and 1% for HA-tagged proteins) and bound fractions (15% for GFP-tagged proteins and 30% for HA-tagged proteins) were analysed by WB using anti-HA and anti-GFP antibodies. **(C)** Anti-HA immunoprecipitation assay displaying the interaction between HA-4EHP and GFP-4E-T. HA-eIF4E served as positive control and HA-MBP as a negative control. The input (1.5% for HA-tagged proteins and 1% for GFP-tagged proteins) and bound fractions (25% for HA-tagged proteins and 30% for GFP-tagged proteins) were analysed by WB using anti-HA and anti-GFP antibodies.

6.1.3 4EHP requires GIGYF to repress mRNA expression

To determine the functional significance of the 4EHP-GIGYF interaction, I employed a luciferase-based tethering assay. In this assay, an mRNA reporter (F-Luc-5BoxB) containing an open reading frame coding for the firefly luciferase (F-Luc) enzyme and five copies of the RNA element BoxB hairpins (5BoxB) at the 3' UTR, is expressed in S2 cells. The BoxB hairpins of the reporter are recognized with high affinity by the λN peptide (λN) (Gehring et al., 2005) which is co-expressed in the cells fused to a protein of interest. Hence, in the tethering assay, a protein of interest is physically anchored to the 3' UTR of the F-Luc-5BoxB reporter, bypassing and mimicking its recruitment to an mRNA. To monitor possible changes in F-Luc expression upon tethering of a specific protein, the luciferase activity is directly measured on a luminometer.

In addition, a F-Luc reporter lacking the 5BoxB hairpins (F-Luc-V5) is used as a negative control to ensure that the overexpression of the λN-fusion protein as no effect on reporter mRNA expression in the absence of tethering. A second luciferase reporter lacking the 5BoxB elements, *Renilla* luciferase (R-Luc), is also used as transfection control. Moreover, the expression of the F-Luc reporter is analysed upon tethering of the HA-tagged λN-peptide (λN-HA), and the ratio between the F-Luc and R-Luc activities is taken as a reference and set to 100%. In the tethering assay, measurement of luciferase activity (protein levels) and F-Luc mRNA steady-state levels via Northern blot analysis (NB) are a direct assessment of the ability of a protein of interest to regulate translation and stability of the reporter mRNA.

Interestingly, tethering of λN-HA-4EHP to the F-Luc-5BoxB reporter resulted in a strong reduction of F-Luc activity and F-Luc mRNA levels, compared to the λN-HA control (Fig. 9 A and B). In the presence of λN-HA-4EHP, F-Luc activity was reduced to 20% and mRNA levels to 40%, compared to λN-HA alone (Fig. 9 A and B, green and blue bars respectively). In addition, this experiment suggested that 4EHP not only induces mRNA decay, as shown by the reduction of mRNA level to 40%, but also determine an additional repressive effect on translation activity, since the F-Luc activity was reduced to 20% (Fig. 9 A and B).

To test the importance of the interaction of 4EHP with GIGYF or with the cap in the regulation of mRNA expression, I tethered the D* and the CAP* mutants

of 4EHP to the F-Luc-5BoxB reporter. Intriguingly, the 4EHP D* mutant, that is unable to interact with GIGYF (Fig. 7 C), was strongly impaired in the ability to reduce F-Luc activity and mRNA levels, compared to WT 4EHP (Fig. 9 A and B). This data indicates that the interaction with GIGYF is essential in 4EHP-mediated translational repression and mRNA decay. Conversely, anchoring the 4EHP CAP* mutant to the mRNA reporter strongly repressed F-Luc activity, suggesting that tethering of 4EHP bypasses its cap binding properties (Fig. 9 A and B). The λN-HA-4EHP WT and mutant proteins did not affect the expression of a F-Luc reporter lacking the 5BoxB hairpins and were expressed at a similar level (Fig. 9 C and D).

To better characterise the role of GIGYF in 4EHP-mediated mRNA repression and to exclude the possibility that other not yet identified 4EHP-binding partners may influence its function, I tethered 4EHP in cells deprived of endogenous GIGYF. To reduce GIGYF expression in S2 cells, I performed knock down (KD) experiments with dsRNA designed to target endogenous GIGYF mRNA. As control, I used a dsRNA directed against the neomycin coding sequence. As there are no antibodies against *Dm* GIGYF, I estimated the efficiency and specificity of the knockdown by analysing the expression of HA-tagged GIGYF in cells treated with dsRNA targeting either neomycin as the control (Ctrl) or the *Dm* GIGYF mRNA (Fig. 9 E). The tethering assay in cells depleted of GIGYF, revealed that the 4EHP (WT and CAP*)-mediated mRNA repression was strongly compromised and affected F-Luc activity and mRNA levels (Fig. 9 A and B). All the 4EHP proteins were expressed at comparable levels (Fig. 9 F). Taken together, these experiments indicated that 4EHP represses translation and promotes degradation of mRNA target in a GIGYF-dependent manner.

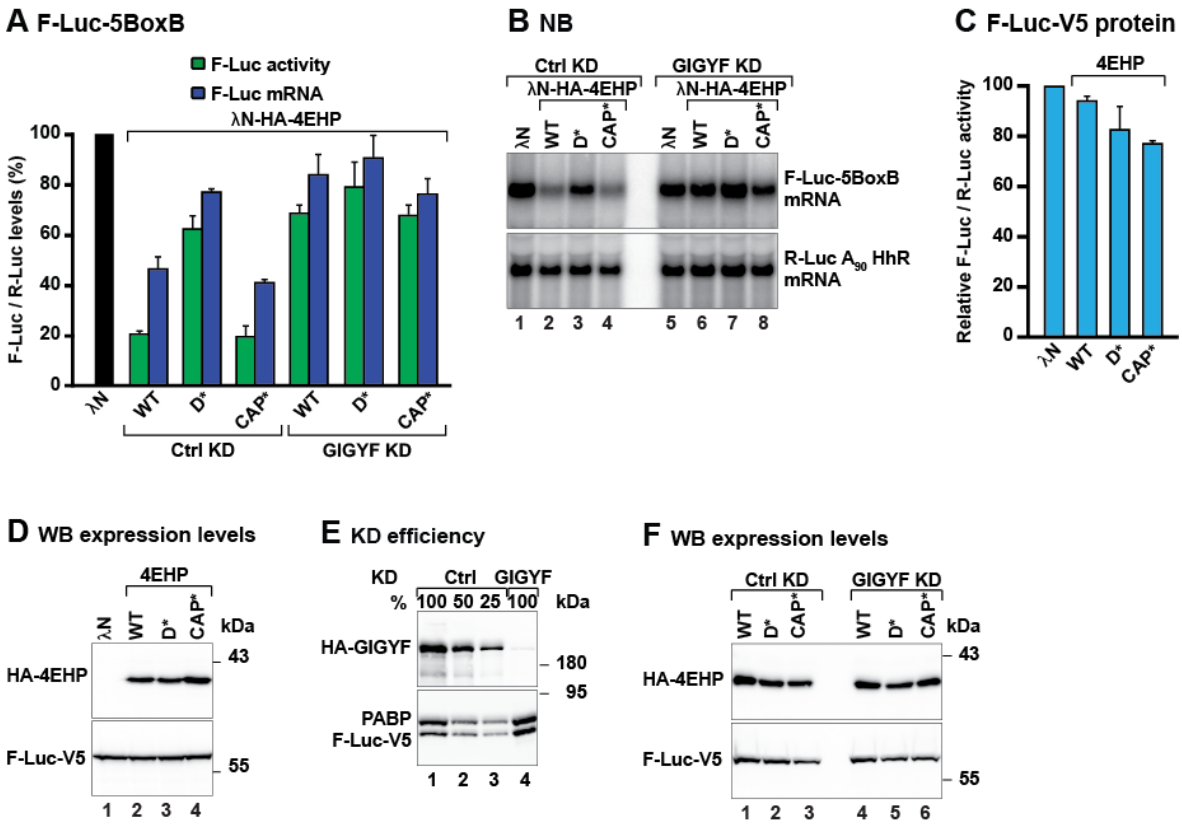

Figure 9. 4EHP represses mRNA expression in a GIGYF-dependent manner

(A) Tethering assay of 4EHP WT and indicated mutants to the F-Luc-5BoxB reporter in S2 cells. The R-Luc-A_{90}-HhR reporter served as transfection control. The bar graph shows the quantification of the luciferase activity (protein levels, green bars) and the mRNA levels (from NB analysis, blue bars). F-Luc activity and mRNA levels in cells expressing the λN-HA peptide were normalized to those of the R-Luc transfection control and set to 100%. Bars represent the mean values and error bars denote the standard deviation from at least three independent experiments. Control (Ctrl) KD cells were treated with dsRNA Neomycin, while GIGYF KD cells were treated with dsRNA GIGYF. **(B)** NB of a representative experiment shown in (A). **(C)** Tethering assay of WT and mutant 4EHP proteins on the F-Luc-V5 reporter. F-Luc activity in cells expressing the λN-HA peptide was normalized to the R-Luc activity and set to 100%. Bars represent the mean values and error bars denote the standard deviation from at least three independent experiments. **(D)** Representative WB analysis of samples in (C). **(E)** WB showing the KD efficiency of GIGYF-depleted cells. HA-GIGYF was overexpressed after the cells were treated with either dsRNA neomycin (Ctrl KD) or dsRNA GIGYF (GIGYF KD). Samples were analysed by WB with anti-HA antibody. Serial dilutions of Ctrl KD sample were loaded in lanes 1-3 to better estimate KD efficiency. F-Luc-V5 was used as transfection control and PABP as a loading control. **(F)** Representative WB showing the expression levels of the proteins tethered in (A).

6.2 GIGYF recruits mRNA decay factors to induce mRNA decay

6.2.1 The N-term of GIGYF represses translation and induces mRNA decay

4EHP requires GIGYF to repress translation and to induce mRNA decay. In order to define GIGYF function in the control of mRNA expression, I tethered λN-HA-GIGYF to the F-Luc-5BoxB reporter. Binding of λN-HA-GIGYF to the 3' UTR of the F-Luc mRNA reporter induced a strong reduction of F-Luc activity to 20% and mRNA levels to 45% (Fig. 10 A and B). As observed for 4EHP, repression of F-Luc activity was again more prominent than the changes on mRNA levels, suggesting that GIGYF mainly promotes translational repression (Fig. 10 A and B).

To gain detailed molecular knowledge on the mechanism of mRNA repression, I generated two GIGYF fragments: the N-terminal (N-term, 1-640 AA), which contained the 4EHP-binding motif and the GYF domain, and the C-terminal (C-term, 641-1574 AA) regions (Fig. 4 A). The tethering of the λN-HA-GIGYF N-term to the F-Luc-5BoxB reporter caused a reduction of F-Luc activity and mRNA levels, in a fashion comparable to GIGYF full length (FL; Fig. 10 A and B). Conversely, GIGYF C-term only partially affected the expression of the F-Luc reporter and had a similar effect on F-Luc activity and mRNA levels (Fig. 10 A and B). The observed effects did not depend on different protein expression, since the three GIGYF proteins (FL, N-term and C-term) were expressed at similar levels (Fig. 10 C). The expression of the F-Luc-V5 mRNA lacking the 5BoxB hairpins in the presence of the different λN-HA-GIGYF proteins remained unaltered, indicating that GIGYF-mediated mRNA repression is specific and only occurs upon binding of GIGYF proteins to the 3' UTR of the reporter mRNA (Fig. 10 D and E). Thus, these results identified the N-term region as the effector part of GIGYF and pointed toward a role of this protein in the direct regulation of mRNA expression

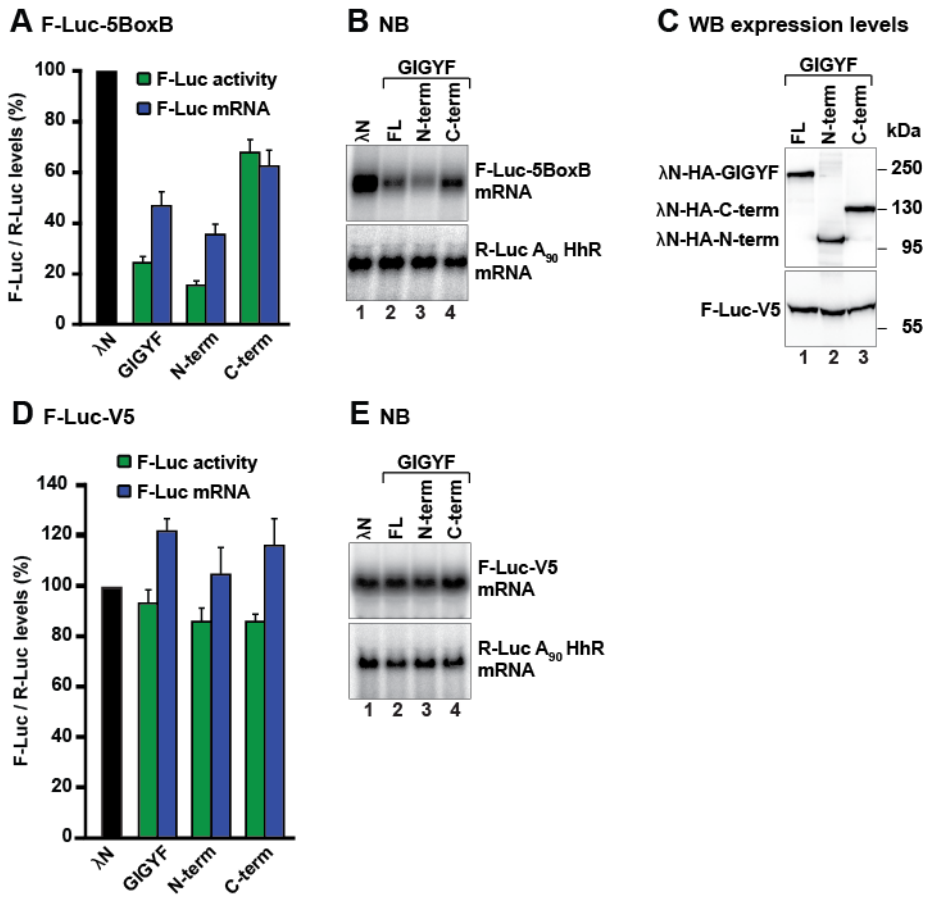

Figure 10. GIGYF N-term region represses mRNA expression
(A) Tethering assay of GIGYF WT and indicated fragments to F-Luc-5BoxB reporter in S2 cells. The R-Luc-A_{90}-HhR served as transfection control. The bar graph shows the quantification of luciferase activity (protein levels, green bars) and NB (RNA levels, blue bars). The ratio between the F-Luc and R-Luc levels in cells expressing the λN-HA peptide are set to 100%. Bars represent the mean values and error bars denote the standard deviation from at least three independent experiments. **(B)** NB of one representative experiment shown in (A). **(C)** Representative WB analysis of samples used in (A) and decorated with anti-HA and anti-V5 antibodies. **(D)** Tethering of GIGYF WT and indicated fragments to the F-Luc-V5 reporter. F-Luc levels normalized to those of the R-Luc in cells expressing the λN-HA peptide are set to 100%. Bars represent the mean values and error bars denote the standard deviation from at least three independent experiments. **(E)** NB of one representative experiment shown in (D).

6.2.2 GIGYF regulates mRNA stability

3' UTR-bound GIGYF repressed mRNA expression. To determine if changes on reporter mRNA abundance were a consequence of post-transcriptional regulation of mRNA stability, I tethered λN-HA-GIGYF FL to the F-Luc-5BoxB reporter and performed a time-course experiment to quantify reporter mRNA levels upon transcriptional inhibition with Actinomycin D (Fig. 11 A and B). The half-life,

the time required to degrades the 50% of the mRNA, in the presence of GIGYF, normalized with the stable ribosomal protein 49 (rp49) mRNA, was drastically shorter compared to the λN-HA alone, indicating that GIGYF accelerated mRNA degradation (Fig. 11 A and B). Furthermore, tethering of GIGYF to the reporter induced mRNA deadenylation as evidenced from the faster migration of the mRNA after 240 minutes compared to time zero, marked as polyA tail length A_n versus A_0 (Fig. 11 A, red line). Moreover, the F-Luc activity was still inhibited by the tethering of GIGYF at the end of experiment indicating that GIGYF protein was still active after 240 minutes (Fig. 11 C). In conclusion, this experiment showed the influence of GIGYF on mRNA post-transcriptional regulation.

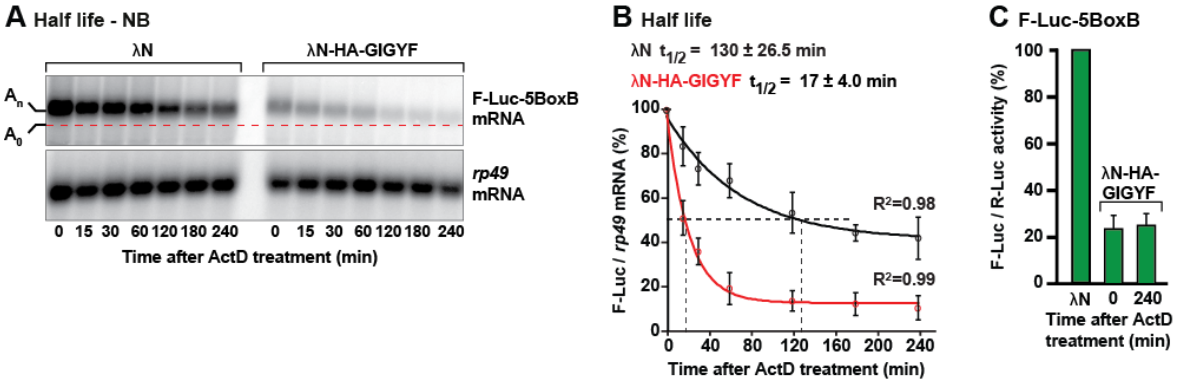

Figure 11. GIGYF induces mRNA degradation

(A) Representative NB of an RNA half-life experiment performed upon tethering of λN-HA-GIGYF, or λN-HA, to the F-Luc-5BoxB reporter. The cells were treated with Actinomycin D (ActD) and samples were collected at the indicated time-points. The stable ribosomal RNA *rp49* was used as a loading control. A_n indicates the position of the mRNA reporter containing the polyA tail, while A_0 and the red dashed line highlight the deadenylated mRNA. **(B)** Quantification of F-Luc-5BoxB reporter mRNA half-life experiment as in (A). The circles represent the mean values and error bars denote the standard deviation of three independent experiments. The grey dashed lines indicate the time after the treatment with ActD, required for the degradation of 50% of the total mRNA (half-life, $t_{1/2}$) of the reporter upon tethering of λN-HA-GIGYF (red curve) or λN-HA (black curve). $t_{1/2}$ is represented as the mean of three independent experiments ± standard deviation and the R^2 has been calculated with SciDAVis. **(C)** Quantification of the F-Luc activity (protein levels) at the indicated time points after ActD addition, in samples with λN-HA-GIGYF or λN tethered to F-Luc-5BoxB reporter in S2 cell line. The R-Luc served as transfection control and is used for normalization of the F-Luc values. The ratio F-Luc to R-Luc activity in cells expressing the λN peptide is set to 100%. Bars represent the mean values and error bars denote the standard deviation from at least three independent experiments.

6.2.3 GIGYF promotes deadenylation-dependent decapping

The degradation of mRNA is a fundamental step for gene expression and eukaryotes have evolved different mechanisms to control mRNA abundance. Considering the relevance of the mRNA decay pathways, I investigated which mechanism is induced by GIGYF to mediate mRNA degradation. To analyse whether GIGYF triggers deadenylation-dependent mRNA decay (Fig. 5), I tethered GIGYF in cells overexpressing a DCP1 protein mutated in the DCP2-activation loop (DCP1-GSSG), known to inhibit decapping in a dominant negative manner (Chang et al., 2014; Kuzuoglu-Ozturk et al., 2016). Upon decapping inhibition, deadenylated mRNA decay intermediates accumulate in the cell since the 5' to 3' exonuclease activity of XRN1 exonuclease is blocked. Using λN-HA-GW182 as a known example of a protein reported to trigger deadenylation-dependent decapping (Behm-Ansmant et al., 2006; Jonas and Izaurralde, 2015), I analysed if tethering of λN-HA-GIGYF results in the accumulation of a stable and deadenylated F-Luc-5BoxB mRNA in the presence of the DCP1-GSSG mutant (Fig. 12 A and B). In cells overexpressing GFP instead of the DCP1 mutant, λN-HA-GIGYF or λN-HA-GW182 induced the degradation of the reporter compared to the λN-HA negative control vector (Fig. 12 A and B, lanes 2 and 3). Conversely, tethering of λN-HA-GIGYF, or λN-HA-GW182, in the presence of DCP1-GSSG resulted in the accumulation of the deadenylated reporter mRNA decay intermediate (Fig. 12 A and B, lanes 5 and 6). Not surprisingly the deadenylated mRNA reporter was translationally silenced in all tethering conditions (Fig. 12 A). The expression levels of the tethered proteins and of GFP and GFP-DCP1-GSSG were assessed by WB (Fig. 12 C). This experiment showed that GIGYF induces deadenylation-dependent 5' to 3' mRNA degradation.

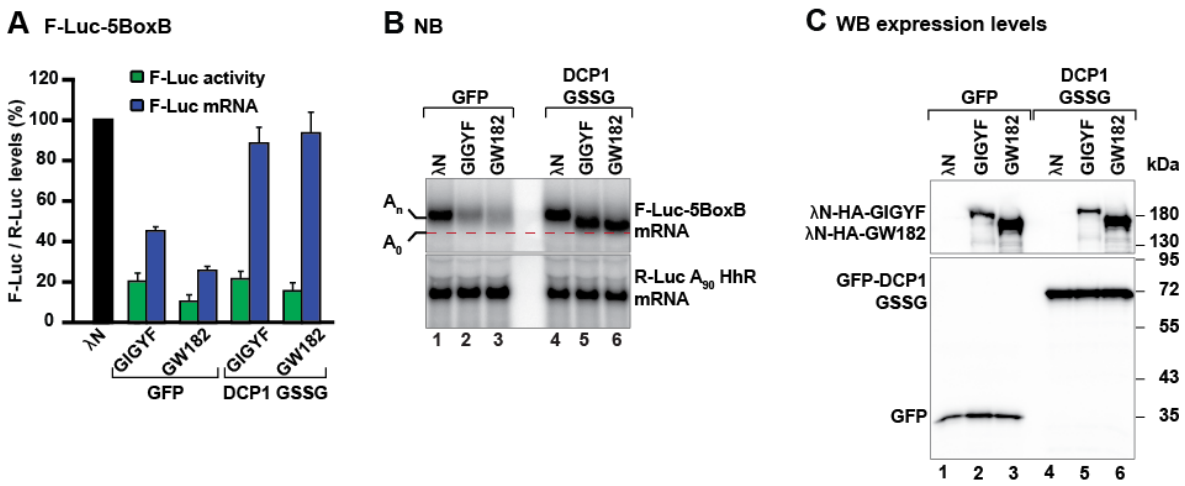

Figure 12. GIGYF promotes deadenylation-dependent decapping
(A) Tethering of GIGYF or GW182 to the F-Luc-5BoxB reporter performed in cells overexpressing either GFP-V5 or the DCP1-GSSG mutant. The bar graph shows the quantification of the luciferase activity (protein level, green bars) and luciferase mRNA abundance (RNA level, blue bars). The R-Luc served as transfection control and is used for normalization of the F-Luc values. F-Luc to R-Luc ratio in cells expressing the λN peptide is set to 100%. Bars represent the mean values and error bars denote the standard deviation from at least three independent experiments. **(B)** NB of one representative experiment shown in (A). A_n indicates the position of the mRNA reporter containing the polyA tail, while A_0 and the red dashed line highlight the deadenylated mRNA. **(C)** Representative WB for the analysis of the samples as in (A).

6.2.4 GIGYF interacts with mRNA decay factors

The observation that GIGYF induces 5' to 3' mRNA degradation prompted me to identify the interaction network of GIGYF with mRNA decay factors. Therefore, I performed co-immunoprecipitation assays of GIGYF with components of the two deadenylation machineries (PAN2/PAN3 and CCR4-NOT complexes), the decapping complex (DCP1/DCP2) and associated proteins, and the exonuclease XRN1 (Fig. 13 and 14). Interestingly, GIGYF interacted with different subunits of the CCR4-NOT deadenylase complex and with different decapping activators. In detail, GIGYF efficiently bound to the scaffold subunit of the CCR4-NOT complex, NOT1 (Fig. 13 A) and to the decapping activators, Me31B (Fig. 13 B) and HPat (Fig. 13 C).

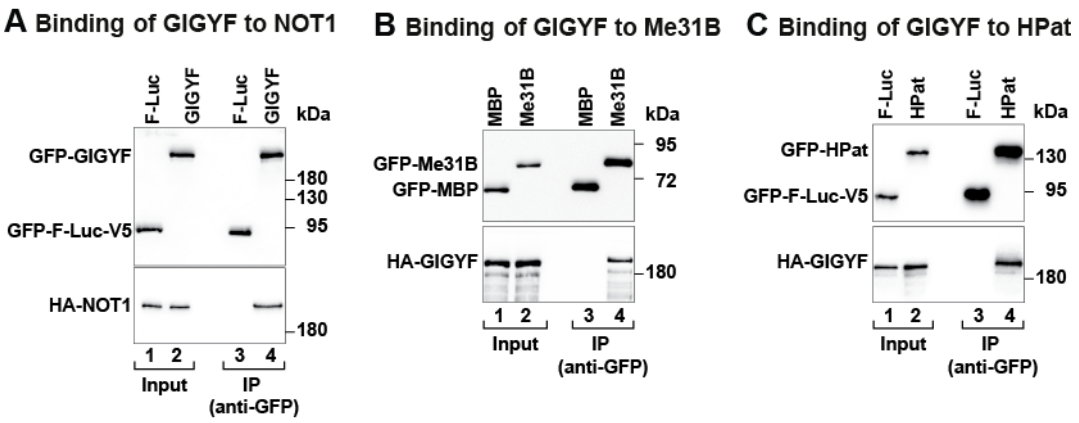

Figure 13. NOT1, Me31B, and HPat efficiently interact with GIGYF
(A) Immunoprecipitation assay displaying the interaction between GFP-GIGYF and HA-NOT1. GFP-F-Luc-V5 served as a negative control. The input (4% for GFP-tagged proteins and 1% for HA-tagged proteins) and bound fractions (15% for GFP-tagged proteins and 30% for HA-tagged proteins) were analysed by WB using anti-GFP and anti-HA antibodies. **(B)** Immunoprecipitation assay displaying the interaction between GFP-Me31B and HA-GIGYF. GFP-MBP served as a negative control. The input (2% for GFP-tagged proteins and 1% for HA-tagged proteins) and bound fractions (20% for GFP-tagged and HA-tagged proteins) were analysed by WB using anti-GFP and anti-HA antibodies. **(C)** Immunoprecipitation assay displaying the interaction between GFP-HPat and HA-GIGYF. GFP-F-Luc-V5 served as a negative control. The input (2.5% for GFP-tagged proteins and 1% for HA-tagged proteins) and bound fractions (20% for GFP-tagged and HA-tagged proteins) were analysed by WB using anti-GFP and anti-HA antibodies.

Moreover, GIGYF weakly associated with other mRNA decay factors. Among those are the CCR4-NOT complex subunits POP2 (Fig. 14 B, lane 7), NOT2 (Fig. 14 B, lane 8) and NOT3 (Fig. 14 C), and the enhancer of decapping EDC3 (Fig. 14 E, lane 5). In contrast, GIGYF did not interact with the PAN2/PAN3 deadenylase complex (Fig. 14 A), the CCR4-NOT complex subunits CCR4 (Fig. 14 B, lane 6) and CAF40 (Fig. 14 D), the decapping factors Tral (Fig. 14 E, lane 6), EDC4 (Fig. 14 F) and DCP1 (Fig. 14 G), the decapping enzyme DCP2 (Fig. 14 H), or the exonuclease XRN1 (Fig. 14 I).

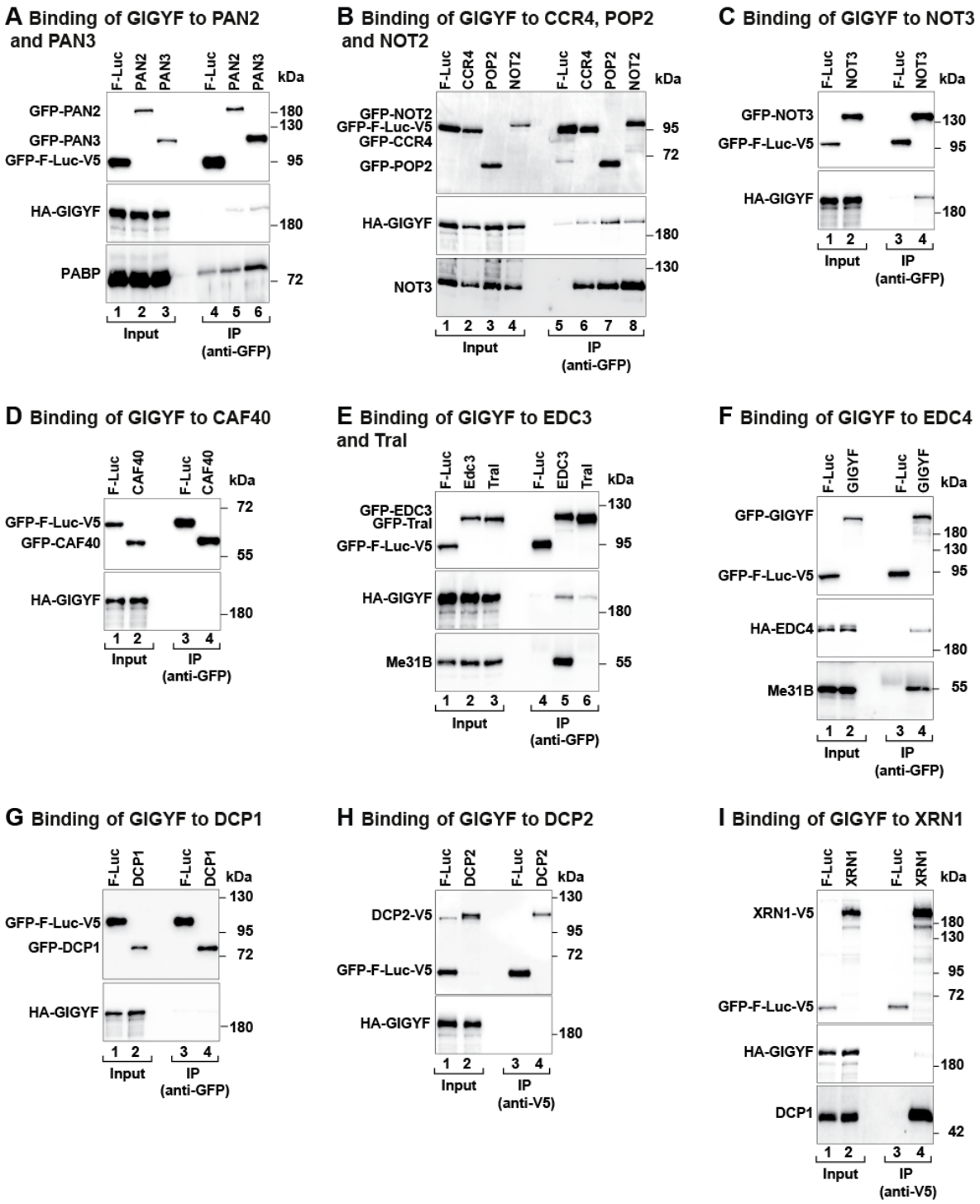

Figure 14. GIGYF associates with components of the mRNA decay complexes
(A-I) Immunoprecipitation assay displaying the interaction between GIGYF and the indicated mRNA decay factors. GFP-F-Luc-V5 served as a negative control. Immunoprecipitation was performed using anti-GFP or anti-V5 antibody as indicated. The input and bound fractions were analysed by WB using anti-GFP, anti-HA antibodies, and the indicated antibodies. **(A)** Interaction of GIGYF with PAN2 and PAN3. Input: 3.5% for GFP-tagged proteins and 1% for HA-tagged proteins. Bound fractions: 15% for GFP-tagged proteins and 30% for HA-tagged proteins. PABP served as positive control for the interaction with the PAN2/PAN3 complex. **(B)** Interaction of GIGYF with CCR4, POP2, and NOT2. Input: 3.5% for GFP-tagged proteins

and 1% for HA-tagged proteins. Bound fractions: 15% for GFP-tagged proteins and 30% for HA-tagged proteins. NOT3 served as a positive control of the interaction with the deadenylase complex. **(C)** Interaction of GIGYF with NOT3. Input: 2.5% for GFP-tagged proteins and 1% for HA-tagged proteins. Bound fractions: 15% for GFP-tagged proteins and 30% for HA-tagged proteins. **(D)** Interaction of GIGYF with CAF40. Input: 3% for GFP-tagged proteins and 1% for HA-tagged proteins. Bound fractions: 20% for GFP-tagged proteins and 30% for HA-tagged proteins. **(E)** Interaction of GIGYF with EDC3 and Tral. Input: 3.5% for GFP-tagged proteins and 1% for HA-tagged proteins. Bound fractions: 15% for GFP-tagged proteins and 30% for HA-tagged proteins. Me31B served as positive control for the interaction with the decapping factors. **(F)** Interaction of GIGYF with EDC4. Input: 3% for GFP-tagged proteins and 1% for HA-tagged proteins. Bound fractions: 15% for GFP-tagged proteins and 30% for HA-tagged proteins. Me31B served as positive control for the interaction with EDC4. **(G)** Interaction of GIGYF with DCP1. Input: 3% for GFP-tagged proteins and 1% for HA-tagged proteins. Bound fractions: 20% for GFP-tagged proteins and 30% for HA-tagged proteins. **(H)** Interaction of GIGYF with DCP2. Input: 2% for GFP-tagged proteins and 1% for HA-tagged proteins. Bound fractions: 20% for GFP-tagged proteins and 30% for HA-tagged proteins. **(I)** Interaction of GIGYF with XRN1. Input: 2% for GFP-tagged proteins and 1% for HA-tagged proteins. Bound fractions: 20% for GFP-tagged proteins and 30% for HA-tagged proteins. DCP1 served as positive control for the interaction with XRN1.

6.2.5 TTP, ZNF598, and GW182 do not recruit GIGYF on RNA in S2 cells

In addition to the CCR4-NOT complex, mammalian GIGYF2 interacts with TTP, ZNF598 and GW182. These RBPs direct the activity of GIGYF by recruiting it to the mRNA in a transcript-specific manner (Fu et al., 2016; Morita et al., 2012; Schopp et al., 2017). In order to assess whether these interactions are conserved in *Drosophila* S2 cells, I tested the binding of GIGYF to *Dm* ZNF598, Tis11 (TTP), and GW182 (Fig. 15). Interestingly the GFP-tagged *Dm* ZNF598 did not co-immunoprecipitated GIGYF FL. Conversely GFP-4EHP, used as a positive control, efficiently interacted with GIGYF (Fig. 15 A and 7). Since in human GIGYF2 interacts with TTP (*Dm* Tis11) and GW182 through the GYF domain located at the N-term of the protein (Fig. 4 A), beside the GIGYF FL, I employed the GYF* mutant or the N-term and C-term fragments to test the interaction with Tis11 (Fig. 15 B) and GW182 (Fig. 15 C), respectively. Interesting, none of the interactions reported for the mammalian GIGYF2 are conserved in *D. melanogaster*, suggesting that the 4EHP/GIGYF complex might regulate different transcripts in different organisms and subsequently control different biological processes. However, the RBPs that recruit GIGYF complexes on the mRNA in S2 cells remain still unknown.

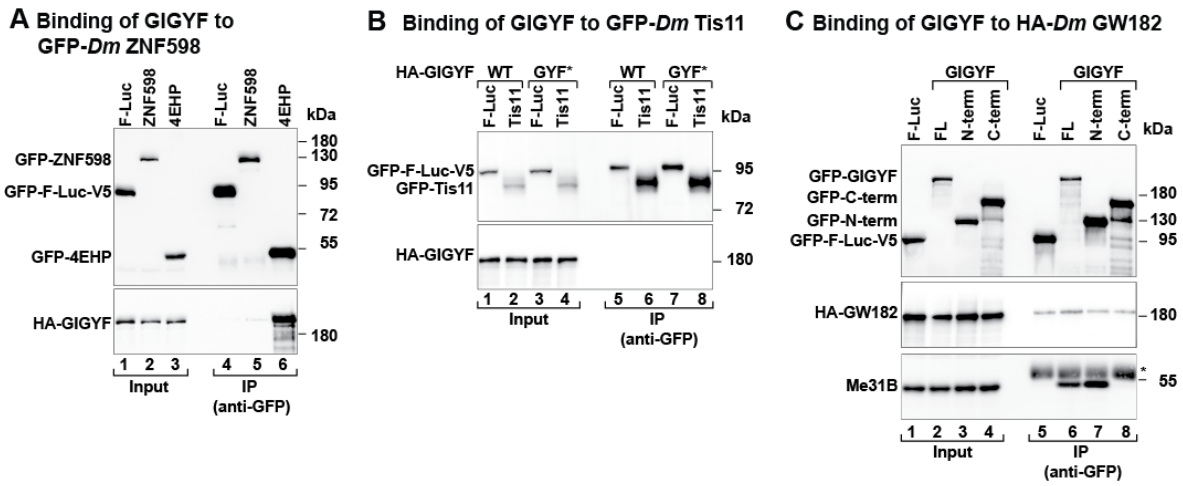

Figure 15. GIGYF does not interact with ZNF598, Tis11 or GW182
(A-C) Immunoprecipitation assays displaying the interaction between GIGYF and the indicated RBPs. GFP-F-Luc-V5 served as a negative control. Immunoprecipitations were performed using anti-GFP antibody. The input and bound fractions were analysed by WB using anti-GFP, anti-HA antibodies, and the indicated antibodies. **(A)** Interaction of GIGYF with ZNF598. Input: 3% for GFP-tagged proteins and 1% for HA-tagged proteins. Bound fractions: 15% for GFP-tagged proteins and 30% for HA-tagged proteins. 4EHP served as positive control for the interaction with GIGYF. **(B)** Interaction of GIGYF WT and GYF* mutant with Tis11. Input: 3% for GFP-tagged proteins and 1% for HA-tagged proteins. Bound fractions: 15% for GFP-tagged proteins and 30% for HA-tagged proteins. **(C)** Interaction of GIGYF FL and indicated mutants with GW182. Input: 3% for GFP-tagged proteins and 1.5% for HA-tagged proteins. Bound fractions: 15% for GFP-tagged proteins and 15% for HA-tagged proteins. Me31B served as positive control for the interaction with GIGYF. The asterisk indicated an unspecific band.

6.2.6 Me31B and HPat interact with the effector domain of GIGYF

The previous results indicate that GIGYF interacts with Me31B, HPat and NOT1 (Fig. 13). To delineate the binding regions on GIGYF for these proteins, I performed co-immunoprecipitation assays between GIGYF FL, N-term, and C-term regions and Me31B, HPat, and NOT1 (Fig. 16). As expected, GIGYF FL efficiently interacted with the three decay factors (Fig. 16 A and B, lanes 6). Interestingly, the N-term fragment interacted with Me31B as efficiently as the FL and with HPat, albeit in a weaker manner (Fig. 16 A, lanes 7). Conversely, GIGYF C-term did not associate with neither of the two decay factors (Fig. 16 A, lanes 8). Instead, none of the GIGYF fragments were able to bind to NOT1, suggesting that both N-term and C-term participate in this interaction (Fig. 16 B, lanes 7 and 8 versus 6). In summary, the N-term region, which represent the effector part of GIGYF associates with the

decay factors Me31B and HPat, while the it remains unclear where NOT1 binds on GIGYF.

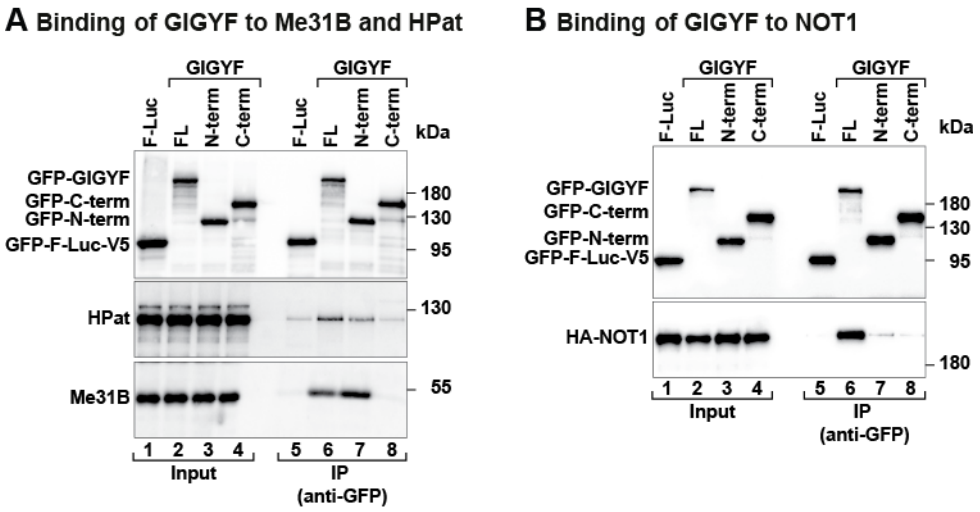

Figure 16. The N-term region of GIGYF binds to Me31B and HPat
(A) Immunoprecipitation assay displaying the interaction between GFP-GIGYF FL and the indicated fragments with endogenous HPat and Me31B. GFP-F-Luc-V5 served as a negative control. The proteins were immunoprecipitated using an anti-GFP antibody. The input (3% for GFP-tagged proteins, 0.2% for endogenous HPat, and 0.4% for endogenous Me31B) and bound fractions (30% for GFP-tagged proteins, 30% for endogenous HPat, and 40% for endogenous Me31B) were analysed by WB using anti-GFP, anti-HPat, and anti-Me31B antibodies. **(B)** Immunoprecipitation assay displaying the interaction between GFP-GIGYF FL and indicated fragments with HA-NOT1. GFP-F-Luc-V5 served as a negative control. The proteins were immunoprecipitated using an anti-GFP antibody. The input (3% for GFP-tagged proteins and 1% for HA-tagged proteins) and bound fractions (15% for GFP-tagged proteins and 30% for HA-tagged proteins) were analysed by WB using anti-GFP and anti-HA antibodies.

6.2.7 GIGYF contains a conserved Me31B-binding motif

GIGYF is conserved in all metazoan and the highest similarity is in the N-term region (1-640 AA), containing the 4EHP-binding motif and the GYF domain (Fig. 4 A). To identify the binding region between GIGYF and Me31B, I performed several sequence analyses between insects GIGYF N-term orthologues that revealed multiple highly conserved blocks, including the 4EHP-binding region and the GYF domain. Extending the analysis to human orthologues, allowed to identify a conserved motif in the N-term of GIGYF proteins, subsequently named Me31B-binding motif (MBM) (Fig. 17 A). This motif has partial sequence similarity with the CHD present in other Me31B/DDX6-interacting partners, like *Dm* CUP and 4E-T

proteins (Fig. 17 A). To verify if this sequence constitutes an Me31B-binding motif (MBM), I generated a GIGYF deletion mutant lacking this region (GIGYF ΔMBM) and tested its interaction with endogenous Me31B in S2 cells (Fig. 17 B and C). GIGYF WT, or the GYF* mutant, efficiently immunoprecipitated Me31B, whereas the GIGYF ΔMBM protein did not (Fig. 17 B, lanes 6 and 8 versus 7, and Fig. 17 C, lanes 8 and 10 versus 9 and 11). This data indicates that the MBM is required for the interaction between GIGYF and Me31B. Moreover, in co-immunoprecipitation assays, the GIGYF MBM alone retained the ability to strongly interact with Me31B (Fig. 17 C, lane 12). Thus, the MBM is necessary and sufficient to mediate GIGYF-Me31B interaction *in vivo*.

Me31B is an RNA helicase with a typical structure constituted mainly by two RecA-like domains (Fig. 17 D, scheme). To map the region of Me31B mediating the interaction with GIGYF, I performed an immunoprecipitation assay with Me31B FL or the two separated RecA domains and GIGYF N-term (Fig. 17 D). GIGYF interacted with the RecA2 domain as efficiently as with FL Me31B, while no interaction was detected with the RecA1 domain (Fig. 17 D, lane 6 and 8 versus 7). Taken together, these results show that a newly identified Me31B-binding domain present in the N-term region of GIGYF is necessary and sufficient to mediate interaction with the RecA2 domain of Me31B.

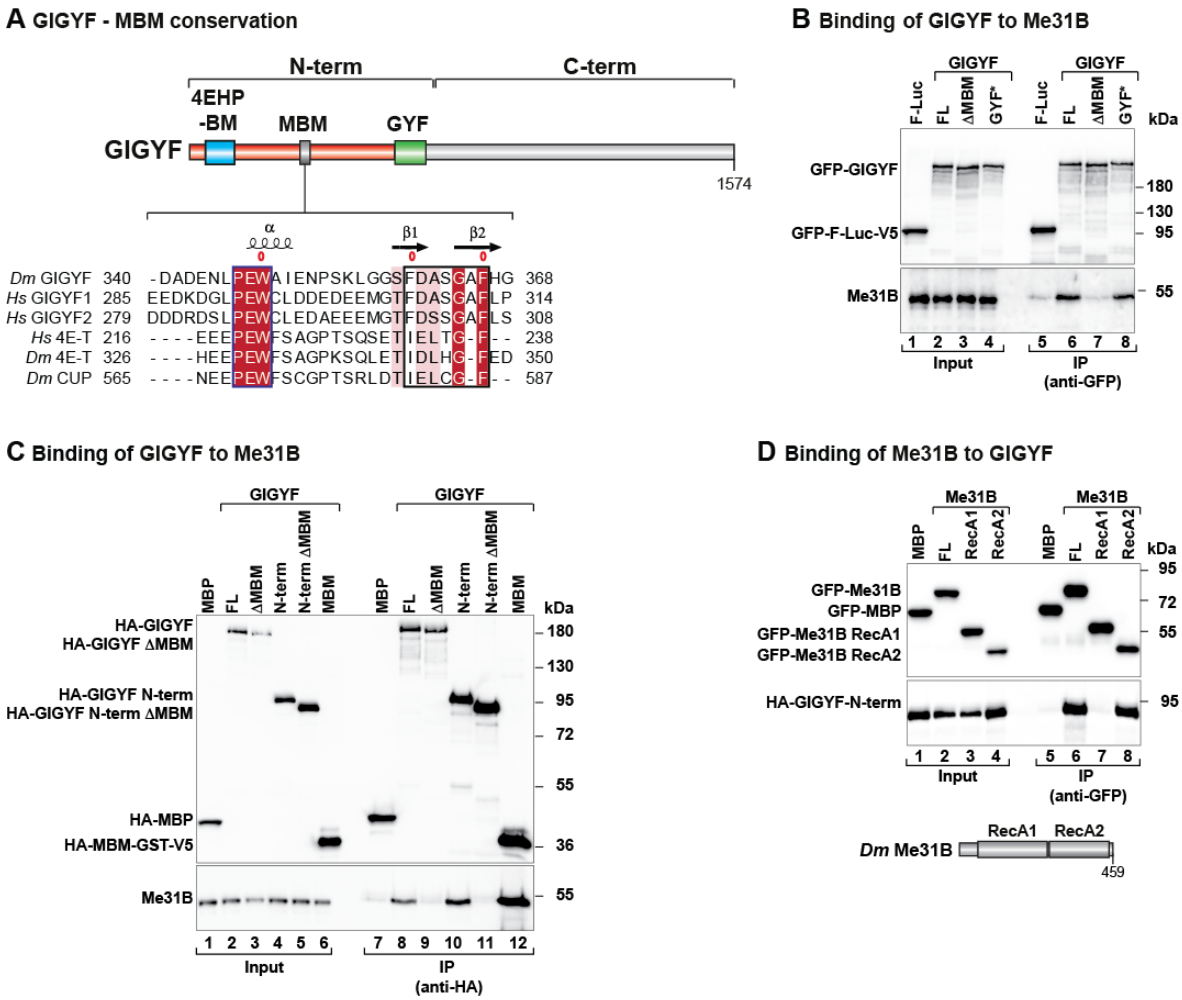

Figure 17. GIGYF interacts with Me31B RecA2 domain via a distinct motif

(A) GIGYF schematic domain organization. The N-term is depicted in red and the C-term in grey. The different domains/motifs are marked: 4EHP-binding motif (4EHP-BM blue), Me31B-binding motif (MBM, grey), and GYF domain (green). Below the scheme is shown the sequence alignment of the *Dm* and *Hs* GIGYF proteins MBM with the CHD present in *Hs* and *Dm* 4E-T proteins and *Dm* CUP. The numbers at the sides of the alignment indicate the amino acid position on the protein. Identical residues are shown in red boxes and white text, similar residues (>70%) are in pink. The blue box highlights the first Me31B-binding sequence containing the PEW motif whereas the black box points out to the second Me31B-binding sequence, the discontinuous FDF motif. The red circle above the sequences indicate the residues mutated according to the crystal structure. The secondary structure of the MBM is depicted above the sequence. **(B)** Immunoprecipitation assay displaying the interaction between GFP-GIGYF FL or the indicated mutants and endogenous Me31B. GFP-F-Luc-V5 served as a negative control. The proteins were immunoprecipitated using an anti-GFP antibody. The input (4% for GFP-tagged proteins, 0.18% for endogenous Me31B) and bound fractions (40% for GFP-tagged proteins, 45% for endogenous Me31B) were analysed by WB using anti-GFP and anti-Me31B antibodies. **(C)** Immunoprecipitation assay displaying the interaction between GFP-GIGYF FL or the indicated mutants and endogenous Me31B. HA-MBP served as a negative control. The proteins were immunoprecipitated using an anti-HA antibody. The input (1.5% for HA-tagged proteins and 0.2% for endogenous Me31B) and bound fractions (30% for HA-tagged proteins and 45% for endogenous Me31B) were analysed

by WB using anti-HA and anti-Me31B antibodies. **(D)** Immunoprecipitation assay displaying the interaction between GFP-Me31B FL or the indicated fragments and HA-GIGYF N-term. GFP-MBP served as a negative control. The proteins were immunoprecipitated using an anti-GFP antibody. The input (3% for GFP-tagged proteins, 3% HA-tagged proteins) and bound fractions (15% for GFP-tagged proteins and 30% for HA-tagged proteins) were analysed by WB using anti-GFP and anti-HA antibodies. At the bottom of the image a schematic representation of the domain organization of Me31B is shown. The number indicate the last residue of the protein.

6.2.8 GIGYF and Me31B interact through a unique structural arrangement

To determine if the interaction between GIGYF and Me31B is direct, I expressed MBP-tagged GIGYF MBM (348-368 AA) and GST-tagged Me31B RecA2 domain (268-459 AA) in *E. coli.* These proteins were then used in a GST-pulldown assay. The pulled down proteins were visualized after Coomassie blue staining of an SDS-PAGE acrylamide gel (Fig. 18 A). This assay showed that the two proteins interact *in vitro*, suggesting that the interaction between Me31B and GIGYF is direct.

To uncover the structural arrangement adopted by the complex, in collaboration with Daniel Peter, a former PhD student in the department, we determined the crystal structure of the GIGYF-MBM (348-368 AA) bound to the RecA2 domain of Me31B (264-433 AA) at 2.4 Å resolution. The crystal structure revealed that GIGYF adopts a bipartite binding mode to associate with Me31B and highlighted two distinct structural arrangements assumed by the Me31B-binding motifs of GIGYF (Fig. 18 B). In the first contact point between the two proteins, the side chain of Trp348 (W348) present in a small helix of GIGYF, initiated by a Pro-Glu-Trp (P346, E347, W348, PEW) sequence, interacted with a hydrophobic pocket lying between helices 10 and 11 of Me31B (Fig. 18 C). Interestingly, the PEW sequence is conserved also in other Me31B/DDX6-interacting proteins (Ozgur et al., 2015), as shown in fig. 17 A. C-terminally of the PEW sequence, a flexible link connected this motif with the second structural element of GIGYF formed by two β-hairpins that position a Phe-Asp-Phe (F360, D361, F366) motif of GIGYF in a second hydrophobic pocket of Me31B (Fig. 18 D). The FDF motif has also been structurally characterized in other Me31B/DDX6-binding proteins (Ozgur et al., 2015; Tritschler et al., 2009), however in GIGYF it assumed a different arrangement characterized by the presence of four amino acids between the FD residues and the last F residue, in a discontinuous FDx_4F motif. Despite the difference in the

sequence, the two phenylalanine residues still occupied the same hydrophobic pocket of Me31B, with the same structural arrangement of the previously described FDF or IEL motif, a variation of the sequence in some Me31B/DDX6-binding proteins (Fig. 17 A). In addition, the interaction between GIGYF and Me31B is stabilized by a network of hydrogen bonds occurring at both contact sites that guarantee backbone-backbone stabilization (Fig. 18 E).

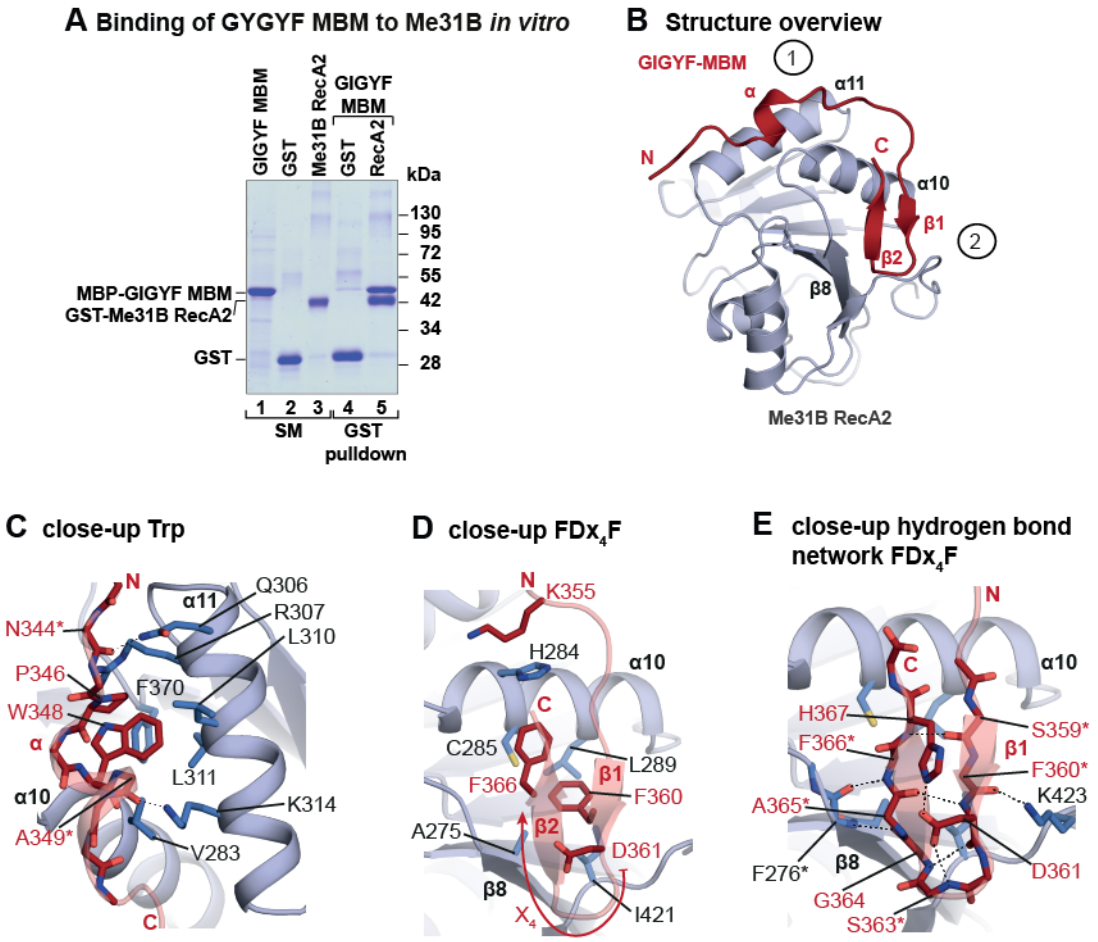

Figure 18. GIGYF and Me31B directly interact with a bipartite binding mode
(A) GST pulldown assay performed with purified recombinant MBP-tagged GIGYF MBM and GST-tagged Me31B RecA2 domain. GST served as a negative control. The starting material (SM; 6.25% for GST-proteins, 2% for the MBP-proteins) and bound fractions (20%) were analysed by SDS-PAGE followed by Coomassie blue staining. **(B)** Crystal structure overview. The GIGYF-MBM peptide is depicted in red and the Me31B RecA2 domain in grey. Secondary structural elements of both peptides are indicated in the figure. GIGYF peptide orientation is indicated as N-term (N) and C-term (C). The circles with numbers 1 and 2 indicate the first and second contact site between GIGYF and Me31B and are enlarged in panel C and D, respectively. **(C-E)** Details of the crystal structure showing the contact points of the tryptophan (W348) of the PEW sequence (C) and of the discontinuous FDx_4F motif (D) of GIGYF with the RecA2 domain of Me31B. The structural arrangement of the discontinuous FDx_4F motif in two β-hairpins and the hydrogen bonding network around the FDx_4F motif are shown in D and E,

respectively. The GIGYF-MBM peptide is depicted in red and the Me31B RecA2 domain in grey. The asterisks indicate residues where the lateral side chain has not been depicted.

To validate the structure, GIGYF mutants carrying point mutations (Ala substitution) in the W348 (PEW motif; W*), F360 and F366 (FDx$_4$F motif; FF*) residues of GIGYF were generated and used in co-immunoprecipitation assays to tested interaction with Me31B. As expected, overexpressed Me31B efficiently immunoprecipitated GIGYF (Fig. 19 lane 10), whereas the GIGYF single (W*, FF*) and double (WFF*) mutants completely abolished the interaction between Me31B and GIGYF (Fig. 19, lanes 12, 14, and 16 versus 10), indicating a pivotal role for both binding motifs in the *in vivo* interaction.

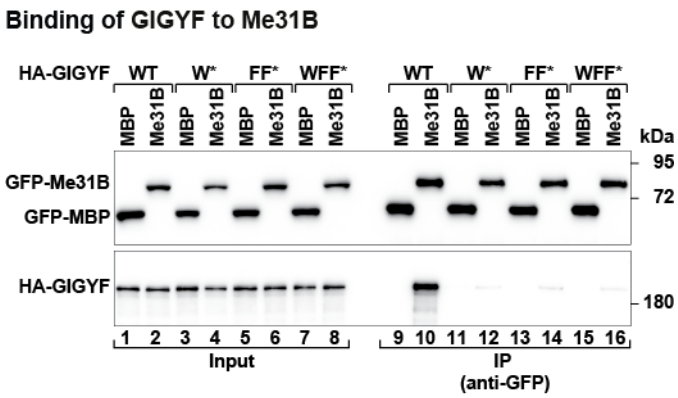

Figure 19. Validation of the crystal structure
Immunoprecipitation assay displaying the interaction between GFP-Me31B and HA-GIGYF WT or indicated mutants. GFP-MBP served as a negative control. The proteins were immunoprecipitated using an anti-GFP antibody. The input (3% for GFP-tagged proteins, 1% HA-tagged proteins) and bound fractions (15% for GFP-tagged proteins and 30% for HA-tagged proteins) were analysed by WB using anti-GFP and anti-HA antibodies.

6.2.9 HPat is a GYF domain-interacting protein

HPat is a GIGYF-binding partner (Fig. 13 C). To gain further insights into this interaction, I investigated which regions of the two proteins are responsible for it. HPat is a protein containing two proline rich sequences (PPGF) in a central portion of the protein, called P-rich region (Fig. 20 A). Since the PPGΦ motifs bind to the GYF domain (Kofler and Freund, 2006), I verified if HPat interacts to the GYF domain of GIGYF, by analysing the interaction of the GIGYF GYF* mutant with endogenous HPat in co-immunoprecipitation assays (Fig. 20 B). In contrast to the

GIGYF WT or the ΔMBM mutant, the GIGYF GYF* mutant did not interact with HPat (Fig. 20 B lanes 6 and 7 versus 8). These results indicate that HPat is a GYF domain-binding protein. To demonstrate that the PPGF sequences present in HPat mediated this interaction, a HPat protein mutated in the two proline-rich motifs (PPGF*) was used in a co-immunoprecipitation assay with overexpressed HA-GIGYF N-term (Fig. 20 C). As expected, HPat WT strongly immunoprecipitated HA-GIGYF while the HPat PPGF* mutant drastically impaired the interaction (Fig. 20 C, lanes 5 versus 6).

Since Me31B binds to the N-term region of HPat (Fig. 20 D) (Haas et al., 2010) and to the MBM of GIGYF (Fig. 17), it was possible that HPat-GIGYF interaction was bridged by Me31B. However, the GIGYF ΔMBM mutant, which no longer binds to Me31B, immunoprecipitated HPat as efficiently as the WT protein (Fig. 20 B, lane 7). In agreement with this result, a HPat mutant lacking the N-term region (HPat ΔN-term) (Haas et al., 2010), associated with GIGYF and not with Me31B in co-immunoprecipitation assays (Fig. 20 D, lane 5 versus 6). Moreover, the interaction of GIGYF with NOT1 is not mediated by either Me31B or HPat (two CCR4-NOT complex binding proteins) as both GIGYF ΔMBM and GYF* mutants still immunoprecipitated overexpressed HA-NOT1 (Fig. 20 B). In summary, these experiments demonstrated that the interaction between HPat and GIGYF requires the GYF domain and the PPGF motifs and was not mediated by Me31B. Although it remains unclear how NOT1 binds to GIGYF, this interaction does not depend on the binding of GIGYF to HPat or Me31B.

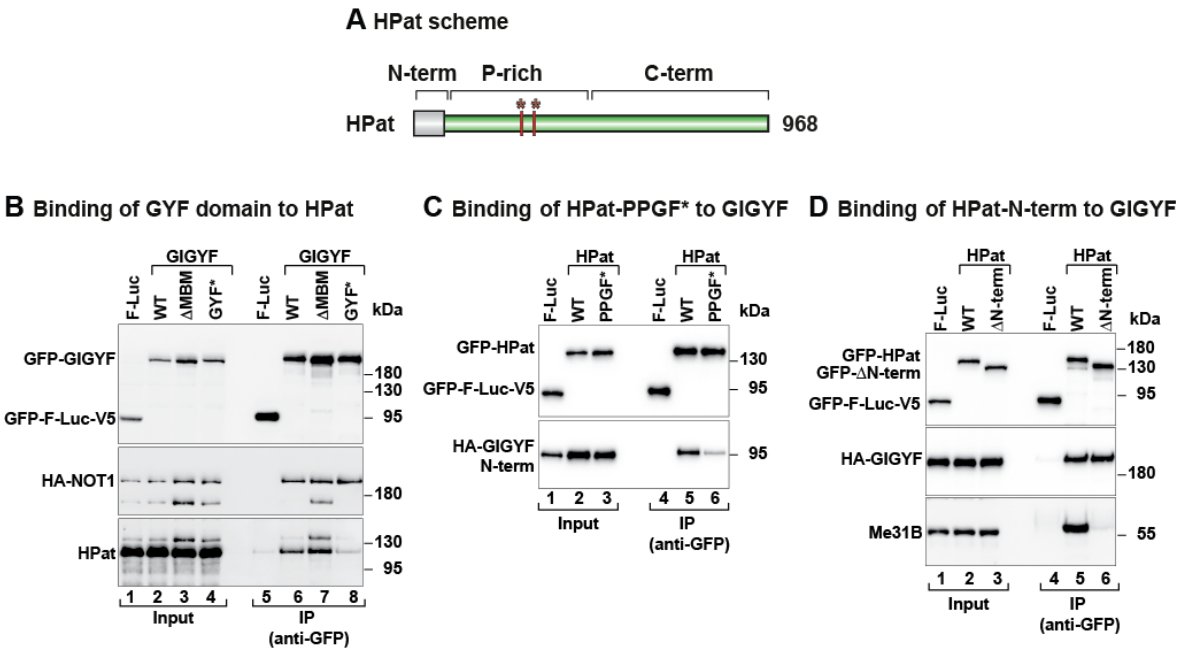

Figure 20. GIGYF and HPat interact via their GYF domain and P-rich motifs, respectively **(A)** Schematic representation of HPat domain organization. The brackets indicate the boundaries of the N-term, proline-rich (P-rich), and C-term regions. The number represents the last amino acid of the protein. The red bars designate the location of the PPGF sequences in the P-rich region and the red asterisks indicate the mutated residues. **(B)** Immunoprecipitation assay displaying the interaction between GFP-GIGYF WT or indicated mutants, HA-NOT1 and endogenous HPat. GFP-F-Luc-V5 served as a negative control. The proteins were immunoprecipitated using an anti-GFP antibody. The input (4% for GFP-tagged proteins, 0.8% for HA-tagged protein and endogenous HPat) and bound fractions (15% for GFP-tagged proteins, 35% for HA-tagged protein and endogenous HPat) were analysed by WB using anti-GFP, anti-HA, and anti-HPat antibodies. **(C)** Immunoprecipitation assay displaying the interaction between GFP-HPat WT or PPGF* mutant and HA-GIGYF N-term. GFP-F-Luc-V5 served as a negative control. The proteins were immunoprecipitated using an anti-GFP antibody. The input (2% for GFP-tagged proteins and 0.8% for HA-tagged protein) and bound fractions (10% for GFP-tagged and 20% for HA-tagged protein) were analysed by WB using anti-GFP and anti-HA antibodies. **(D)** Immunoprecipitation assay displaying the interaction between GFP-HPat WT or the indicated mutant, HA-GIGYF and endogenous Me31B. GFP-F-Luc-V5 served as a negative control. The proteins were immunoprecipitated using an anti-GFP antibody. The input (3% for GFP-tagged proteins and 1% for HA-tagged protein and endogenous Me31B) and bound fractions (15% for GFP-tagged and 30% for HA-tagged and endogenous Me31B protein) were analysed by WB using anti-GFP, anti-HA, and anti-Me31B antibodies.

6.2.10 GIGYF requires Me31B and HPat to induce translational repression and mRNA decay

Since GIGYF binds 4EHP and the decay factors Me31B and HPat, I investigated whether these interactions are required for its repressor function.

Therefore, I tethered the different GIGYF mutants, which abolish the interaction with single or double partners, to the F-Luc-5BoxB reporter (Fig. 21). To study the role of 4EHP in GIGYF-mediated mRNA repression, I tethered λN-HA-GIGYF WT and C* mutant, which cannot bind 4EHP (Fig. 7 A), to the F-Luc-5BoxB mRNA reporter (Fig. 21 A and B). Interestingly, λN-HA-GIGYF C* mutant repressed translation and induced mRNA decay to a similar extent as λN-HA-GIGYF WT, reducing the luciferase activity to 20% and the RNA levels to 40% compared to the negative control λN-HA (Fig. 21 A and B, lanes 1, 2, and 3). This result suggests that, when bound to the mRNA, GIGYF does not require 4EHP to repress target mRNA expression. Similarly, tethering of λN-HA-GIGYF GYF* mutant, which does not bind to HPat (Fig. 20), promoted mRNA decay of the F-Luc mRNA reporter, in a manner similar to GIGYF WT. Nevertheless, the GIGYF GYF* mutant showed a slight reduction in the translational repressor function (Fig. 21 A and B). In addition, tethering of a double GIGYF C*+GYF* mutant to the F-Luc-5BoxB reporter also did not compromise the repressor function of GIGYF (Fig. 21 A and B). All λN-HA-GIGYF protein variants were expressed at comparable levels (Fig. 21 C). These experiments suggest that 4EHP is not relevant for GIGYF function, when it is tethered to the reporter, and that the disruption of HPat binding alone might not be sufficient to hamper GIGYF repressor function.

Beside 4EHP and HPat, I also identified Me31B as a new GIGYF-interacting protein. To investigate the role of this protein in GIGYF-mediated repression, I tethered the λN-HA-GIGYF ΔMBM mutant, which does not interact with Me31B (Fig. 17), to the F-Luc-5BoxB mRNA reporter (Fig. 21 D and E). λN-HA-GIGYF ΔMBM repressed translation of the reporter to 40% compared to the λN-HA, while λN-HA-GIGYF WT reduced it to 20% (Fig. 21 D). Reporter mRNA was also less degraded by the GIGYF ΔMBM mutant (Fig. 21 D and E), indicating that Me31B may be relevant for GIGYF-mediated mRNA repression. The double GIGYF ΔMBM+GYF* mutant, which cannot interact with Me31B and HPat, repressed luciferase activity to 60% indicating that GIGYF repressor function is strongly impaired (Fig. 21 D and E). As a control, I verified that all the tested proteins were expressed to a similar level (Fig. 21 F). These tethering assays showed that Me31B is involved in GIGYF-mediated control of gene expression, with an additional contribution of HPat.

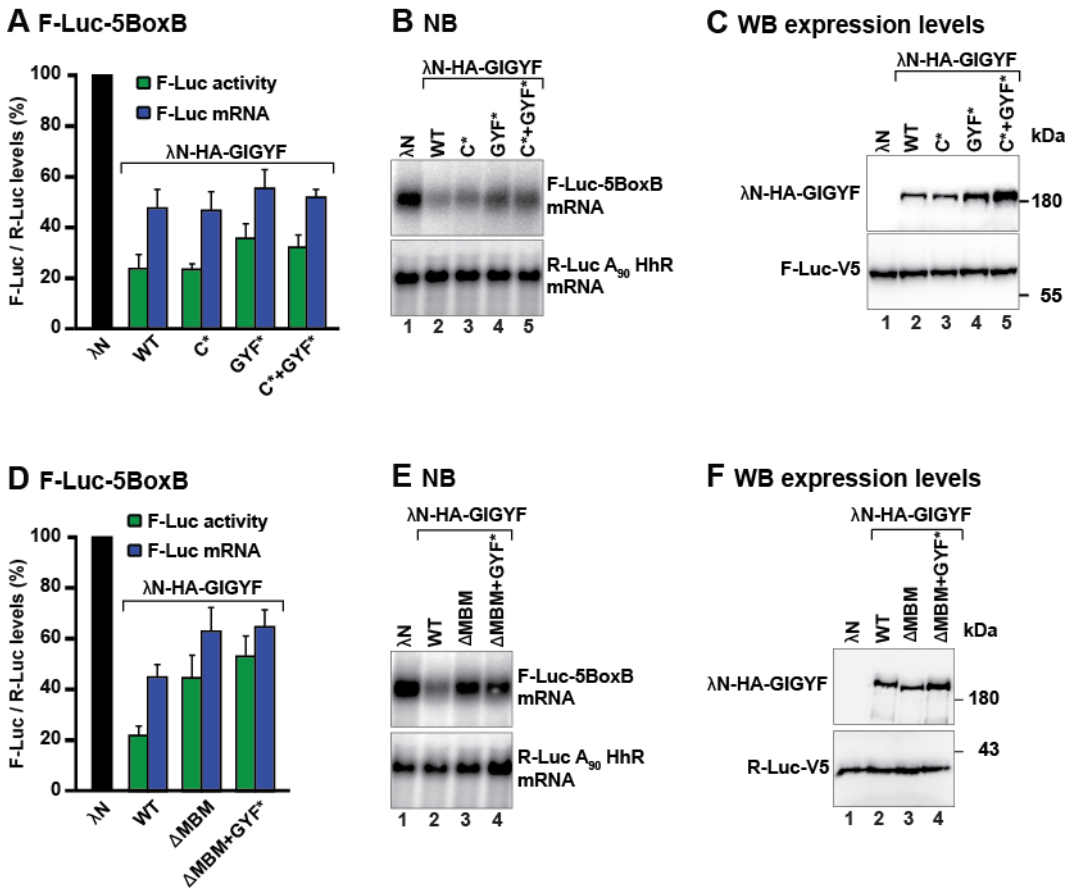

Figure 21. GIGYF requires Me31B and HPat to repress mRNA expression
(A) Tethering of λN-HA-GIGYF WT and indicated mutants to the F-Luc-5BoxB reporter in S2 cells. The R-Luc-A_{90}-HhR served as transfection control. The bar graph shows the quantification of the luciferase activity (protein level, green bars) and NB (RNA level, blue bars). F-Luc levels in cells expressing the λN-HA peptide were normalized to those of the R-Luc and set to 100%. Bars represent the mean values and error bars denote the standard deviation from at least three independent experiments. **(B)** NB of one representative experiment shown in (A). **(C)** Samples as in (A) were analyzed by WB and stained with anti-HA and anti-V5 antibodies. **(D)** Tethering of λN-HA-GIGYF WT and indicated mutants to the F-Luc-5BoxB reporter in S2 cells. The R-Luc-A_{90}-HhR served as transfection control. The bar graph shows the quantification of the luciferase activity (protein level, green bars) and NB (RNA level, blue bars). F-Luc levels in cells expressing the λN-HA peptide were normalized to those of the R-Luc and set to 100%. Bars represent the mean values and error bars denote the standard deviation from at least three independent experiments. **(E)** NB of one representative experiment shown in (D). **(F)** Samples as in (D) were analyzed by WB and stained with anti-HA and anti-V5 antibodies.

6.2.11 Me31B and HPat are required for GIGYF-mediated translational repression

The results of the tethering assays employing λN-HA-GIGYF proteins (Fig. 10), pointed toward a role of GIGYF not only in promoting mRNA decay but also in

repressing translation. To better characterize the mechanism by which GIGYF induces translational repression, I performed tethering assays with the mRNA reporter F-Luc-5BoxB-A_{96}-HhR, which lacks the polyadenylation site and contains 96 adenosines (internal polyA) followed by a self-cleaving RNA element (hammerhead ribozyme, HhR) that generates a non-processable product that is resistant to deadenylation and degradation because it lacks the polyA tail (Zekri et al., 2013). Employing this reporter allows to specifically study the ability of a protein of interest to regulate translation, in the absence of mRNA decay. To understand how different binding partners contribute to GIGYF-mediated translational repression, I tethered λN-HA-GIGYF WT or the C*, GYF* and C*+GYF* mutants (Fig. 22 A, B, and C) as well as the ΔMBM and ΔMBM+GYF* mutants (Fig. 22 D, E, and F) to the F-Luc-5BoxB-A_{96}-HhR reporter. These experiments showed that disrupting the interaction with either HPat (GIGYF GYF* and C*+GYF* mutants; Fig. 22 A), or Me31B (GIGYF ΔMBM mutant; Fig. 22 D) partially affected the repressor function of GIGYF, increasing the F-Luc activity to around 40% instead of the 20% observed with the GIGYF WT. However, the ability to repress translation of the GIGYF ΔMBM+GYF* mutant, which cannot interact with neither HPat nor Me31B, is strongly impaired, as indicated by an increase in the luciferase activity to 60% compared to the 20% of GIGYF WT (Fig. 22 D). These results indicated that GIGYF function as a translational repressor requires its simultaneous interaction with Me31B and HPat. Conversely, the interaction with 4EHP is dispensable for GIGYF-mediated translational repression, as shown by the fact that the GIGYF C* mutant reduces F-Luc activity to the same extent as GIGYF WT (Fig. 22 A). As expected, the mRNA levels were not affected (Fig. 22 B and E) and all the tethered proteins were similarly expressed (Fig. 22 C and F).

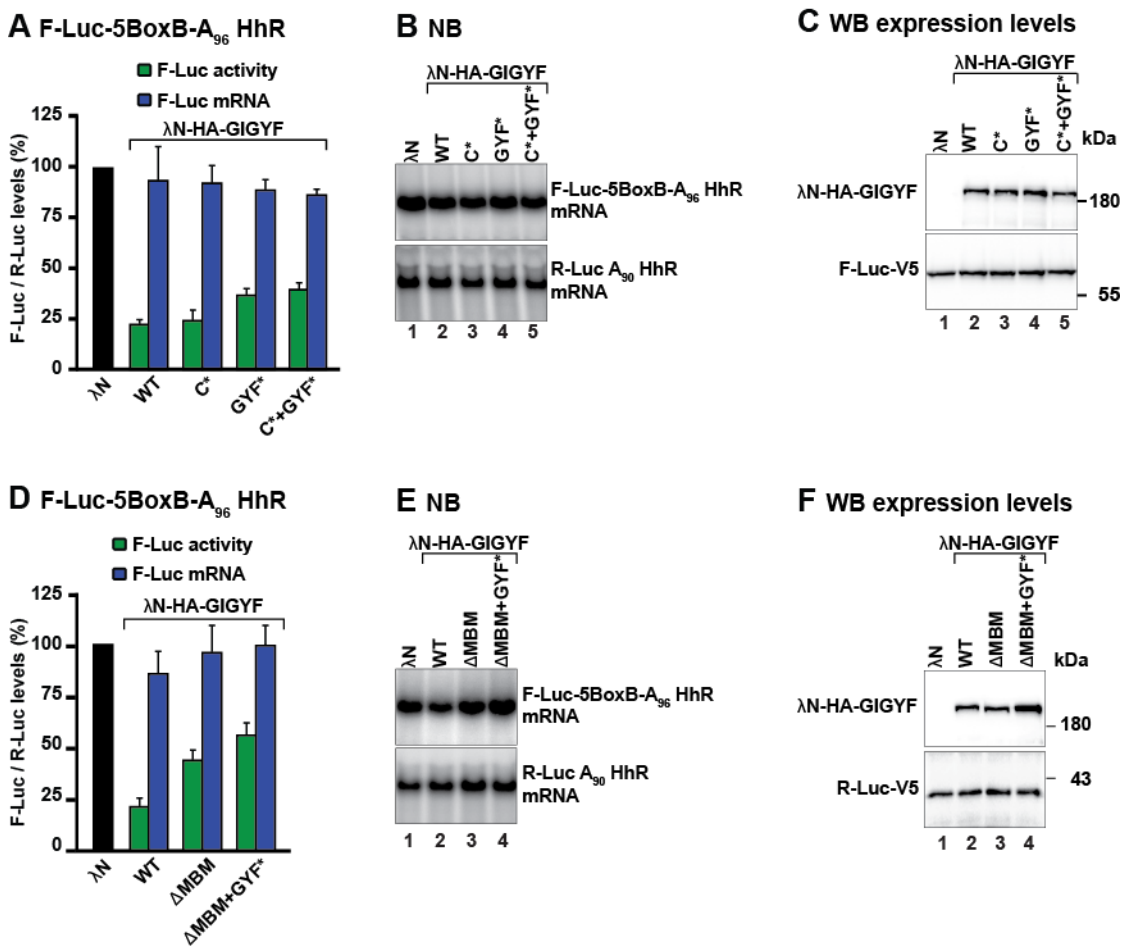

Figure 22. GIGYF requires Me31B and HPat to induce translation repression
(A) Tethering of λN-HA-GIGYF WT and indicated mutants to the F-Luc-5BoxB-A_{96}-HhR reporter in S2 cells. The R-Luc-A_{90}-HhR served as transfection control. The bar graph shows the quantification of the luciferase activity (protein levels, green bars) and mRNA abundance (RNA levels, blue bars). F-Luc levels in cells expressing the λN-HA peptide were normalized to those of the R-Luc and set to 100%. Bars represent the mean values and error bars denote the standard deviation from at least three independent experiments. **(B)** NB of one representative experiment shown in (A). **(C)** Samples as in (A) were analyzed by WB and probed with anti-HA and anti-V5 antibodies. **(D)** Tethering of λN-HA-GIGYF WT and indicated mutants to the F-Luc-5BoxB-A_{96}-HhR reporter in S2 cells. The R-Luc-A_{90}-HhR served as transfection control. The bar graph shows the quantification of the luciferase activity (protein levels, green bars) and mRNA abundance (RNA levels, blue bars). F-Luc levels in cells expressing the λN-HA peptide were normalized to those of the R-Luc and set to 100%. Bars represent the mean values and error bars denote the standard deviation from at least three independent experiments. **(E)** NB of one representative experiment shown in (D). **(F)** Samples as in (D) were analyzed by WB and probed with anti-HA and anti-V5 antibodies.

To confirm that Me31B and HPat are essential for GIGYF-mediated translational repression, I analysed the ability of λN-HA-GIGYF to reduce F-Luc-5BoxB-A_{96}-HhR expression in cells depleted of Me31B or HPat (Fig. 23 D and G). Cellular depletion

of Me31B reduced the repressor function of GIGYF, leading to an increase of F-Luc activity to a 40% compared to 20% in control cells (Fig. 23 A). This result is in line with the data obtained with the GIGYF ΔMBM mutant (Fig. 22 D) and further validated the relevance of Me31B in GIGYF-mediated translational repression. Additionally, tethering of the GIGYF GYF* mutant in Me31B-depleted cells strongly compromised the translational repression function of the protein, as indicated by the increase of F-Luc activity to 70% compared to 40% observed in control cells (Fig. 23 A). This striking result clearly highlighted the importance of the synergic recruitment of Me31B and HPat to a GIGYF-repressed mRNA (Fig. 23 A). As expected, reporter mRNA was not degraded (Fig. 23 B) and the expression levels of GIGYF WT and GYF* mutant were similar in the tested conditions (Fig. 23 C).

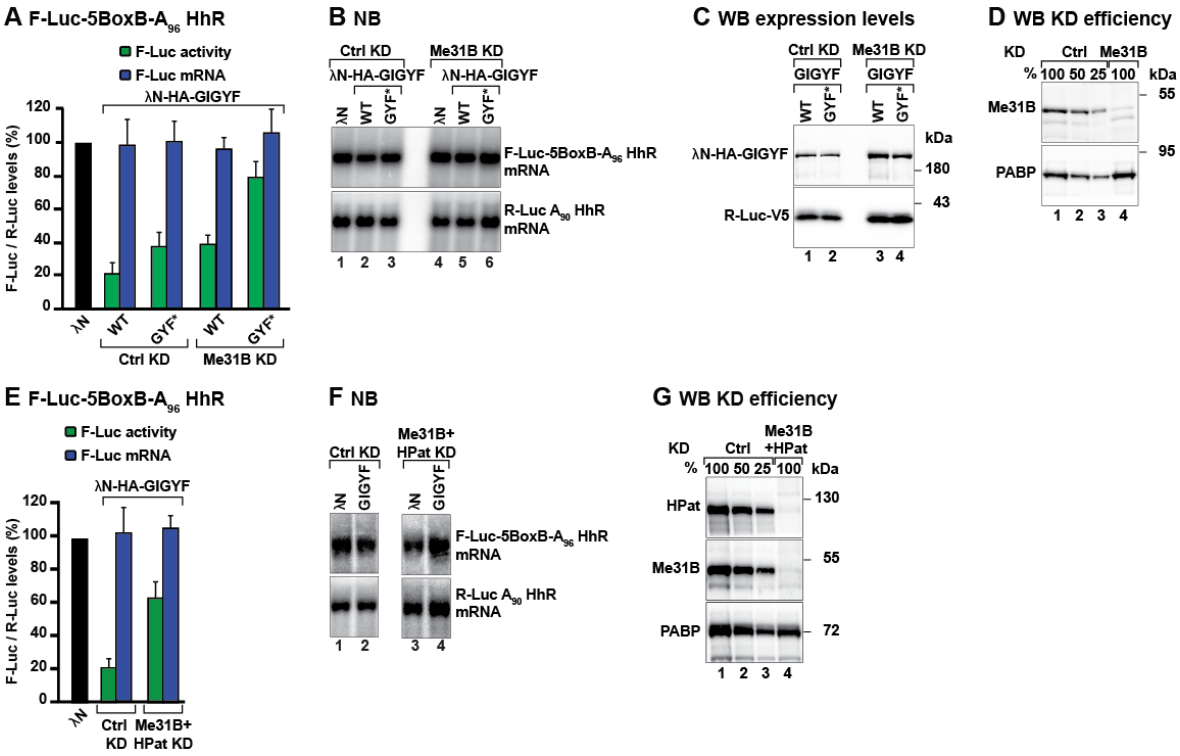

Figure 23. Me31B and HPat contribute to GIGYF-mediated translation repression
(A) Tethering of λN-HA-GIGYF WT or indicated mutant to the F-Luc-5BoxB-A_{96}-HhR reporter. The R-Luc-A_{90}-HhR served as transfection control. The bar graph shows the quantification of the luciferase activity (protein levels, green bars) and mRNA abundance (RNA levels, blue bars). F-Luc levels in cells expressing the λN-HA peptide were normalized to those of the R-Luc and set to 100%. Bars represent the mean values and error bars denote the standard deviation from at least three independent experiments. Cells were treated with dsRNA targeting neomycin (Ctrl KD) or Me31B mRNAs (Me31B KD). **(B)** NB of one representative experiment shown in (A). **(C)** Samples as in (A) were analyzed by WB and stained with anti-HA and anti-V5 antibodies. **(D)** Samples as in (A) were analyzed by WB and stained with anti-

Me31B and anti-PABP antibodies. **(E)** Tethering of λN-HA-GIGYF WT to the F-Luc-5BoxB-A_{96}-HhR reporter. The R-Luc-A_{90}-HhR served as transfection control. The bar graph shows the quantification of the luciferase activity (protein levels, green bars) and mRNA abundance via NB (RNA levels, blue bars). F-Luc levels in cells expressing the λN-HA peptide were normalized to those of the R-Luc and set to 100%. Bars represent the mean values and error bars denote the standard deviation from at least three independent experiments. Cells were treated with dsRNA targeting neomycin mRNA (Ctrl KD) or a combination of dsRNAs targeting Me31B and HPat mRNAs (Me31B+HPat KD). **(F)** NB of one representative experiment shown in (E). **(G)** Samples as in (E) were analyzed by WB and stained with anti-HPat, anti-Me31B, and anti-PABP antibodies.

To strengthen these results, I tethered λN-HA-GIGYF to the F-Luc-5BoxB-A_{96}-HhR reporter in cells depleted of both Me31B and HPat. Coherently with the previous results, the translational repression function of GIGYF was strongly compromised in conditions where GIGYF is unable to interact with the two decay factors (Fig. 23 E and G). Once more, reporter mRNA levels did not change (Fig. 23 F). This experiments finally highlights the involvement of Me31B and HPat in GIGYF-mediated translational repression

6.3 4EHP-mediated mRNA repression requires the recruitment of Me31B and HPat via GIGYF

6.3.1 GIGYF is necessary to recruit Me31B and HPat to 4EHP repressor complexes

GIGYF is required for 4EHP-dependent mRNA repression and it also interacts with decay factors to promote translation repression and mRNA decay. This suggests that binding of GIGYF to HPat and Me31B might be important for 4EHP-mediated translational repression. To verify this hypothesis, I tethered λN-HA-4EHP WT onto the F-Luc-5BoxB-A_{96}-HhR mRNA reporter in cells depleted of endogenous GIGYF (GIGYF KD) and subsequently complemented the cells with dsRNA-resistant versions of HA-GIGYF WT or C*, ΔMBM+GYF*, and N-term mutants (Fig. 24). Overexpression of dsRNA-resistant HA-GIGYF WT in control cells (Ctrl KD), in the absence of 4EHP, did not affect the F-Luc activity compared to the λN-HA (Fig. 24 A), while tethering of λN-HA-4EHP strongly reduced F-Luc activity. As observed previously (Fig. 9 A), in the absence of GIGYF (GIGYF KD) 4EHP repressor function was strongly impaired (Fig. 24 A). 4EHP-mediated

translational repression was restored by transient overexpression of HA-GIGYF WT but not by the expression of the C* mutant, which does not interact with 4EHP (Fig. 24 A). Importantly, overexpression of the HA-GIGYF ΔMBM+GYF* mutant did not restore the repressor function of 4EHP, while the N-term effector region of GIGYF, which contains the interaction sites for HPat and Me31B, was sufficient to entirely restore 4EHP-mediated translational repression (Fig. 24 A). All the proteins were similarly expressed (Fig. 24 B). This complementation assay recapitulates the role of the different factors in mRNA translation repression: 4EHP interacts with GIGYF, which in turn recruits HPat and Me31B to promote mRNA repression.

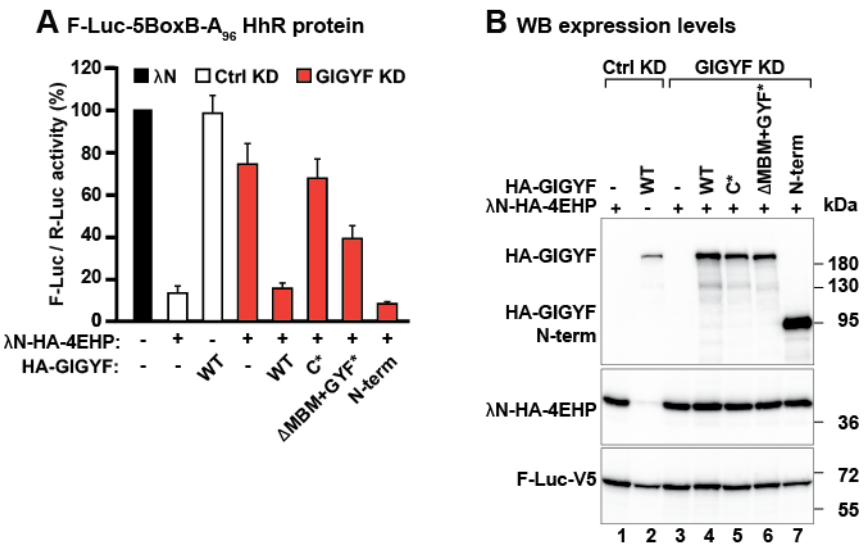

Figure 24. 4EHP requires GIGYF, HPat, and Me31B to repress target mRNA expression
(A) Complementation assay in GIGYF-depleted S2 cells. λN-HA-4EHP WT was tethered to the F-Luc-5BoxB-A_{96}-HhR reporter. The R-Luc-A_{90}-HhR served as transfection control. The bar graph shows the quantification of the luciferase activity (protein levels). F-Luc levels in cells expressing the λN-HA peptide were normalized to those of the R-Luc and set to 100%. Bars represent the mean values and error bars denote the standard deviation from at least three independent experiments. Cells were treated with dsRNA targeting either the neomycin (Ctrl KD, white bars) or GIGYF mRNAs (GIGYF KD, red bars). A vector expressing a dsRNA-resistant version of HA-GIGYF WT or indicated mutants was added to the transfection mixture as indicated. **(B)** Samples as in (A) were analyzed by WB and stained with anti-HA, and anti-V5 antibodies.

6.3.2 GIGYF bridges 4EHP to Me31B and HPat

To verify that GIGYF acts as a bridging factor between 4EHP, HPat, and Me31B, I immunoprecipitated GFP-4EHP in the presence or absence of HA-GIGYF

and analysed its interaction with HPat and Me31B. Interestingly, GFP-4EHP did not efficiently immunoprecipitate endogenous HPat and Me31B unless HA-GIGYF was simultaneously expressed (Fig. 25, lane 7 versus 8). Moreover, the assembly of the 4EHP/GIGYF/Me31B/HPat complex was compromised in cells expressing HA-GIGYF C* or HA-GIGYF ΔMBM+GYF* (Fig. 25, lanes 8 versus 9 and 10), demonstrating the key role of GIGYF in the recruitment of the decay factors to 4EHP repressor complexes.

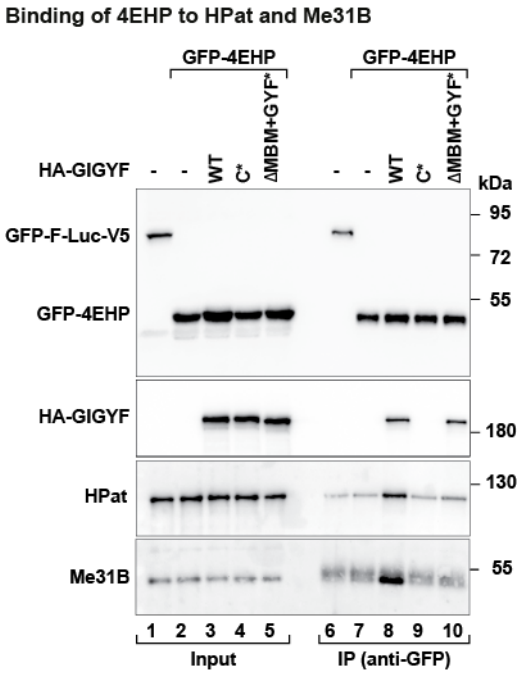

Figure 25. GIGYF bridges 4EHP to the decay factors HPat and Me31B
Immunoprecipitation assay displaying the interaction between GFP-4EHP and endogenous HPat and Me31B in the absence (-) or presence of overexpressed HA-GIGYF WT or indicated mutants. GFP-F-Luc-V5 served as a negative control. The proteins were immunoprecipitated using an anti-GFP antibody. The inputs (4% for GFP- and HA-tagged proteins and 0.1% for endogenous Me31B and HPat) and bound fractions (5% for GFP- and HA-tagged proteins and 20% for endogenous Me31B and HPat) were analyzed by WB and stained with anti-GFP, anti-HA, anti-HPat, and anti-Me31B antibodies.

6.3.3 4EHP requires HPat and Me31B to repress target mRNA expression

To further corroborate the importance of HPat and Me31B for 4EHP-mediated translational repression, λN-HA-4EHP WT was tethered to the F-Luc-5BoxB-A_{96}-HhR reporter in HPat and Me31B co-depleted cells (Fig. 26) (this experiment was performed by Dr. Praveen Bawankar). While in the control cells

tethering of 4EHP lead to a reduction of F-Luc activity to 20%, the depletion of Me31B and HPat strongly impaired the repressor function of 4EHP as shown by an increase of the F-Luc activity to 70% (Fig. 26 A). As expected, the mRNA levels were not affected in this experiment (Fig. 26 B). This result restates the importance of HPat and Me31B in 4EHP-mediated mRNA repression.

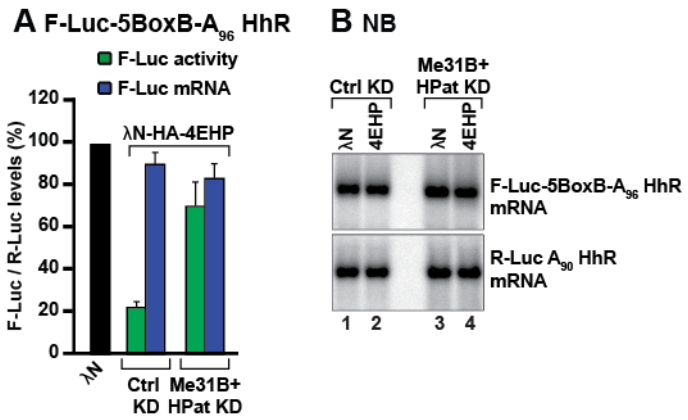

Figure 26. HPat and Me31B are required for 4EHP activity
(A) Tethering of 4EHP to the F-Luc-5BoxB-A96-HhR reporter. The R-Luc-A90-HhR served as transfection control. The bar graph shows the quantification of the luciferase activity (protein levels) and mRNA abundance by NB (blue bars). F-Luc levels in cells expressing the λN-HA peptide were normalized to those of the R-Luc and set to 100%. Bars represent the mean values and error bars denote the standard deviation from at least three independent experiments. Cells were treated with dsRNA targeting neomycin mRNA (Ctrl KD) or a combination of dsRNA targeting Me31B and HPat mRNAs (Me31B+HPat KD). **(B)** NB of one representative experiment shown in (A).

6.3.4 NOT1 might be involved in 4EHP/GIGYF-mediated translational repression

4EHP collaborates with the CCR4-NOT complex in miRNA-mediated gene silencing (Chapat et al., 2017). Moreover, GIGYF also associates with NOT1, the scaffold subunit of the CCR4-NOT complex (Fig. 27 A) and (Amaya Ramirez et al., 2018). Depletion of both HPat and Me31B strongly affects but does not abolish the translational repressor function of both GIGYF and 4EHP (Fig. 23 E and 26 A). To verify if the CCR4-NOT complex, and specifically NOT1, is responsible for the remaining activity of the 4EHP/GIGYF repressor complex, I evaluated the ability of λN-HA-GIGYF and λN-HA-4EHP to inhibit translation of the F-Luc-5BoxB-A_{96}-HhR reporter in NOT1-depleted cells (Fig. 27). Unexpectedly, reduction in NOT1 protein

amount (Fig. 27 B) did not alter the repressor function of either GIGYF or 4EHP. To eliminate the possibility that the remaining NOT1 molecules are recruited to GIGYF via Me31B and/or HPat, known NOT1-binding partners (Haas et al., 2010; Lee et al., 2017; Ozgur et al., 2010), I analysed the ability of the GIGYF ΔMBM+GYF* mutant to repress the translation of the F-Luc-5BoxB-A_{96}-HhR in NOT1-depleted cells. Although the repressor function of this GIGYF mutant is strongly impaired compared to WT protein, no significant changes were observed in cells depleted of NOT1. A similar result was obtained in the tethering of the 4EHP D* mutant upon NOT1 depletion (Fig. 27 A). The results did not depend on different expression levels since the tested proteins were expressed at similar levels (Fig. 27 C). These data indicate that NOT1 might be involved in the translational repressor function of both GIGYF and 4EHP in S2 cells. Nevertheless, more studies need to clarify the precise role of NOT1, and the identification of the binding sites between 4EHP/GIGYF and NOT1 will be extremely important to pin-point the role of NOT1 in 4EHP/GIGYF-mediated translation repression.

Taken together, all the presented experiments strongly support a model where 4EHP interacts with GIGYF, which in turn is essential to recruit Me31B, HPat and NOT1 to the repressor complexes. The recruitment of multiple decays factors by the 4EHP/GIGYF complex ensures that redundant mechanisms operate in the repression of translation and in the control of mRNA stability. Namely, inhibition of eIF4F recruitment to the cap structure coupled with deadenylation and decapping guarantees the successful repression of mRNA expression.

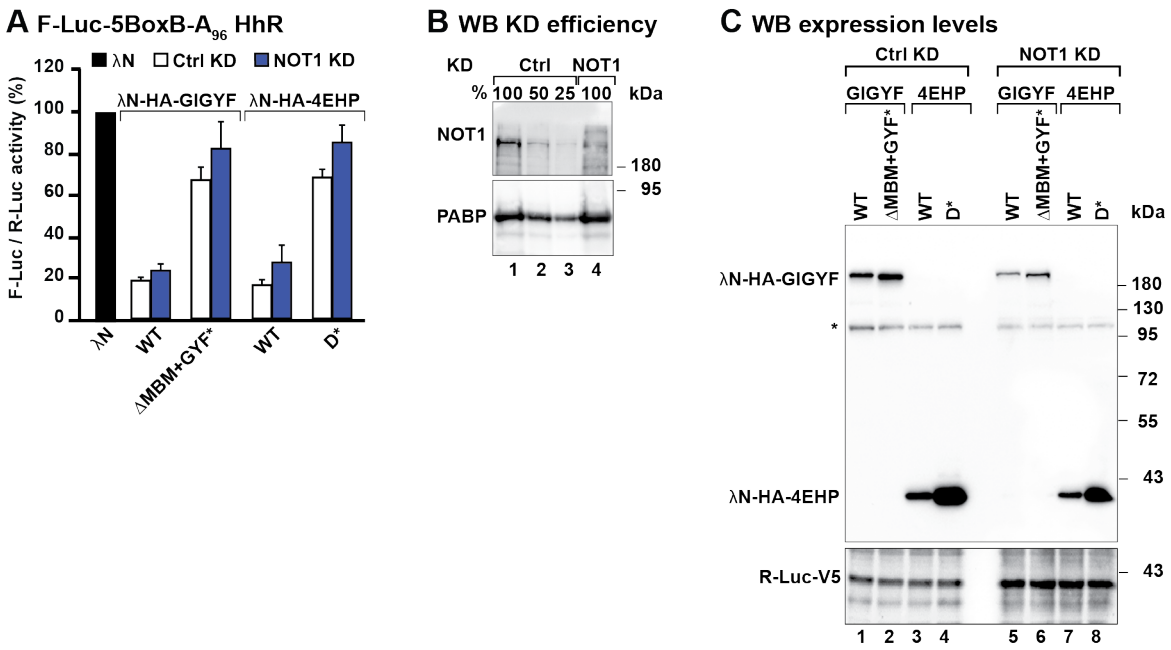

Figure 27. NOT1 has minor contribution in 4EHP/GIGYF-mediated translational repression

(A) Tethering of GIGYF and 4EHP WT or indicated mutants to the F-Luc-5BoxB-A_{96} HhR reporter. The R-Luc-A_{90}-HhR served as transfection control. The bar graph shows the quantification of the luciferase activity. F-Luc levels in cells expressing the λN-HA peptide were normalized to those of the R-Luc and set to 100%. Bars represent the mean values and error bars denote the standard deviation from at least three independent experiments. In this experiment cells were treated with dsRNA targeting neomycin (Ctrl KD, white bars) or NOT1 mRNAs (NOT1 KD, blue bars). **(B)** Samples as in (A) were analyzed by WB and stained with anti-NOT1 and anti-PABP antibodies. **(C)** Samples as in (A) were analyzed by WB and stained with anti-HA and anti-V5 antibodies.

7 Discussion

7.1 *D. melanogaster* 4EHP and GIGYF are different from their cognate human proteins

4EHP is a cap binding protein, that acts as a transcript-specific translational repressor in complex with different partner proteins required for the specificity of its action. For example, in *D. melanogaster* embryos, the binding of 4EHP to the RBPs Brat and Bicoid is necessary to inhibit the expression of mRNAs required to define the anterior-posterior body axes of the fly (Cho et al., 2006; Cho et al., 2005). In human cells, the scaffold proteins GIGYF1/2 have been identified as a 4EHP-interacting proteins important for translational repression (Peter et al., 2017). Moreover, the role of 4EHP in human cell lines has been expanded to miRNA-mediated gene silencing via its association with 4E-T (Chapat et al., 2017), an important actor on this regulative mechanism. Nevertheless, the molecular mechanism by which 4EHP and its interacting partners mediate translation repression has not been defined yet.

To obtain molecular detail on the mechanism employed by 4EHP to repress target mRNA expression, I studied the function of the uncharacterized *Dm* 4EHP. Thus, I analysed the interaction with known *D. melanogaster* RBPs such as Brat and Bicoid. Immunoprecipitation assays revealed that the aforementioned did not interact with 4EHP in S2 cells (Fig. 8 A and B). A possible explanation for this difference is that the interaction with those RBPs might be indirect and mediated by a bridging protein, which could be absent in S2 cells or be specific for *D. melanogaster* embryos (Cho et al., 2006; Peter et al., 2017). This opens the possibility that 4EHP might regulate translation in different ways according to the cell type. Very surprising was also the observation that *Dm* 4EHP failed to interact with *Dm* 4E-T (Fig. 8 C), an important regulator of the RISC complex. However, the molecular principals that explain the binding affinity difference between *Dm* 4E-T and 4EHP are not yet understood. More experiments are required to address the structural binding properties of these two proteins in S2 cells.

Intriguingly, I identified *Dm* GIGYF as a 4EHP-interacting protein in S2 cells (Fig. 7) and the fact that this is, so far, the only conserved partner, opens several important questions on their biological roles and functional interaction. Interestingly,

taking the structure of the human 4EHP/GIGYF complex (Peter et al., 2017) as a model, it has been possible to verify that the interaction mode between these two proteins is conserved in *D. melanogaster* and it maintains the same molecular principles, adopting a tripartite binding mode (Fig. 7). In human, this architecture is fundamental to increase the binding specificity of GIGYF for 4EHP instead of eIF4E and it is possible that this high specific interaction is important in *D. melanogaster* as well. The conservation of the binding mode highlights also the relevance of the functions mediated by this two proteins. In my doctoral studies, I extensively studied the role of 4EHP and GIGYF in translation repression, which I will discuss more in detail afterwards. Nevertheless, GIGYF is the only *Dm* 4EHP-binding protein identified so far, suggesting that the GIGYF/4EHP complex could regulate functions that in other species are regulated by complexes of 4EHP with other proteins.

Since none of the known 4EHP-interacting RBPs, as Bicoid and Brat, bind 4EHP in S2 cells, it is possible that GIGYF could interact with some RBPs, to ensure the recruitment of the complex on the mRNA. Indeed, two GIGYF interactors have been identified in mammals, such as the RBPs TTP and ZNF598, which directs the 4EHP/GIGYF complex on specific mRNA transcripts (Fu et al., 2016; Morita et al., 2012). These are GYF domain-binding proteins that possess the typical PPGΦ motifs and, given the highly sequence similarity of the GYF domains in human *and Dm* GIGYF, it is likely that it might be recruited to target mRNA by these proteins. However, Tis11, the insect orthologue of TTP, and *Dm* ZNF598 failed to bind to GIGYF in S2 cells (Fig. 15 A and B). Sequence analysis highlighted the absence of the typical PPGΦ sequence in Tis11, which could explain the lack of interaction with GIGYF, while *Dm* ZNF598 possess a tandem PPGΦ motif, thus it is so far not clear why these two proteins do not interact. The lack of conservation of the interaction between RBPs and GIGYF, as well as with 4EHP, leaves an open question concerning their recruitment on the mRNA. It will be important in the future to further investigate the link between the 4EHP/GIGYF complex and the corresponding RBPs in different organisms. Moreover, the identification of GIGYF as an RBP in mammalian cells (Amaya Ramirez et al., 2018) is a very intriguing possibility that will have to be tested in *D. melanogaster*.

These remarking differences in the interaction partners may suggest different transcript-specific regulation of the 4EHP/GIGYF complex in different species,

opening several questions about the mechanism employed to repress target mRNA expression in these cells.

7.2 4EHP/GIGYF-mediated mRNA-repression

The 4EHP/GIGYF translational repressive complex regulates the expression of specific mRNA transcripts. The data resulting from the tethering assays indicates that in S2 cells 4EHP induces translational repression (Fig. 9), in agreement with several previous reports in mammals (Chapat et al., 2017; Fu et al., 2016; Morita et al., 2012). Additionally, my data point towards a previously uncharacterised role of 4EHP in regulating mRNA stability (Fig. 9). Moreover, 4EHP activities are dependent on GIGYF binding (Fig. 9), in line with a study concerning translation repression performed in human cells (Peter et al., 2017).

In this work, I show in great detail the relevance of GIGYF interaction for 4EHP-mediated mRNA decay. In fact, in S2 cells, GIGYF associates with different decay factors and subunits of the CCR4-NOT complex (Fig. 13 and 14). These data confirm recent findings that associated the human GIGYF2 with the CCR4-NOT complex, to regulate the expression of a subset of mRNAs (Amaya Ramirez et al., 2018). Moreover, GIGYF, like 4EHP, has been associated to the regulation of miRNA-mediated gene silencing, since GIGYF2 is an Ago2 and TNRC6/GW182-binding partner, in human cells (Chapat et al., 2017; Kryszke et al., 2016; Schopp et al., 2017). However, *Dm* GIGYF does not interact with GW182 (Fig. 15 C) and *Dm* 4EHP failed to interact with 4E-T (Fig. 8 C), also involved in the miRNA mediated translational repression (Chapat et al., 2017), possibly suggesting that *Dm* 4EHP/GIGYF complex may be important to regulate mRNA expression in a miRNA-independent manner. Coherently, I demonstrated that GIGYF directs mRNA targets towards the cytoplasmic 5’ to 3’ decay pathway (Fig. 11), a hypothesis supported by the several interactions with factors belonging to this regulative mechanism (Fig. 13 and 14), never described before. Although my data suggest that GIGYF triggers the 5’ to 3’ decay pathway, experiments employing miRNA-responsive mRNA reporter will be important to clarify the possible role of GIGYF in miRNA-mediated silencing pathway.

Taken together these experiments demonstrate a role for GIGYF in the 4EHP-repressive mechanism. They also suggest that the cap binding activity might

be important in anchoring 4EHP onto the mRNA, in combination with an RBP. This would allow GIGYF to recruit the decay machineries thus promoting mRNA decay. In fact, in experimental condition where the anchorage requirement is bypassed, for example in the tethering assay, the cap-binding function of 4EHP is dispensable (Fig. 9). It would be interesting to study the effect of the cap-binding 4EHP defective mutant in more physiological condition, for example by analysing the effect on the target mRNA *in vivo*. Consequently, it will be important to identify endogenous mRNA targets of GIGYF/4EHP, since at the moment there is limited knowledge and only few examples of target mRNA are reported for the single proteins (Amaya Ramirez et al., 2018; Jafarnejad et al., 2018).

7.3 GIGYF allows the formation of a network of interactions

As aforementioned, GIGYF is a major regulator of mRNA stability that links 4EHP to the deadenylation and decapping machinery (Fig. 12, 24, and 26). In fact, it interacts with HPat, Me31B and NOT1 (Fig. 13), as well as POP2, NOT3, and EDC3 (Fig. 14). Moreover, detailed studies on the molecular interaction with these partners showed that GIGYF binds to HPat and Me31B through different, previously unidentified, discrete motifs (Fig.17 and 20). Therefore, multiple binding partners can be simultaneously docked on GIGYF, which recruits them to the mRNA target. This suggests that GIGYF might be a newly identified stable component that links decapping complex and deadenylation machinery.

7.3.1 GIGYF-HPat interaction

In this work, I described for the first time that *Dm* HPat is a GIGYF-binding protein (Fig. 13 C). HPat is a conserved scaffold protein in eukaryotes that links deadenylation and decapping by binding to different factors involved in translational repression and mRNA decay (Haas et al., 2010; Marnef and Standart, 2010). It has a Proline-rich region containing two PPGΦ motifs (Fig. 20 A); the PPGΦ, in different proteins, have been previously described to be involved in the interaction with the GYF (Ash et al., 2010; Giovannone et al., 2003). Although it has never been reported the interaction of HPat- PPGF to GIGYF.

The interaction studies with mutated proteins demonstrated that the GIGYF-HPat binding requires the GYF domain of GIGYF and two PPGF motifs in HPat (Fig. 20

C). This interaction is likely to be direct and is independent on Me31B (Fig. 20 D), a known interactor partner of both HPat (Haas et al., 2010) and GIGYF (Fig.13 B). Interestingly, HPat is the only GYF-binding protein identified in *D. melanogaster*, while many others GIGYF-binding proteins interacting with the GYF domain have been identified in mammals (Ajiro et al., 2009; Fu et al., 2016; Kryszke et al., 2016; Morita et al., 2012; Schopp et al., 2017). Although this interaction is conserved in human cells (data from our lab, not shown), the recruitment of *Dm* HPat will most probably be different because the human orthologues PATL1 does not contain the PPGΦ motifs. This illustrates how diverse is the recruitment of the actors between *D. melanogaster* and human, a common feature of the decapping associated factors. Even though it is different, the interaction between *Dm* HPat and *Hs* PATL1 with GIGYF is conserved, suggesting that the role mediated by these proteins is maintained in the two species. Both of them appear to have a similar scaffolding function that allow the reinforcement and redundant repressive activity, which, as observed by the interaction with 4EHP/GIGYF, has also a prominent translational repressive activity.

7.3.2 GIGYF-NOT1 interaction

NOT1 is the scaffold subunit of the CCR4-NOT complex, one of the most studied deadenylase machinery in the cell, and it is recruited to mRNA targets by several RBPs, which highlight the fundamental role of this protein in regulating gene expression. Interestingly, GIGYF strongly interacts with NOT1 and the CCR4-NOT complex (Fig. 13 and 14) and this binding does not require either Me31B or HPat (Fig. 20 B), both NOT1 and CCR4-NOT complex binding partners (Haas et al., 2010; Lee et al., 2017). However, although the interaction with NOT1 is very efficient (Fig. 13 A), it was not possible to pin-point the exact interaction region, since the separation of GIGYF in N- and C-term strongly decreased its interaction with NOT1 (Fig. 16 B), possibly indicating that GIGYF uses multiple binding sites, located in both N- and C-term, to associate with NOT1. Once more, it seems that there are differences between human and *D. melanogaster* GIGYF, since in human cell lines it has been identified that NOT1 interacts with the N-term region of GIGYF (Amaya Ramirez et al., 2018). Nevertheless, employing multiple binding sites is a common way to recruit the deadenylase machinery to the mRNA. It has been observed for

other RNA-associated factors, such as CUP in recruiting NOT1 in *D. melanogaster* (Igreja and Izaurralde, 2011), or a multitude of different proteins that bind different subunit of the CCR4-NOT complex (Bawankar et al., 2013; Fabian et al., 2013; Raisch et al., 2016; Sgromo et al., 2018; Zekri et al., 2013). In conclusion, NOT1 is a stable binding partner of GIGYF, however more experiments are required to precisely identify the NOT1 binding regions on *Dm* GIGYF.

7.3.3 GIGYF-Me31B interaction

Another crucial GIGYF-interactor partner identified in this study is Me31B (Fig. 13 B), an ATP-dependent RNA helicase. Its human orthologues, DDX6, is activated by the binding with NOT1 and is required in miRNA-mediated gene silencing (Mathys et al., 2014; Presnyak and Coller, 2013). Moreover, Me31B/DDX6 has many roles in regulating translational repression and mRNA decay and has been widely studied in different species, from yeast to human (Jonas and Izaurralde, 2013; Wang et al., 2017). Interestingly, the interaction of Me31B to *Dm* GIGYF is direct and independent on HPat (Fig. 18 and 17), another known Me31B-interactor partner (Fig. 20 D). Revealing the details of the interaction between GIGYF and Me31B has an extremely relevant role for understanding the functions mediated by these two proteins in translation repression. By several interaction studies I identified a Me31B-binding motif (MBM), necessary and sufficient for the binding (Fig. 13, 17 and 18), and, as shown by bioinformatics analysis, has sequence similarity with the known Me31B-interacting CHD domain, present in both human and *Dm* 4E-T and in *Dm* CUP (Fig. 17 A). Similarly, to the known interacting domain, GIGYF adopts a bipartite binding mode in complex with Me31B defined by a PEW motif that folds into a small coiled element upon binding to Me31B and a discontinuous FDx_4F motif characterized by two beta hairpins (Fig. 18). Both binding motifs insert the side chain of the aromatic residues (W348 and F360 F366) into two hydrophobic pockets of the RecA2 domain of Me31B (Fig. 18). The FDx_4F motif is a newly identified and unique version of the known FDF motif, that mediates the interaction of DDX6/Me31B with EDC3, LSM14 and HPat (Brandmann et al., 2018; Jonas and Izaurralde, 2013; Ozgur et al., 2015; Tritschler et al., 2009), where structural arrangements occupy the same hydrophobic pockets with the two Phe of the FDF motif (or similarly with IEL motif of 4E-T and CUP). Interestingly, this

Me31B/DDX6 binding surface is shared between several subunits of translational repression and decay complexes, such as 4E-T, EDC3, HPat (Brandmann et al., 2018; Jonas and Izaurralde, 2013; Mathys et al., 2014; Ozgur et al., 2015; Tritschler et al., 2009; Valkov et al., 2017). This would exclude the binding of Me31B/DDX6 with more than one of the aforementioned partner in the same repressor complex and the consequent formation of different and specific RNPs that might have different functions.

7.3.4 4EHP/GIGYF and HPAT/Me31B/NOT1 interaction

Intriguingly, the newly identified GIGYF-interacting decay factors can also independently associate with each other (Haas et al., 2010).

Different proteins, as GIGYF, 4E-T, HPat, EDC3, share the same binding surface on Me31B/DDX6, while NOT1 interacts with Me31B/DDX6 through another region located more towards the C-terminus in the RecA2 domain (Mathys et al., 2014; Ozgur et al., 2015). Therefore, it is conceivable the formation of a trimeric complex between Me31B/DDX6, NOT1, and any of the mentioned protein. However, structural studies reported that the formation of the trimeric complex is favourable only between 4E-T, DDX6 and NOT1, due to a chemically favourable environment formed by a polar residue preceding the IEL (FDF-like motif) of 4E-T, which, when bound to Me31B/DDX6, points towards a negatively charged residue of NOT1 (Mathys et al., 2014; Ozgur et al., 2015). Conversely, EDC3 and Pat1 (orthologue of HPat in *S. cerevisiae*) cannot form a trimeric complex with Me31B/DDX6 and NOT1, because of a negatively charged residue preceding the FDF motif that locates in close proximity of a negatively charged residue of NOT1 (Ozgur et al., 2015). Interestingly, the crystal structure and the sequence analysis obtained in this study (Fig. 16 and 17), show that the interaction with Me31B/DDX6 forms on GIGYF a similar chemically favourable environment as identified in 4E-T, with a polar residue preceding the FDx_4F motif, which would allow the formation of the trimeric complex with NOT1. The constitution of a complex between Me31B/DDX6, NOT1 and either GIGYF (this thesis) or 4E-T (Ozgur et al., 2015) would be important to ensure a strong repression of an mRNA target, combining the recruitment of deadenylation machinery and decapping complex, and blocking translation.

Moreover, Me31B and HPat interact with GIGYF independently to each other (Fig. 17 and 20) and, although GIGYF and HPat cannot interact with Me31B at the same time, it is possible that HPat and Me31B can simultaneously dock onto GIGYF, which could theoretically allow the concomitant binding of NOT1. In addition, HPat is also interacting with the CCR4-NOT complex via a region located C-terminally of the P-rich region (Haas et al., 2010), therefore it could interact simultaneously with GIGYF and subunits of the CCR4-NOT.

Despite no data are currently available to specifically address these details, the speculation about the formation of such network of interactions raises many questions concerning the assembly of one or many repressive complexes and their composition in different organisms, due also to the presence of many other decay factors that are not taken in consideration in this model. Moreover, most the interactions, identified in this thesis, such as HPat Me31B/DDX6, NOT1 and subunits of the CCR4-NOT complex, are preserved in human, indicating that this mechanism is conserved also in other species, pointing towards its functional relevance. Thus, the identification of GIGYF as a huge docking platform opens the possibility for many additional experiments required to clarify the composition of these intricate network of interactions.

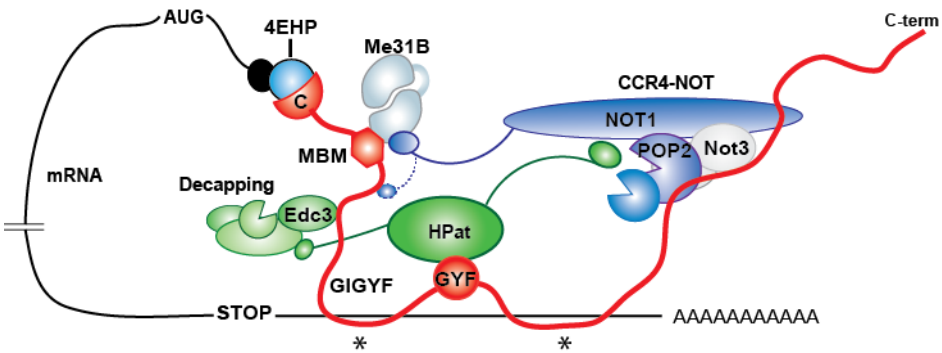

Figure 28. Interaction network between GIGYF and the downstream effectors
This model describes the possible interaction network of the 4EHP/GIGYF complex with the decay factors identified in this study. GIGYF (red) interacts with 4EHP (light blue), which binds the cap structure of the target mRNA (black). GIGYF might also directly interact with mRNA target (asterisks) as suggested by (Amaya Ramirez et al., 2018), or via different RBPs (not shown). Moreover, GIGYF interacts with Me31B (grey), HPat (green), and NOT1 (blue), by a simultaneous interaction in distinct binding sites (MBM and GYF for Me31B and HPat, respectively). The weaker interaction with EDC3, NOT3 and POP2 are also depicted. Furthermore, these decay factors can interact with each other and recruit additional subunits of the decapping and deadenylation machineries.

7.4 4EHP/GIGYF require HPat and Me31B for mRNA regulation

The identification of HPat and Me31B as GIGYF direct interacting partners and the characterization of the binding domain/motif allowed the detailed study of the molecular mechanism employed by GIGYF and 4EHP in the control of translation and mRNA stability. The newly identified GIGYF-interacting partners Me31B and HPat, cooperate in GIGYF-mediated mRNA repression (Fig. 22). In fact, single binding mutants or knockdowns that impair the interaction of Me31B or HPat partially compromised GIGYF repressor function, whereas the double mutations or knockdowns greatly diminished GIGYF activity (Fig. 21, 22, and 23). Moreover, the interaction of GIGYF with HPat and Me31B is also required for 4EHP-mediated translational repression (Fig. 24). These results support and expand our understanding on the regulation of mRNA expression by the 4EHP/GIGYF complex. Specifically, multiple and redundant protein-protein interactions mediated by GIGYF allow the assembly of an efficient 4EHP/GIGYF-repressor complex that inhibits translation and directs target mRNAs to decay (Fig. 29).

The recruitment of DDX6, Me31B human orthologue, to target mRNA is a known mechanism employed to regulate translation repression. In particular, it has been described the role of 4E-T in linking 4EHP to DDX6 and the CCR4-NOT complex to induce translation repression and mRNA decay in miRNA-mediated gene silencing (Chapat et al., 2017). Both 4E-T and GIGYF link 4EHP to downstream effector partners, but have mutually exclusive interaction with DDX6/Me31B, therefore they are part of different RNPs, and most probably, regulate different mRNA targets. Additional studies on endogenous target will be required to better understand the different mode of action of these two proteins.

Nevertheless, in the absence of HPat and Me31B the repressor function of 4EHP and GIGYF is not completely blocked, indicating that other factors may be involved (Fig. 23 E and 26 A). Indeed, GIGYF also interacts with the components of the CCR4-NOT complex, NOT1, NOT3, and POP2 (Fig. 13 and 14). The binding of GIGYF to the deadenylation complex has been recently shown to be important for the regulation of several endogenous mRNA targets (Amaya Ramirez et al., 2018). However, in S2 cells knockdown of NOT1 did not significantly altered the ability of GIGYF or 4EHP to repress translation (Fig. 27). The different requirement for the deadenylation complex in *Dm* 4EHP/GIGYF-mediated mRNA repression indicates

that the repressive mechanism is ensured by a multitude of redundant repressors. For example, reduced levels of NOT1 may not be sufficient to hamper the deadenylase activity of the CCR4-NOT complex and KD of multiple CCR4-NOT associated proteins may be required to block GIGYF-mediated repressor function. In agreement with this, it has been recently shown the requirement of concomitant KDs of different deadenylase enzymes of the CCR4-NOT complex in order to reduce GIGYF-repressor functions (Amaya Ramirez et al., 2018). Additional experiments altering the participation in the repressive mechanism of the different RNA decay-associated enzymes, will be important to clarify the selective involvement of the repressive mechanism. Moreover, GIGYF also interacts with other factors of the CCR4-NOT complex, such as POP2 (CNOT8 in human) and NOT3 (Fig. 14 and 28), together with the decapping-associated protein EDC3, ensuring a robust stability and coordination of the repressive events, which may begin with the translation block and the binding of 4EHP to the cap, followed by the recruitment of the deadenylation machinery and the decapping complex (Fig. 29).

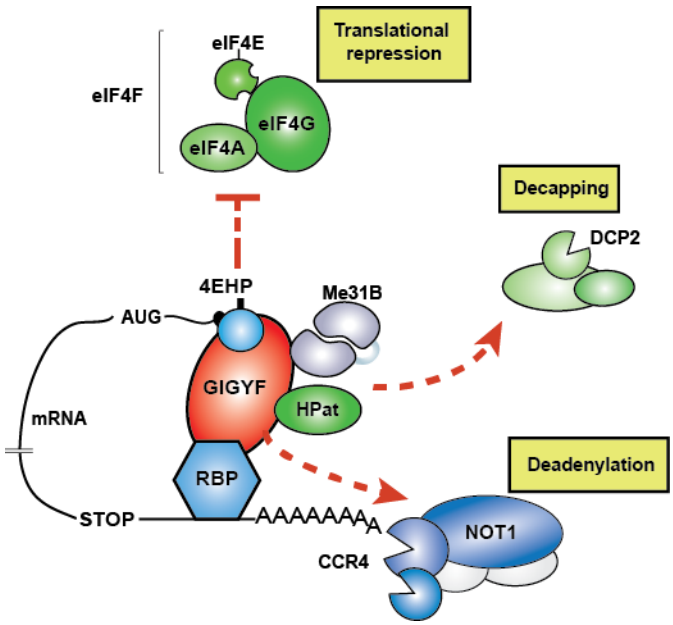

Figure 29. Mechanistic model of 4EHP/GIGYF complex repressive function
This model describes the presence of redundant protein-protein interactions established by the 4EHP/GIGYF complex. 4EHP binds the cap structure at the 5' end of the mRNA (black dot) and GIGYF connects 4EHP to the mRNA, through the interaction with specific RBPs or possibly by directly binding to the mRNA. In addition, GIGYF uses multiple binding motifs to simultaneously bind to Me31B and HPat. Furthermore, GIGYF recruits the CCR4-NOT complex. Therefore, the 4EHP/GIGYF complex competes with eIF4F for binding to the cap

structure of the mRNA and recruits the decapping and the deadenylation complexes to the mRNA to ultimately promote translational repression and mRNA decay.

7.5 GIGYF biological role

In this work, I proposed a working model describing the function of GIGYF as a repressor of mRNA expression (Fig. 29). This is a scaffold protein that elicits translational repression and decay of a 4EHP-bound mRNA via multiple protein-protein interactions. During my doctorate studies, I obtained significant knowledge on the interaction network and repression function of GIGYF proteins (Fig. 28 and 29), which will be helpful for studying also other biological roles described for these proteins. For examples my data will be valuable to better elucidate the molecular mechanism of action of 4EHP/GIGYF and Me31B/HPat/NOT1 complex/es with TTP and to further understand the regulation of ARE-containing mRNA that are linked to cytokines and immune regulation (Fu et al., 2016). Moreover, these experiments will clarify the involvement of 4EHP/GIGYF in embryonic development, which has been suggested by different lines of evidence, since both proteins are important for the vitality and correct development of mouse embryos (Morita et al., 2012). Additionally, the identification of DDX6, NOT3, and EDC3 as GIGYF-interactors strongly support a role of this protein in the regulation of stem cells renewal. In fact, those proteins have a relevant role in stem cell regulation. For example, DDX6, in association with EDC3, is important to repress key mRNA targets of differentiation inducing transcription factors, maintaining progenitor cell function. Moreover, also CNOT3 has been reported to maintain pluripotent cell state via mRNA deadenylation (Nicklas et al., 2015; Wang et al., 2015; Zheng et al., 2012; Zheng et al., 2016; Zhou et al., 2017).

Additionally, GIGYF proteins have been related to a multitude of different cellular activities not directly connected with each other. They were initially identified in human cells as interactors of the adaptor protein Grb10, which binds the intracellular domain of an activated tyrosine kinase receptor (Giovannone et al., 2003). This interaction is important in the regulation of insulin-like growth factor receptor signalling and has been linked to neurodegeneration and cognitive impairments in mice (Giovannone et al., 2003; Giovannone et al., 2009; Xie et al., 2014). Moreover, in *D. melanogaster* GIGYF participates in the regulation of

physiological autophagy required for proper neuron and muscle homeostasis (Kim et al., 2015). Furthermore, GIGYF proteins have also been associated to Parkinson disease (Tan and Schapira, 2010; Zhang et al., 2015) and are connected to the regulation of EGFR-induced phosphorylation pathway and the subsequent activation of the AKT kinase in mammary carcinogenesis (Ajiro et al., 2009; Ajiro et al., 2010; Desbuquois et al., 2013).

To date it is still unclear if these biological functions of GIGYF proteins are related to the mRNA repression function investigated in this work. Since they are large scaffold proteins that can be engaged in multiple protein-protein interactions, it is possible that GIGYF proteins also have functional roles unrelated to mRNA control. Indeed, this work highlights that all the identified GIGYF elements required for mRNA regulation, as 4EHP-BM, MBM, and the GYF domain, are limited to the N-term of the protein (Fig. 17 A). So far it seems that the C-term region of GIGYF contributes only to a minor extent in reporter mRNA repression and no conserved motif or functional role has been identified for this region. Characterization of the functions of the C-term of GIGYF in mRNA regulation or other unrelated cellular processes is therefore a new challenge to elucidate the biological roles of GIGYF proteins. Future studies that will aim to identify new binding partners of GIGYF interacting with its C-term region will be helpful to answer these questions.

In conclusion, this work gives more detailed information concerning the role of GIGYF in mRNA regulation and opens new possible lines of study of the function of this protein in multiple and apparently unrelated processes.

8 References

Afonine, P.V., R.W. Grosse-Kunstleve, N. Echols, J.J. Headd, N.W. Moriarty, M. Mustyakimov, T.C. Terwilliger, A. Urzhumtsev, P.H. Zwart, and P.D. Adams. 2012. Towards automated crystallographic structure refinement with phenix.refine. *Acta crystallographica. Section D, Biological crystallography*. 68:352-367.

Ajiro, M., T. Katagiri, K. Ueda, H. Nakagawa, C. Fukukawa, M.L. Lin, J.H. Park, T. Nishidate, Y. Daigo, and Y. Nakamura. 2009. Involvement of RQCD1 overexpression, a novel cancer-testis antigen, in the Akt pathway in breast cancer cells. *International journal of oncology*. 35:673-681.

Ajiro, M., T. Nishidate, T. Katagiri, and Y. Nakamura. 2010. Critical involvement of RQCD1 in the EGFR-Akt pathway in mammary carcinogenesis. *International journal of oncology*. 37:1085-1093.

Amaya Ramirez, C.C., P. Hubbe, N. Mandel, and J. Bethune. 2018. 4EHP-independent repression of endogenous mRNAs by the RNA-binding protein GIGYF2. *Nucleic Acids Res*.

Andreou, A.Z., and D. Klostermeier. 2014. eIF4B and eIF4G jointly stimulate eIF4A ATPase and unwinding activities by modulation of the eIF4A conformational cycle. *J Mol Biol*. 426:51-61.

Antonchuk, J., G. Sauvageau, and R.K. Humphries. 2002. HOXB4-induced expansion of adult hematopoietic stem cells ex vivo. *Cell*. 109:39-45.

Arribas-Layton, M., D. Wu, J. Lykke-Andersen, and H. Song. 2013. Structural and functional control of the eukaryotic mRNA decapping machinery. *Biochim Biophys Acta*. 1829:580-589.

Ash, M.R., K. Faelber, D. Kosslick, G.I. Albert, Y. Roske, M. Kofler, M. Schuemann, E. Krause, and C. Freund. 2010. Conserved beta-hairpin recognition by the GYF domains of Smy2 and GIGYF2 in mRNA surveillance and vesicular transport complexes. *Structure*. 18:944-954.

Aylett, C.H.S., and N. Ban. 2017. Eukaryotic aspects of translation initiation brought into focus. *Philosophical transactions of the Royal Society of London. Series B, Biological sciences*. 372:20160186.

Baralle, M., and F.E. Baralle. 2018. The splicing code. *Biosystems*. 164:39-48.

Bartel, D.P. 2018. Metazoan MicroRNAs. *Cell*. 173:20-51.

Bawankar, P., B. Loh, L. Wohlbold, S. Schmidt, and E. Izaurralde. 2013. NOT10 and C2orf29/NOT11 form a conserved module of the CCR4-NOT complex that docks onto the NOT1 N-terminal domain. *RNA Biol*. 10:228-244.

Beck, M., and E. Hurt. 2016. The nuclear pore complex: understanding its function through structural insight. *Nature Reviews Molecular Cell Biology*. 18:73.

Behm-Ansmant, I., J. Rehwinkel, T. Doerks, A. Stark, P. Bork, and E. Izaurralde. 2006. mRNA degradation by miRNAs and GW182 requires both CCR4:NOT deadenylase and DCP1:DCP2 decapping complexes. *Genes Dev*. 20:1885-1898.

Bicknell, A.A., and E.P. Ricci. 2017. When mRNA translation meets decay. *Biochem Soc Trans*. 45:339-351.

Biffo, S., N. Manfrini, and S. Ricciardi. 2018. Crosstalks between translation and metabolism in cancer. *Curr Opin Genet Dev*. 48:75-81.

Björk, P., and L. Wieslander. 2014. Mechanisms of mRNA export. *Seminars in Cell & Developmental Biology*. 32:47-54.

Brandmann, T., H. Fakim, Z. Padamsi, J.Y. Youn, A.C. Gingras, M.R. Fabian, and M. Jinek. 2018. Molecular architecture of LSM14 interactions involved in the assembly of mRNA silencing complexes. *The EMBO Journal*.

Braun, J.E., E. Huntzinger, M. Fauser, and E. Izaurralde. 2011. GW182 proteins directly recruit cytoplasmic deadenylase complexes to miRNA targets. *Mol Cell*. 44:120-133.

Cao, R. 2018. mTOR Signaling, Translational Control, and the Circadian Clock. *Frontiers in genetics*. 9:367.

Carmody, S.R., and S.R. Wente. 2009. mRNA nuclear export at a glance. *Journal of cell science*. 122:1933-1937.

Cate, J.H.D. 2017. Human eIF3: from 'blobology' to biological insight. *Philosophical transactions of the Royal Society of London. Series B, Biological sciences*. 372:20160176.

Chang, C.T., N. Bercovich, B. Loh, S. Jonas, and E. Izaurralde. 2014. The activation of the decapping enzyme DCP2 by DCP1 occurs on the EDC4 scaffold and involves a conserved loop in DCP1. *Nucleic Acids Res*. 42:5217-5233.

Chapat, C., S.M. Jafarnejad, E. Matta-Camacho, G.G. Hesketh, I.A. Gelbart, J. Attig, C.G. Gkogkas, T. Alain, N. Stern-Ginossar, M.R. Fabian, A.C. Gingras, T.F.

Duchaine, and N. Sonenberg. 2017. Cap-binding protein 4EHP effects translation silencing by microRNAs. *Proc Natl Acad Sci U S A*. 114:5425-5430.

Chen, C.A., and A.B. Shyu. 2017. Emerging Themes in Regulation of Global mRNA Turnover in cis. *Trends in biochemical sciences*. 42:16-27.

Chen, Y., A. Boland, D. Kuzuoglu-Ozturk, P. Bawankar, B. Loh, C.T. Chang, O. Weichenrieder, and E. Izaurralde. 2014. A DDX6-CNOT1 complex and W-binding pockets in CNOT9 reveal direct links between miRNA target recognition and silencing. *Mol Cell*. 54:737-750.

Cho, P.F., C. Gamberi, Y.A. Cho-Park, I.B. Cho-Park, P. Lasko, and N. Sonenberg. 2006. Cap-dependent translational inhibition establishes two opposing morphogen gradients in Drosophila embryos. *Current biology : CB*. 16:2035-2041.

Cho, P.F., F. Poulin, Y.A. Cho-Park, I.B. Cho-Park, J.D. Chicoine, P. Lasko, and N. Sonenberg. 2005. A new paradigm for translational control: inhibition via 5'-3' mRNA tethering by Bicoid and the eIF4E cognate 4EHP. *Cell*. 121:411-423.

Chu, J., S.R.Y. Cajal, N. Sonenberg, and J. Pelletier. 2018. Eukaryotic initiation factor 4F-sidestepping resistance mechanisms arising from expression heterogeneity. *Curr Opin Genet Dev*. 48:89-96.

Collart, M.A. 2016. The Ccr4-Not complex is a key regulator of eukaryotic gene expression. *Wiley interdisciplinary reviews. RNA*. 7:438-454.

Collart, M.A., and O.O. Panasenko. 2017. The Ccr4-Not Complex: Architecture and Structural Insights. *In* Macromolecular Protein Complexes: Structure and Function. J.R. Harris and J. Marles-Wright, editors. Springer International Publishing, Cham. 349-379.

Cordin, O., J. Banroques, N.K. Tanner, and P. Linder. 2006. The DEAD-box protein family of RNA helicases. *Gene*. 367:17-37.

de la Parra, C., B.A. Walters, P. Geter, and R.J. Schneider. 2018. Translation initiation factors and their relevance in cancer. *Curr Opin Genet Dev*. 48:82-88.

des Georges, A., V. Dhote, L. Kuhn, C.U. Hellen, T.V. Pestova, J. Frank, and Y. Hashem. 2015. Structure of mammalian eIF3 in the context of the 43S preinitiation complex. *Nature*. 525:491-495.

Desbuquois, B., N. Carre, and A.F. Burnol. 2013. Regulation of insulin and type 1 insulin-like growth factor signaling and action by the Grb10/14 and SH2B1/B2 adaptor proteins. *Febs j*. 280:794-816.

Dever, T.E., J.D. Dinman, and R. Green. 2018. Translation Elongation and Recoding in Eukaryotes. *Cold Spring Harb Perspect Biol*. 10.

Eliscovich, C., and R.H. Singer. 2017. RNP transport in cell biology: the long and winding road. *Current Opinion in Cell Biology*. 45:38-46.

Emsley, P., B. Lohkamp, W.G. Scott, and K. Cowtan. 2010. Features and development of Coot. *Acta crystallographica. Section D, Biological crystallography*. 66:486-501.

Eulalio, A., J. Rehwinkel, M. Stricker, E. Huntzinger, S.F. Yang, T. Doerks, S. Dorner, P. Bork, M. Boutros, and E. Izaurralde. 2007. Target-specific requirements for enhancers of decapping in miRNA-mediated gene silencing. *Genes Dev*. 21:2558-2570.

Fabian, M.R., F. Frank, C. Rouya, N. Siddiqui, W.S. Lai, A. Karetnikov, P.J. Blackshear, B. Nagar, and N. Sonenberg. 2013. Structural basis for the recruitment of the human CCR4-NOT deadenylase complex by tristetraprolin. *Nature structural & molecular biology*. 20:735-739.

Frye, M., B.T. Harada, M. Behm, and C. He. 2018. RNA modifications modulate gene expression during development. *Science*. 361:1346-1349.

Fu, R., M.T. Olsen, K. Webb, E.J. Bennett, and J. Lykke-Andersen. 2016. Recruitment of the 4EHP-GYF2 cap-binding complex to tetraproline motifs of tristetraprolin promotes repression and degradation of mRNAs with AU-rich elements. *RNA*. 22:373-382.

Galloway, A., and V.H. Cowling. 2018. mRNA cap regulation in mammalian cell function and fate. *Biochimica et Biophysica Acta (BBA) - Gene Regulatory Mechanisms*.

Garcia-Garcia, C., K.L. Frieda, K. Feoktistova, C.S. Fraser, and S.M. Block. 2015. RNA BIOCHEMISTRY. Factor-dependent processivity in human eIF4A DEAD-box helicase. *Science*. 348:1486-1488.

Gehring, N.H., J.B. Kunz, G. Neu-Yilik, S. Breit, M.H. Viegas, M.W. Hentze, and A.E. Kulozik. 2005. Exon-junction complex components specify distinct routes of nonsense-mediated mRNA decay with differential cofactor requirements. *Mol Cell*. 20:65-75.

Ghosh, S., and A. Jacobson. 2010. RNA decay modulates gene expression and controls its fidelity. *Wiley Interdisciplinary Reviews: RNA*. 1:351-361.

Gingras, A.C., S.P. Gygi, B. Raught, R.D. Polakiewicz, R.T. Abraham, M.F. Hoekstra, R. Aebersold, and N. Sonenberg. 1999. Regulation of 4E-BP1 phosphorylation: a novel two-step mechanism. *Genes Dev*. 13:1422-1437.

Gingras, A.C., S.G. Kennedy, M.A. O'Leary, N. Sonenberg, and N. Hay. 1998. 4E-BP1, a repressor of mRNA translation, is phosphorylated and inactivated by the Akt(PKB) signaling pathway. *Genes Dev*. 12:502-513.

Giovannone, B., E. Lee, L. Laviola, F. Giorgino, K.A. Cleveland, and R.J. Smith. 2003. Two novel proteins that are linked to insulin-like growth factor (IGF-I) receptors by the Grb10 adapter and modulate IGF-I signaling. *J Biol Chem*. 278:31564-31573.

Giovannone, B., W.G. Tsiaras, S. de la Monte, J. Klysik, C. Lautier, G. Karashchuk, S. Goldwurm, and R.J. Smith. 2009. GIGYF2 gene disruption in mice results in neurodegeneration and altered insulin-like growth factor signaling. *Hum Mol Genet*. 18:4629-4639.

Graifer, D., and G. Karpova. 2015. Interaction of tRNA with eukaryotic ribosome. *International journal of molecular sciences*. 16:7173-7194.

Grudzien-Nogalska, E., and M. Kiledjian. 2017. New insights into decapping enzymes and selective mRNA decay. *Wiley interdisciplinary reviews. RNA*. 8.

Gruner, S., D. Peter, R. Weber, L. Wohlbold, M.Y. Chung, O. Weichenrieder, E. Valkov, C. Igreja, and E. Izaurralde. 2016. The Structures of eIF4E-eIF4G Complexes Reveal an Extended Interface to Regulate Translation Initiation. *Mol Cell*. 64:467-479.

Gruner, S., R. Weber, D. Peter, M.Y. Chung, C. Igreja, E. Valkov, and E. Izaurralde. 2018. Structural motifs in eIF4G and 4E-BPs modulate their binding to eIF4E to regulate translation initiation in yeast. *Nucleic Acids Res*. 46:6893-6908.

Ha, M., and V.N. Kim. 2014. Regulation of microRNA biogenesis. *Nat Rev Mol Cell Biol*. 15:509-524.

Haas, G., J.E. Braun, C. Igreja, F. Tritschler, T. Nishihara, and E. Izaurralde. 2010. HPat provides a link between deadenylation and decapping in metazoa. *J Cell Biol*. 189:289-302.

Hanson, G., and J. Coller. 2018. Codon optimality, bias and usage in translation and mRNA decay. *Nat Rev Mol Cell Biol*. 19:20-30.

Heck, A.M., and J. Wilusz. 2018. The Interplay between the RNA Decay and Translation Machinery in Eukaryotes. *Cold Spring Harb Perspect Biol*. 10.

Hellen, C.U.T. 2018. Translation Termination and Ribosome Recycling in Eukaryotes. *Cold Spring Harb Perspect Biol*. 10.

Hernandez, G., M. Altmann, and P. Lasko. 2010. Origins and evolution of the mechanisms regulating translation initiation in eukaryotes. *Trends in biochemical sciences*. 35:63-73.

Higashi, S., E. Iseki, M. Minegishi, T. Togo, T. Kabuta, and K. Wada. 2010. GIGYF2 is present in endosomal compartments in the mammalian brains and enhances IGF-1-induced ERK1/2 activation. *Journal of neurochemistry*. 115:423-437.

Hinnebusch, A.G. 2014. The Scanning Mechanism of Eukaryotic Translation Initiation. *Annual Review of Biochemistry*. 83:779-812.

Hinnebusch, A.G., and J.R. Lorsch. 2012. The mechanism of eukaryotic translation initiation: new insights and challenges. *Cold Spring Harb Perspect Biol*. 4.

Hollerer, I., K. Grund, M.W. Hentze, and A.E. Kulozik. 2014. mRNA 3′end processing: A tale of the tail reaches the clinic. *EMBO Molecular Medicine*. 6:16-26.

Hoshino, S. 2012. Mechanism of the initiation of mRNA decay: role of eRF3 family G proteins. *Wiley interdisciplinary reviews. RNA*. 3:743-757.

Houseley, J., and D. Tollervey. 2009. The many pathways of RNA degradation. *Cell*. 136:763-776.

Igreja, C., and E. Izaurralde. 2011. CUP promotes deadenylation and inhibits decapping of mRNA targets. *Genes Dev*. 25:1955-1967.

Igreja, C., D. Peter, C. Weiler, and E. Izaurralde. 2014. 4E-BPs require non-canonical 4E-binding motifs and a lateral surface of eIF4E to repress translation. *Nat Commun*. 5:4790.

Iwakawa, H.O., and Y. Tomari. 2015. The Functions of MicroRNAs: mRNA Decay and Translational Repression. *Trends in cell biology*. 25:651-665.

Jackson, R.J., C.U. Hellen, and T.V. Pestova. 2010. The mechanism of eukaryotic translation initiation and principles of its regulation. *Nat Rev Mol Cell Biol*. 11:113-127.

Jafarnejad, S.M., C. Chapat, E. Matta-Camacho, I.A. Gelbart, G.G. Hesketh, M. Arguello, A. Garzia, S.H. Kim, J. Attig, M. Shapiro, M. Morita, A. Khoutorsky, T. Alain, C.G. Gkogkas, N. Stern-Ginossar, T. Tuschl, A.C. Gingras, T.F. Duchaine, and N. Sonenberg. 2018. Translational control of ERK signaling through miRNA/4EHP-directed silencing. *Elife*. 7.

Jamar, N.H., P. Kritsiligkou, and C.M. Grant. 2017. The non-stop decay mRNA surveillance pathway is required for oxidative stress tolerance. *Nucleic acids research*. 45:6881-6893.

Jamar, N.H., P. Kritsiligkou, and C.M. Grant. 2018. Loss of mRNA surveillance pathways results in widespread protein aggregation. *Sci Rep*. 8:3894.

Jia, Y., V. Polunovsky, P.B. Bitterman, and C.R. Wagner. 2012. Cap-dependent translation initiation factor eIF4E: an emerging anticancer drug target. *Med Res Rev*. 32:786-814.

Jonas, S., and E. Izaurralde. 2013. The role of disordered protein regions in the assembly of decapping complexes and RNP granules. *Genes Dev*. 27:2628-2641.

Jonas, S., and E. Izaurralde. 2015. Towards a molecular understanding of microRNA-mediated gene silencing. *Nat Rev Genet*. 16:421-433.

Jones, C.I., M.V. Zabolotskaya, and S.F. Newbury. 2012. The 5' --> 3' exoribonuclease XRN1/Pacman and its functions in cellular processes and development. *Wiley interdisciplinary reviews. RNA*. 3:455-468.

Joshi, B., A. Cameron, and R. Jagus. 2004. Characterization of mammalian eIF4E-family members. *European journal of biochemistry*. 271:2189-2203.

Joshi, B., K. Lee, D.L. Maeder, and R. Jagus. 2005. Phylogenetic analysis of eIF4E-family members. *BMC evolutionary biology*. 5:48.

Kabir, N.N., and J.U. Kazi. 2014. Grb10 is a dual regulator of receptor tyrosine kinase signaling. *Molecular Biology Reports*. 41:1985-1992.

Kabsch, W. 2010. XDS. *Acta crystallographica. Section D, Biological crystallography*. 66:125-132.

Kamenska, A., W.T. Lu, D. Kubacka, H. Broomhead, N. Minshall, M. Bushell, and N. Standart. 2014a. Human 4E-T represses translation of bound mRNAs and enhances microRNA-mediated silencing. *Nucleic Acids Res*. 42:3298-3313.

Kamenska, A., C. Simpson, and N. Standart. 2014b. eIF4E-binding proteins: new factors, new locations, new roles. *Biochem Soc Trans*. 42:1238-1245.

Kamenska, A., C. Simpson, C. Vindry, H. Broomhead, M. Benard, M. Ernoult-Lange, B.P. Lee, L.W. Harries, D. Weil, and N. Standart. 2016. The DDX6-4E-T interaction mediates translational repression and P-body assembly. *Nucleic Acids Res*. 44:6318-6334.

Kilchert, C., S. Wittmann, and L. Vasiljeva. 2016. The regulation and functions of the nuclear RNA exosome complex. *Nature Reviews Molecular Cell Biology*. 17:227.

Kim, M., I. Semple, B. Kim, A. Kiers, S. Nam, H.W. Park, H. Park, S.H. Ro, J.S. Kim, G. Juhasz, and J.H. Lee. 2015. Drosophila Gyf/GRB10 interacting GYF protein is an autophagy regulator that controls neuron and muscle homeostasis. *Autophagy*. 11:1358-1372.

Kofler, M.M., and C. Freund. 2006. The GYF domain. *FEBS J*. 273:245-256.

Kong, J., and P. Lasko. 2012. Translational control in cellular and developmental processes. *Nat Rev Genet*. 13:383-394.

Kozak, M. 1991. An analysis of vertebrate mRNA sequences: intimations of translational control. *J Cell Biol*. 115:887-903.

Kryszke, M.H., B. Adjeriou, F. Liang, H. Chen, and F. Dautry. 2016. Post-transcriptional gene silencing activity of human GIGYF2. *Biochem Biophys Res Commun*. 475:289-294.

Kubacka, D., A. Kamenska, H. Broomhead, N. Minshall, E. Darzynkiewicz, and N. Standart. 2013. Investigating the consequences of eIF4E2 (4EHP) interaction with 4E-transporter on its cellular distribution in HeLa cells. *PLoS One*. 8:e72761.

Kuzuoglu-Ozturk, D., D. Bhandari, E. Huntzinger, M. Fauser, S. Helms, and E. Izaurralde. 2016. miRISC and the CCR4-NOT complex silence mRNA targets independently of 43S ribosomal scanning. *EMBO J*. 35:1186-1203.

Labno, A., R. Tomecki, and A. Dziembowski. 2016. Cytoplasmic RNA decay pathways - Enzymes and mechanisms. *Biochim Biophys Acta*. 1863:3125-3147.

Lafontaine, D.L. 2015. Noncoding RNAs in eukaryotic ribosome biogenesis and function. *Nat Struct Mol Biol*. 22:11-19.

Lee, J., E. Yoo, H. Lee, K. Park, J.H. Hur, and C. Lim. 2017. LSM12 and ME31B/DDX6 Define Distinct Modes of Posttranscriptional Regulation by ATAXIN-2 Protein Complex in Drosophila Circadian Pacemaker Neurons. *Mol Cell*. 66:129-140 e127.

Leppek, K., R. Das, and M. Barna. 2017. Functional 5′ UTR mRNA structures in eukaryotic translation regulation and how to find them. *Nature Reviews Molecular Cell Biology*. 19:158.

Lewis, C.J.T., T. Pan, and A. Kalsotra. 2017. RNA modifications and structures cooperate to guide RNA–protein interactions. *Nature Reviews Molecular Cell Biology*. 18:202.

Lindqvist, L.M., K. Tandoc, I. Topisirovic, and L. Furic. 2018. Cross-talk between protein synthesis, energy metabolism and autophagy in cancer. *Curr Opin Genet Dev*. 48:104-111.

Lykke-Andersen, S., and T.H. Jensen. 2015. Nonsense-mediated mRNA decay: an intricate machinery that shapes transcriptomes. *Nature Reviews Molecular Cell Biology*. 16:665.

Mader, S., H. Lee, A. Pause, and N. Sonenberg. 1995. The translation initiation factor eIF-4E binds to a common motif shared by the translation factor eIF-4 gamma and the translational repressors 4E-binding proteins. *Mol Cell Biol*. 15:4990-4997.

Majumdar, R., A. Bandyopadhyay, and U. Maitra. 2003. Mammalian Translation Initiation Factor eIF1 Functions with eIF1A and eIF3 in the Formation of a Stable 40 S Preinitiation Complex. *Journal of Biological Chemistry*. 278:6580-6587.

Marcotrigiano, J., A.C. Gingras, N. Sonenberg, and S.K. Burley. 1999. Cap-dependent translation initiation in eukaryotes is regulated by a molecular mimic of eIF4G. *Mol Cell*. 3:707-716.

Marnef, A., and N. Standart. 2010. Pat1 proteins: a life in translation, translation repression and mRNA decay. *Biochemical Society Transactions*. 38:1602-1607.

Mathys, H., J. Basquin, S. Ozgur, M. Czarnocki-Cieciura, F. Bonneau, A. Aartse, A. Dziembowski, M. Nowotny, E. Conti, and W. Filipowicz. 2014. Structural and biochemical insights to the role of the CCR4-NOT complex and DDX6 ATPase in microRNA repression. *Mol Cell*. 54:751-765.

McCoy, A.J., R.W. Grosse-Kunstleve, P.D. Adams, M.D. Winn, L.C. Storoni, and R.J. Read. 2007. Phaser crystallographic software. *Journal of applied crystallography*. 40:658-674.

Meng, D., A.R. Frank, and J.L. Jewell. 2018. mTOR signaling in stem and progenitor cells. *Development (Cambridge, England)*. 145.

Mitchell, S.F., and R. Parker. 2014. Principles and properties of eukaryotic mRNPs. *Mol Cell*. 54:547-558.

Moore, M.J. 2005. From birth to death: the complex lives of eukaryotic mRNAs. *Science*. 309:1514-1518.

Morita, M., L.W. Ler, M.R. Fabian, N. Siddiqui, M. Mullin, V.C. Henderson, T. Alain, B.D. Fonseca, G. Karashchuk, C.F. Bennett, T. Kabuta, S. Higashi, O. Larsson, I. Topisirovic, R.J. Smith, A.C. Gingras, and N. Sonenberg. 2012. A novel 4EHP-GIGYF2 translational repressor complex is essential for mammalian development. *Mol Cell Biol*. 32:3585-3593.

Nagarajan, V.K., C.I. Jones, S.F. Newbury, and P.J. Green. 2013. XRN 5'-->3' exoribonucleases: structure, mechanisms and functions. *Biochim Biophys Acta*. 1829:590-603.

Nakamura, A., K. Sato, and K. Hanyu-Nakamura. 2004. Drosophila cup is an eIF4E binding protein that associates with Bruno and regulates oskar mRNA translation in oogenesis. *Developmental cell*. 6:69-78.

Nasif, S., L. Contu, and O. Muhlemann. 2018. Beyond quality control: The role of nonsense-mediated mRNA decay (NMD) in regulating gene expression. *Semin Cell Dev Biol*. 75:78-87.

Nelson, M.R., A.M. Leidal, and C.A. Smibert. 2004. Drosophila Cup is an eIF4E-binding protein that functions in Smaug-mediated translational repression. *Embo j*. 23:150-159.

Nicklas, S., S. Okawa, A.-L. Hillje, L. González-Cano, A. del Sol, and J.C. Schwamborn. 2015. The RNA helicase DDX6 regulates cell-fate specification in neural stem cells via miRNAs. *Nucleic Acids Research*. 43:2638-2654.

Nishimura, T., Z. Padamsi, H. Fakim, S. Milette, Wade H. Dunham, A.-C. Gingras, and Marc R. Fabian. 2015. The eIF4E-Binding Protein 4E-T Is a Component of the mRNA Decay Machinery that Bridges the 5′ and 3′ Termini of Target mRNAs. *Cell Reports*. 11:1425-1436.

Okumura, F., W. Zou, and D.E. Zhang. 2007. ISG15 modification of the eIF4E cognate 4EHP enhances cap structure-binding activity of 4EHP. *Genes Dev*. 21:255-260.

Ostareck, D.H., I.S. Naarmann-de Vries, and A. Ostareck-Lederer. 2014. DDX6 and its orthologs as modulators of cellular and viral RNA expression. *Wiley interdisciplinary reviews. RNA*. 5:659-678.

Ozgur, S., J. Basquin, A. Kamenska, W. Filipowicz, N. Standart, and E. Conti. 2015. Structure of a Human 4E-T/DDX6/CNOT1 Complex Reveals the Different Interplay of DDX6-Binding Proteins with the CCR4-NOT Complex. *Cell Rep*. 13:703-711.

Ozgur, S., M. Chekulaeva, and G. Stoecklin. 2010. Human Pat1b connects deadenylation with mRNA decapping and controls the assembly of processing bodies. *Mol Cell Biol*. 30:4308-4323.

Pakos-Zebrucka, K., I. Koryga, K. Mnich, M. Ljujic, A. Samali, and A.M. Gorman. 2016. The integrated stress response. *EMBO reports*. 17:1374-1395.

Passmore, L.A., T.M. Schmeing, D. Maag, D.J. Applefield, M.G. Acker, M.A. Algire, J.R. Lorsch, and V. Ramakrishnan. 2007. The eukaryotic translation initiation factors eIF1 and eIF1A induce an open conformation of the 40S ribosome. *Mol Cell*. 26:41-50.

Peña, C., E. Hurt, and V.G. Panse. 2017. Eukaryotic ribosome assembly, transport and quality control. *Nature Structural &Amp; Molecular Biology*. 24:689.

Pérez-Ortín, J.E., P. Alepuz, S. Chávez, and M. Choder. 2013. Eukaryotic mRNA Decay: Methodologies, Pathways, and Links to Other Stages of Gene Expression. *Journal of Molecular Biology*. 425:3750-3775.

Pestova, T.V., S.I. Borukhov, and C.U. Hellen. 1998. Eukaryotic ribosomes require initiation factors 1 and 1A to locate initiation codons. *Nature*. 394:854-859.

Peter, D., C. Igreja, R. Weber, L. Wohlbold, C. Weiler, L. Ebertsch, O. Weichenrieder, and E. Izaurralde. 2015a. Molecular architecture of 4E-BP translational inhibitors bound to eIF4E. *Mol Cell*. 57:1074-1087.

Peter, D., R. Weber, C. Kone, M.Y. Chung, L. Ebertsch, V. Truffault, O. Weichenrieder, C. Igreja, and E. Izaurralde. 2015b. Mextli proteins use both canonical bipartite and novel tripartite binding modes to form eIF4E complexes that display differential sensitivity to 4E-BP regulation. *Genes Dev*. 29:1835-1849.

Peter, D., R. Weber, F. Sandmeir, L. Wohlbold, S. Helms, P. Bawankar, E. Valkov, C. Igreja, and E. Izaurralde. 2017. GIGYF1/2 proteins use auxiliary sequences to selectively bind to 4EHP and repress target mRNA expression. *Genes Dev*. 31:1147-1161.

Presnyak, V., and J. Coller. 2013. The DHH1/RCKp54 family of helicases: an ancient family of proteins that promote translational silencing. *Biochim Biophys Acta*. 1829:817-823.

Radhakrishnan, A., and R. Green. 2016. Connections Underlying Translation and mRNA Stability. *J Mol Biol*. 428:3558-3564.

Raisch, T., D. Bhandari, K. Sabath, S. Helms, E. Valkov, O. Weichenrieder, and E. Izaurralde. 2016. Distinct modes of recruitment of the CCR4-NOT complex by Drosophila and vertebrate Nanos. *EMBO J*. 35:974-990.

Ramanathan, A., G.B. Robb, and S.-H. Chan. 2016. mRNA capping: biological functions and applications. *Nucleic Acids Research*. 44:7511-7526.

Rehwinkel, J., I. Behm-Ansmant, D. Gatfield, and E. Izaurralde. 2005. A crucial role for GW182 and the DCP1:DCP2 decapping complex in miRNA-mediated gene silencing. *Rna*. 11:1640-1647.

Rissland, O.S. 2017. The organization and regulation of mRNA-protein complexes. *Wiley interdisciplinary reviews. RNA*. 8.

Robichaud, N., N. Sonenberg, D. Ruggero, and R.J. Schneider. 2018. Translational Control in Cancer. *Cold Spring Harbor Perspectives in Biology*.

Rom, E., H.C. Kim, A.-C. Gingras, J. Marcotrigiano, D. Favre, H. Olsen, S.K. Burley, and N. Sonenberg. 1998. Cloning and Characterization of 4EHP, a Novel Mammalian eIF4E-related Cap-binding Protein. *Journal of Biological Chemistry*. 273:13104-13109.

Rosettani, P., S. Knapp, M.G. Vismara, L. Rusconi, and A.D. Cameron. 2007. Structures of the human eIF4E homologous protein, h4EHP, in its m7GTP-bound and unliganded forms. *J Mol Biol*. 368:691-705.

Roy, B., and A. Jacobson. 2013. The intimate relationships of mRNA decay and translation. *Trends in Genetics*. 29:691-699.

Saxton, R.A., and D.M. Sabatini. 2017. mTOR Signaling in Growth, Metabolism, and Disease. *Cell*. 168:960-976.

Schimmel, P. 2017. The emerging complexity of the tRNA world: mammalian tRNAs beyond protein synthesis. *Nature Reviews Molecular Cell Biology*. 19:45.

Schoenberg, D.R., and L.E. Maquat. 2012. Regulation of cytoplasmic mRNA decay. *Nature Reviews Genetics*. 13:246.

Schopp, I.M., C.C. Amaya Ramirez, J. Debeljak, E. Kreibich, M. Skribbe, K. Wild, and J. Bethune. 2017. Split-BioID a conditional proteomics approach to monitor the composition of spatiotemporally defined protein complexes. *Nat Commun*. 8:15690.

Schuller, A.P., and R. Green. 2018. Roadblocks and resolutions in eukaryotic translation. *Nat Rev Mol Cell Biol*. 19:526-541.

Sgromo, A., T. Raisch, C. Backhaus, C. Keskeny, V. Alva, O. Weichenrieder, and E. Izaurralde. 2018. Drosophila Bag-of-marbles directly interacts with the CAF40 subunit of the CCR4-NOT complex to elicit repression of mRNA targets. *RNA*. 24:381-395.

Shi, Y. 2017. Mechanistic insights into precursor messenger RNA splicing by the spliceosome. *Nature Reviews Molecular Cell Biology*. 18:655.

Shirokikh, N.E., and T. Preiss. 2018. Translation initiation by cap-dependent ribosome recruitment: Recent insights and open questions. *Wiley Interdisciplinary Reviews: RNA*. 9:e1473.

Simms, C.L., and H.S. Zaher. 2016. Quality control of chemically damaged RNA. *Cellular and Molecular Life Sciences*. 73:3639-3653.

Singh, P., U. Saha, S. Paira, and B. Das. 2018. Nuclear mRNA Surveillance Mechanisms: Function and Links to Human Disease. *J Mol Biol*. 430:1993-2013.

Sonenberg, N., and A.G. Hinnebusch. 2009. Regulation of translation initiation in eukaryotes: mechanisms and biological targets. *Cell*. 136:731-745.

Sriram, A., J. Bohlen, and A.A. Teleman. 2018. Translation acrobatics: how cancer cells exploit alternate modes of translational initiation. *EMBO Rep*. 19.

Standart, N., and D. Weil. 2018. P-Bodies: Cytosolic Droplets for Coordinated mRNA Storage. *Trends in Genetics*. 34:612-626.

Steitz, T.A., and P.B. Moore. 2017. Perspectives on the ribosome. *Philosophical Transactions of the Royal Society B: Biological Sciences*. 372.

Tahmasebi, S., A. Khoutorsky, M.B. Mathews, and N. Sonenberg. 2018. Translation deregulation in human disease. *Nat Rev Mol Cell Biol*.

Tan, E.K., and A.H. Schapira. 2010. Summary of GIGYF2 studies in Parkinson's disease: the burden of proof. *Eur J Neurol*. 17:175-176.

Tao, X., and G. Gao. 2015. Tristetraprolin Recruits Eukaryotic Initiation Factor 4E2 To Repress Translation of AU-Rich Element-Containing mRNAs. *Mol Cell Biol*. 35:3921-3932.

Terenin, I.M., V.V. Smirnova, D.E. Andreev, S.E. Dmitriev, and I.N. Shatsky. 2017. A researcher's guide to the galaxy of IRESs. *Cellular and molecular life sciences : CMLS*. 74:1431-1455.

Topisirovic, I., and N. Sonenberg. 2011. mRNA translation and energy metabolism in cancer: the role of the MAPK and mTORC1 pathways. *Cold Spring Harb Symp Quant Biol*. 76:355-367.

Treiber, T., N. Treiber, and G. Meister. 2018. Regulation of microRNA biogenesis and its crosstalk with other cellular pathways. *Nature Reviews Molecular Cell Biology*.

Tritschler, F., J.E. Braun, A. Eulalio, V. Truffault, E. Izaurralde, and O. Weichenrieder. 2009. Structural basis for the mutually exclusive anchoring of P body components EDC3 and Tral to the DEAD box protein DDX6/Me31B. *Mol Cell*. 33:661-668.

Tritschler, F., A. Eulalio, S. Helms, S. Schmidt, M. Coles, O. Weichenrieder, E. Izaurralde, and V. Truffault. 2008. Similar modes of interaction enable Trailer Hitch and EDC3 to associate with DCP1 and Me31B in distinct protein complexes. *Mol Cell Biol*. 28:6695-6708.

Tritschler, F., A. Eulalio, V. Truffault, M.D. Hartmann, S. Helms, S. Schmidt, M. Coles, E. Izaurralde, and O. Weichenrieder. 2007. A divergent Sm fold in EDC3 proteins mediates DCP1 binding and P-body targeting. *Mol Cell Biol*. 27:8600-8611.

Tucker, M., M.A. Valencia-Sanchez, R.R. Staples, J. Chen, C.L. Denis, and R. Parker. 2001. The transcription factor associated Ccr4 and Caf1 proteins are components of the major cytoplasmic mRNA deadenylase in Saccharomyces cerevisiae. *Cell*. 104:377-386.

Valkov, E., S. Jonas, and O. Weichenrieder. 2017. Mille viae in eukaryotic mRNA decapping. *Curr Opin Struct Biol*. 47:40-51.

Valkov, E., S. Muthukumar, C.T. Chang, S. Jonas, O. Weichenrieder, and E. Izaurralde. 2016. Structure of the Dcp2-Dcp1 mRNA-decapping complex in the activated conformation. *Nat Struct Mol Biol*. 23:574-579.

van Hoof, A., and E.J. Wagner. 2011. A brief survey of mRNA surveillance. *Trends in biochemical sciences*. 36:585-592.

Villa, N., A. Do, J.W. Hershey, and C.S. Fraser. 2013. Human eukaryotic initiation factor 4G (eIF4G) protein binds to eIF3c, -d, and -e to promote mRNA recruitment to the ribosome. *J Biol Chem*. 288:32932-32940.

Villaescusa, J.C., C. Buratti, D. Penkov, L. Mathiasen, J. Planaguma, E. Ferretti, and F. Blasi. 2009. Cytoplasmic Prep1 interacts with 4EHP inhibiting Hoxb4 translation. *PLoS One*. 4:e5213.

von Stechow, L., D. Typas, J. Carreras Puigvert, L. Oort, R. Siddappa, A. Pines, H. Vrieling, B. van de Water, L.H. Mullenders, and E.H. Danen. 2015. The E3 ubiquitin ligase ARIH1 protects against genotoxic stress by initiating a 4EHP-mediated mRNA translation arrest. *Mol Cell Biol*. 35:1254-1268.

Wahle, E., and G.S. Winkler. 2013. RNA decay machines: Deadenylation by the Ccr4–Not and Pan2–Pan3 complexes. *Biochimica et Biophysica Acta (BBA) - Gene Regulatory Mechanisms*. 1829:561-570.

Wang, M., M. Ly, A. Lugowski, J.D. Laver, H.D. Lipshitz, C.A. Smibert, and O.S. Rissland. 2017. ME31B globally represses maternal mRNAs by two distinct mechanisms during the Drosophila maternal-to-zygotic transition. *Elife*. 6.

Wang, Y., M. Arribas-Layton, Y. Chen, J. Lykke-Andersen, and George L. Sen. 2015. DDX6 Orchestrates Mammalian Progenitor Function through the mRNA Degradation and Translation Pathways. *Molecular Cell*. 60:118-130.

Wu, X., and D.P. Bartel. 2017. Widespread Influence of 3′-End Structures on Mammalian mRNA Processing and Stability. *Cell*. 169:905-917.e911.

Xie, J., Q. Wei, H. Deng, G. Li, L. Ma, and H. Zeng. 2014. Negative regulation of Grb10 Interacting GYF Protein 2 on insulin-like growth factor-1 receptor signaling pathway caused diabetic mice cognitive impairment. *PLoS One*. 9:e108559.

Yamaji, M., M. Jishage, C. Meyer, H. Suryawanshi, E. Der, M. Yamaji, A. Garzia, P. Morozov, S. Manickavel, H.L. McFarland, R.G. Roeder, M. Hafner, and T. Tuschl. 2017. DND1 maintains germline stem cells via recruitment of the CCR4-NOT complex to target mRNAs. *Nature*. 543:568-572.

Yamamoto, H., A. Unbehaun, and C.M.T. Spahn. 2017. Ribosomal Chamber Music: Toward an Understanding of IRES Mechanisms. *Trends in biochemical sciences*. 42:655-668.

Yamashita, A., and O. Takeuchi. 2017. Translational control of mRNAs by 3'-Untranslated region binding proteins. *BMB reports*. 50:194-200.

Yu, S.F., P. Lujan, D.L. Jackson, M. Emerman, and M.L. Linial. 2011. The DEAD-box RNA helicase DDX6 is required for efficient encapsidation of a retroviral genome. *PLoS pathogens*. 7:e1002303-e1002303.

Yusupova, G., and M. Yusupov. 2017. Crystal structure of eukaryotic ribosome and its complexes with inhibitors. *Philosophical transactions of the Royal Society of London. Series B, Biological sciences*. 372:20160184.

Zekri, L., E. Huntzinger, S. Heimstadt, and E. Izaurralde. 2009. The silencing domain of GW182 interacts with PABPC1 to promote translational repression and degradation of microRNA targets and is required for target release. *Mol Cell Biol*. 29:6220-6231.

Zekri, L., D. Kuzuoglu-Ozturk, and E. Izaurralde. 2013. GW182 proteins cause PABP dissociation from silenced miRNA targets in the absence of deadenylation. *EMBO J*. 32:1052-1065.

Zhang, Y., Q.Y. Sun, R.H. Yu, J.F. Guo, B.S. Tang, and X.X. Yan. 2015. The contribution of GIGYF2 to Parkinson's disease: a meta-analysis. *Neurological sciences : official journal of the Italian Neurological Society and of the Italian Society of Clinical Neurophysiology*. 36:2073-2079.

Zheng, X., R. Dumitru, B.L. Lackford, J.M. Freudenberg, A.P. Singh, T.K. Archer, R. Jothi, and G. Hu. 2012. Cnot1, Cnot2, and Cnot3 maintain mouse and human ESC identity and inhibit extraembryonic differentiation. *Stem cells (Dayton, Ohio)*. 30:910-922.

Zheng, X., P. Yang, B. Lackford, B.D. Bennett, L. Wang, H. Li, Y. Wang, Y. Miao, J.F. Foley, D.C. Fargo, Y. Jin, C.J. Williams, R. Jothi, and G. Hu. 2016. CNOT3-Dependent mRNA Deadenylation Safeguards the Pluripotent State. *Stem cell reports*. 7:897-910.

Zhou, B., J. Liu, Z. Ren, F. Yao, J. Ma, J. Song, B. Bennett, Y. Zhen, L. Wang, G. Hu, and S. Hu. 2017. Cnot3 enhances human embryonic cardiomyocyte proliferation by promoting cell cycle inhibitor mRNA degradation. *Sci Rep*. 7:1500.

Zinder, J.C., and C.D. Lima. 2017. Targeting RNA for processing or destruction by the eukaryotic RNA exosome and its cofactors. *Genes & development*. 31:88-100.

Zlotorynski, E. 2014. The fates of mRNAs in P bodies. *Nature Reviews Molecular Cell Biology*. 15:632.

9 Acknowledgments

I would like to express my most sincere gratitude to Prof. Dr. Elisa Izaurralde for her scientific guidance and her support during my PhD.

A very special acknowledge to my supervisor Cátia Igreja, who mentored me along this tough but rewarding path. Thank you for having always an open-door policy, I learned a lot from you.

I would like to thank Prof. Dr. Ralf J. Sommer for the important support.

I am grateful to Prof. Dr. Ralf-Peter Jansen for supervising my PhD thesis for so many years and to Dr. Martin Bayer and Dr. Frank Chan for being members of my thesis advisory committee.

I would like to thank Prof. Dr. Doron Rapaport for evaluating my PhD thesis and to Prof. Dr. Dirk Schwarzer and Dr. Patrick Müller for accepting to be in the thesis defence committee.

I am thankful to Dr. Praveen Bawankar, Dr. Daniel Peter, Ramona Weber, and Dr. Eugene Valkov for their contribution in the GIGYF projects.

I also would like to thank Dr. Eugene Valkov and Dr. Dipankar Bhandari for the help and encouragement over these years.

I want to thank Sigrun Helms, Maria Fauser, Min-Yi Chung, Dr. Heike Budde, and Catrin Weiler for the great technical support and contribution.

Many thanks to Maria Gölz for the help during these years and to the PhD program coordinator, Dr. Dagmar Sigurdardottir, for her support throughout my PhD and for the many courses organized at the Max Planck International PhD program.

My thank goes to all the present and former members of the Department 2 for the nice time we had together, I am happy to have such labmates! Thank you for sharing a quality time in and outside the lab and for all the fun we had during these hard years. A special thanks to Felix Raesch for his exceptional German language skills.

I am also very happy to have met many new Brothers and Sisters during my stay in Tübingen, for the time spent together that I will never forget, and I am thankful for Those back home, always a part of me and constantly in my mind, you will always be precious for me. I would like to thank my families and specially Nicholas and Alessandro.

A particular thanks to Dr. Daniela Giulia Vitali for insightful comments on the thesis and the innumerable scientific discussions. You have always been a Friend for me.

And now it’s done!

10 Curriculum vitae

Vincenzo Ruscica

17 May 1988, Treviglio, Bergamo, Italy.

Hegelstraße 9, Tübingen.

Education

2010 – 2013 Master Degree, “Molecular Biology of the Cell” 110/110 with honours, Università degli Studi di Milano, Italy

2007 – 2010 Bachelor Degree, “Biological Sciences”, Università degli Studi di Milano

Work experience

2014 – 2019 Doctoral Research, Max Planck Institute for Developmental Biology, Tübingen, Germany

2013 – 2014 Research Fellowship, Istituto Nazionale dei Tumori (National Cancer Institute), Milano, Italy

2012 – 2013 Master Degree research, Istituto Nazionale dei Tumori (National Cancer Institute), Milano, Italy